Aus dem Theodor-Boveri-Institut für Biowissenschaften
der Universität Würzburg
Lehrstuhl für Bioinformatik
Vorstand: Prof. Dr. med. Thomas Dandekar

The ERK-cascade in the pathophysiology of cardiac hypertrophy

Inauguraldissertation
zur Erlangung der Doktorwürde
der Medizinischen Fakultät
der
Julius-Maximilians-Universität Würzburg

vorgelegt von
Alexandra Classen
aus Oedheim

Würzburg, Oktober 2020

Referent: Prof. Dr. Thomas Dandekar

Koreferentin: Prof. Dr. Kristina Lorenz

Dekan: Prof. Dr. Matthias Frosch

Tag der mündlichen Prüfung: 05.02.2021

Die Promovendin ist Ärztin.

Contents

Part I.

Introduction

1. Motivation

The leading cause of death worldwide are cardiovascular diseases, which include amongst others high blood pressure, peripheral artery occlusive disease, coronary artery disease and stroke [160, 30]. As diverse the well established risk factors, including age, unhealthy diet, obesity, alcohol abuse and others, are, the main pathological mechanism for all above-mentioned diseases is the same: atherosclerosis [217]. In particular for the heart, atherosclerosis leads to coronary artery disease, which is characterized as a stenosis of the coronary arteries and in series an undersupply of the cardiomyocytes with oxygen. Subsequently, this can cause infarction, arrhythmias and congestive heart failure. The last-mentioned can also be caused as elucidated below by high blood pressure itself [119].

Heart failure is specified as a disproportion of the required blood demand of the organisms and the provided blood supply of the heart, thus in any condition the capacity of the heart muscle is exceeded. This can occur by dysfunction of the cardiomyocyte itself, for example after an infarction as a result of coronary artery disease, or by circumstances which increase the force of contraction needed to pump blood as in existence of high blood pressure [218]. The heart has several mechanisms to compensate this disproportion short-term, but these processes lead to more changes and a progression of the disease long-term because of ventricular remodeling [102]. Coronary artery disease and high blood pressure are rather not the only causes of congestive heart failure, but along with atrial fibrillation the most frequent. More rare causes are cardiomyopathies, valvular heart diseases, anaemia and others [29].

For two reasons, heart failure is of special interest in the following thesis: First, one of the underlying pathological mechanisms, namely myocyte growth, is primarily a physiological process in response to increased workload, for instance occurring consecutively to physiological exercise [162]. So it is of special interest, to find the point of time when and the reasons why this physiological process turns maladaptive.

Second, nearly all utilized drugs target risk factors or symptoms, none of the commonly used drug targets at the time-point, where the the physiological turns to an maladaptive answer. So there is a need for further research.

The objective of this thesis is a signaling cascade involved in physiological as well as pathological myocyte growth, the ERK1/2 cascade. For this cascade, it is already known that an additional phosphorylation may lead to maladaptive cardiac hypertrophy [133], whereas the exact time courses for these processes were so far not investigated.

The present thesis demonstrates an in silico model on all events of the signaling cascade. The model reproduces different phosphorylation states of ERK 1/2 and various types of stimuli and allows prediction of their synergistic and antagonistic effects. Feedback loops are considered. Besides, thresholds for receptor activation can be predicted. To confirm the results of the in silico model, simulated time courses were experimentally validated. Furthermore, gene expression analysis are introduced, which show if and in which way proteins of the ERK1/2 cascade are effected in their gene expression level after inducing heart failure and which other proteins are effected. At last, new possible targets of the ERK1/2 protein, especially with regard on pharmacological treatment, will be presented.

The results presented in this thesis were published in Molecular BioSystems in 2016 and was added to the hot article collection here [25].

2. Heart failure

Heart failure is, as briefed in the previous chapter, a disease with immense meaning in public health, as it is a final point of many diseases. As it applies to one till two percent of adult population it can be termed an epidemic disease [218]. In the following chapter, the main features in the development of heart failure will be pointed out.

Heart failure is a combination of symptoms, signs and their underlying pathophysiology. The current definition of the European Society of Cardiology states that 'Heart failure is a clinical syndrome in which patients have typical symptoms and signs resulting from an abnormality of cardiac structure and function [144]. Heart failure is defined pathophysiologically by the WHO when the heart is not capable of supplying the tissue with enough oxygen to ensure a steady metabolism when resting and exercising. Clinically heart failure is apparent in typical symptoms like fatigue, dyspnoea and retention of fluid. The reason for these dysfunctions can either be on the arterial side as forward heart failure or in the venous side as backward heart failure. The cardiac muscle in these cases is not capable of either supplying sufficient output or providing in adequate turn over to meet the venous side. The WHO further differentiates the more exact location in left heart, right heart or global insufficiency and whether the problem is more on the systolic or diastolic part of the cycle. The most common form of heart failure is the low-output failure. Here, the demand of the circumference is not sufficiently met. The not so common high-output failure describes the situation, when the circumference has an altered requirement through changes in metabolic activity. This case of cause can also be apparent through other pathology for example anemia, hyperthyreosis, septic inflammation or even pregnancy. These are only examples and are not necessarily singular causes for heart failure. However, the most common cause of heart failure is the coronary heart disease. Arterial hypertonia as a singular cause is stated at 9 to 20 percent. In the vast majority of patients showing symptoms of heart failure a reduced ejection fraction can be shown. In more of half of the patients it is reduced under 40 percent. When the chronic pressure or volume overload persists over a long period of time the cardiac muscle growth to a mass that is called overcritical. The

muscle fiber increase leads to a change in texture of the heart muscle that causes dilatation. This again results in an increase of end-diastolic volume which means the sarcomeres as a functional unit of contraction now has to work under more unfavorable conditions. Even in highly hypertrophic hearts the blood supply of the vascular circumference is ensured. The potential shortage is in the bigger subepicardial coronary artery branches which do not grow along. If an even low-grade coronary artery sclerosis is added to this situation a relative coronary insufficiency will result. This means hypoxic myelosis will occur and organize into disseminated myocardial fibrosis. This will further weaken to already insufficient working pump. This can be called a vicious cycle [58].

The hearts action can be influenced in different ways. These include the ability for constriction (called inotropy), the regulation of the frequency of heart rate (called chronotropia) and modification of the degree of excitability (called bathmotropy) only to name the most important for the understanding of the following thesis [211, 55, 94]. In general, sympathomimetics like adrenalin are positive inotropic, whereas sympathoplegic drugs like beta-blockers act negative inotropic. Positive inotropy itself does initially not mean cardiomyocyte growth itself, but can result in it, in case of positive inotropic signals received over a long period of time.

3. MAPK signaling

In response to external influences, for instance signals transmitted by growth factors, cytokines, hormones or environmental stress, the cell requires mechanisms for internal signal transmission. In order to adapt to modified circumstances, for example through changed protein expression, the signals have to reach the nucleus, and the information flow has to make its way from the cell membrane to the interior of the cell. The MAPK (mitogen-activated protein kinase) signaling cascade in this context represents one of the main mechanisms of cellular signal transmission involved in proliferation, differentiation, survival and growth of almost all types of cells [204]. MAPK signaling cascades are multiple-tiered pathways of signal transduction, which include leastwise three kinases, that are connected in series. They are involved in several physiological processes, including for instance response to stress, cell progress, cell survival, cell proliferation and cell differentiation [204, 103]. Quite a few cascades are members of the group of MAPK cascades, and all cascade pathways operate in a similar way: small GTP-binding proteins (smGTP) or adaptor proteins trigger the activation of the pathway, which starts with the phosphorylation of MAPK kinase kinase (MAP3K). In sequence the MAPK kinase (MAP2K) gets activated by the MAP3K. In the following step the signal is transmitted to the MAPK and consecutively to the MAPK-activated protein kinase (MAPKAPK) [174]. The MAPK-component is eponymous for the cascade in order to distinguish them from each other, such as the cascade regarded in this thesis is named ERK1/2 cascade after their MAPK-components ERK 1 and 2.

MAPK cascades transmit as the name implies especially signals influencing the mitosis of the cell, but to a certain extent they also transmit inflammatory and other signals. Most notably this concerns the MAPK p38 and JNK cascades, which basically transmit stress and pro-inflammatory signals, and furthermore the ERK 5 cascade, which transmits stress signals as well as mitogenic signals [238, 117].

ERK (extracellular regulated kinases) cascades as a subcategory of MAPK are of high biological interest as they are involved in many physiological and pathological processes. At this juncture, eight different isoforms of the ERK enzyme are known, they are named ERK 1-8 but partially have proper names beyond that [118, 41].

Thus the focus in the present thesis is on the ERK 1/2 cascade, the accurate functionality will be elucidated only for the this cascade. The activation of the entire cascade is initialized by membrane receptors, which recruit adaptor proteins and exchange factors to the membrane of the cell. G-protein coupled receptors (GPCR), receptor tyrosine kinases (RTK) or ion channels are examples for such membrane receptors. The adaptor proteins and exchange factors induce the activation of Ras. Ras proteins are members of a protein family belonging to a class of protein named small GTPase, phosphatases that are able to bind and hydrolyze guanosine triphosphate (GTP) [236]. In the next step the kinases of the MAP3K level, as there are Raf1, A-Raf and B-Raf kinase, get activated by the (GTP-bound) Ras protein. Raf stands for rapidly accelerated fibrosarcoma. These kinases are a family of serine/threonine protein kinases, which are enzymes known for phosphorylating the hydroxy group of serine or threonine [247].

The kinases of MAP3K level then activate the kinases of MAP2K level by phosphorylating them, in the described cascade are these MEK 1/2 (mitogen-activated protein kinase kinase). MEK 1/2 in turn phosphorylates the kinases of the MAPK level, ERK 1/2 (extracellular signal–regulated kinases 1/2, also known as MAPK 3/1) .The phosphorylation takes place in the TEY motif in the activation loop at a threonine and a tyrosine residue [238, 39]. The now activated ERK is able to phosphorylate its targets, which are for instance transcription factors or further kinases. To mention just a few examples, some of the most investigated targets are Elk1, a transcription factor associated with the development of amongst others breast cancer, Alzheimers disease and Down syndrome and RSK (ribosomal s6 kinase), a kinase involved in signal transduction and the substrate of the first isolated MAPK [19, 40, 7].

ERK cascades are involved in physiological processes as well as, usually when dysregulated, in pathological processes. The results of the last-mentioned processes are diseases, that lead from cancer to degenerative, immunological as well as inflammatory syndromes [170]. As an example ERK dysregulation is involved in more than 30 percent of all types of cancer, well investigated for instance in glioma cells [150, 169].

The focus in the following is the role of ERK 1/2 cascade in the formation of cardiac hypertrophy. This is, as described above, a process, that can result adaptive as well as under certain conditions maladaptive. For instance Raf1, a downstream target of ERK 1/2, is known to protect the heart from ischemic injury and cell death and thereby pathological hypertrophy, but other downstream targets have opposite effects [80]. The exact downstream targets of ERK, reasons and time courses of

these bivalent effects are still uncertain and have to be further investigated [134].

In 2009, an additional autophosphorylation site of ERK2 at Thr188, respectively Thr208 in ERK1, has been identified [133]. Targets located at the nucleus get phosphorylated by ERK subsequently to phosphorylation at this autophosphorylation site and they supposably promote pathological hypertrophy [133]. So if phosphorylation at this site takes place may be the watershed between an adaptive and a maladaptive response to myocyte growth inducing stimuli [197]. Because of the variety of physiological and pathological answers and the great amount of effects ERK promotes, it is of special interest for pharmacological treatment to take aim at specific points of the cascade and not the enzyme altogether. Therefore, this autophosphorylation site is a auspicious pharmacological target.

4. Bioinformatics and systems biology

This thesis is based upon a system biological approach. The aim of systems biology is, to capture a biological system altogether. Therefore, it uses mutliple methods to analyze the genome, proteome, behaviour of a system under certain conditions and often many others, always with the focus on the overall picture. For these complex studies, bioinformatical analysis are a main part.

In dependence on a definition of the National Institute of Health of the United States, bioinformatics include the creation, development and use of computational tools for analyzing, visualization, acquirement or storing biological or medical data. Whereas computational biology is the investigation of for instance biological systems using data-analyzes, theoretical methods, modeling and computational simulation [88]. As both are comparatively new fields of science, for the first time introduced in the 1970 [87], there is yet no broad agreement if computational biology belongs to bioinformatics or rather system biology. Anyway, there is consensus that there is a significant overlap between the two of them and tools of both are used for the following analyses.

Modeling biological systems, which means building a frequently simplified computer model of a biological system, is a basic tool of bioinformatics and computational biology. The represented models can be metabolite networks, gene regulatory networks or signal transduction pathways [11, 21]. In this thesis the focus lies on the last-mentioned.

Biological modeling and analyzing of the networks provided insights in many biological processes including liver cell proliferation and apoptosis [178, 202] as well as platelet activation and inhibition [153, 152]. Above this, there are many models and system biological publications existing, providing insights in the heart. For example models of the cardiac signaling networks [98, 97], models of drug responses in cariomyocytes [96, 90] or models of cardiac cell architecture [74]. There are several biological models representing the MAPK pathways already in existence, as it is an important pathway playing part in many biological processes [111, 20, 4, 77].

Even concerning the heart in particular, there are several models existing, for example a computational model of fibroblast differentiation including the Erk cascade [1] or even of cardiac myocyte hypertrophy signaling [198] . But so far there was none, representing the above described additional phosphorylation and the consequences resulting from it.

Part II.

Material and methods

5. In silico modelling

Network Setup

Simplified, a network is an accumulation of connected objects. In the present thesis, a signal transduction network is presented. It consists of nodes and edges and whereas a node represents a protein or state of protein, an edge represents the connection between two nodes. The connection is directed, which means, there is a direction in which nodes communicate and beyond that, it can be positive or negative, indicating activation or inhibition. To mention a few examples, protein 1 can activate protein 2 (-> direction: protein 1 to protein 2, connection type: positive=activation). Protein 2 in turn further activate protein 1 (-> direction: protein 2 to protein 1, connection type: positive = activation) and inhibit protein 3 (-> direction: protein 2 to protein 3, connection type: negative = inhibition). In addition, the connections can be of different strength, which is indicated by their weight. So if a protein is inhibited by another, but activated by a third one and the activation is stronger then the inhibition, it is still activated.

For the setup of the network an extensive research of published literature, including notably the publications illustrating the above described additional autophosphorylation of ERK [48, 133, 134, 229], was used. Furthermore, databanks as PlateletWeb (http://plateletweb.bioapps.biozentrum.uni-wuerzburg.de/plateletweb.php) [23] and STRING (http://string-db.org/) [215] offered valuable clues to the network setup. A network consisting of 25 nodes and 34 edges comprising all crucial signaling events was established.

CellDesigner version 3.5.1. was used to implement and visualize the model. For the main part, CellDesigner is a tool for modeling and visualization of networks, but it also enables to simulate networks. The last-mentioned tool was not used, rather was taken benefit from the fact, that CellDesigner uses a language, called systems biology markup language (SBML), which functions to import and export in several analyzing tools using the same language [69].

SQUAD simulations

The software SQUAD [49] was used to analyze the model for stable steady states and for simulating different system states under certain stimulatory conditions as well as time courses.

Oftentimes, there is knowledge about the regulatory connection in signaling networks, but there is no information about the underlying biochemical reactions and thereby about the kinetic. So in 2006, a method for the "generation of standardized qualitative dynamical systems of regulatory networks" was introduced by Mendoza et al [149] and in 2007 the advancement SQUAD by Di Cara et al [49]. One aim in simulating signal transmitting networks is always, to elucidate the steady states of a system. Steady states are conditions characterized by a lack of transformation of the system in absences of external influences. During appearance of an external influence, the system can be stable or unstable. Stable means, the system reaches the initial steady state after a perturbation, whereas an unstable system passes into another condition [18]. SQUAD uses Boolean logic to elucidate the steady state initially. Boolean modeling is a discrete modeling technique, each node can reach only two states, value 0 and value 1 (active or inactive, entirely "ON" or "OFF"). The connection between two nodes in the Boolean models used by SQUAD is directed and can either be positive (activatory) or negative (inhibitory). It is a quite simple logic and in many cases not able to constitute the complexity of a biological system, but in lack of broad information as described above it is a pragmatic way to simulate these networks anyway.

Above converting the network into a discrete system, SQUAD converts it into a continuous dynamical system. A dynamical system is a system, in which each node can reach multiple, continous activation levels. The steady states elucidated via the discrete system are used to interpolate exponential functions between the states entirely "ON" (value: 1) and entirely "OFF" (value: 0). Thereby the activating signal can be traced back on its way through the signaling network. The resulting activation pathway can be represented in Western blot-like style, as it is depicted in a time continuous way. Some hypotheses are used for the dynamic analysis: In presence of any activator, the target node is successfully activated and in presence of any inhibitor, the target node is successfully inactivated. Even in presence of any activator, the target node is inactivated in presence of an inhibitor. Anyhow, the nodes and edges can be modified in several ways: SQUAD allows the modification of the initial state or the decay rate of a node or variation of the strength of interactions and so forth. By modifying the decay rate, one can order how strong a node reacts to transformations in general. By modifying the weight of an interaction, one can

order how strong a node reacts to a specific stimulus, an inhibitory or activatory sign upcoming from another node. Thereby, the point, where the presence of an inhibitor always results in inactivation, can be avoided.

In conclusion, SQUAD unites discrete (Boolean) and continuous modeling techniques [149, 49].

CellNetAnalyzer simulation

CellNetAnalyzer (CNA) is a toolbox for MATLAB [143]. MATLAB is an abbreviation for MATrix LABoratory and it is a software to solve and graph mathematical problems. CNA enables the user to analyze structures of metabolic, signaling and regulatory networks [107]. It is an advancement of Flux analyses, which was first introduced by Klamt et al in 2003 and was primarily developed to analyze metabolic (mass-flow) networks [108]. CNA as advancement in turn can be used to analyze metabolic as well as signaling networks. The last are Boolean models in Cell Net Analyzer. The reaction in these networks defined how the activation levels of an "end node" can be reached by "start nodes". The reaction types are defined by the typical Boolean operators AND (conjunction), OR (disjunction) or NOT (negation). In the case of CellNetAnalyzer, conjunction means two start nodes have to be both activated to reach the activation of an end note. By existence of an OR connection (disjunction), one or another start node can reach the activation of the end node. Negation stands for inhibition. In contrast to conventional Boolean models, the nodes cannot only reach levels 1 and 0 (entirely "ON" or "OFF"), they can also be multivalued. This provides for instance discrimination between different degrees of activation [107]. But in contrast to the SQUAD simulations, they cannot reach manifold continuous levels but only by the user predefined ones.

In the present thesis Cell Net Analyzer was used especially to detect steady states and feedback loops and to analyze user-defined perturbations. A feedback loop occurs, when an action leads to an effect and this effect itself influences the original action. Depending on wether the feedback loop intensifies or weakens the originally action, it is called positive or negative feedback loop [251]. A perturbation is defined as a modification of a system caused by internal or external mechanisms. These could be for instance environmental stimuli, inhibition by drugs or gene knockouts [54].

6. New predicted targets

It was searched for new supposable targets of ERK 1/2 by combining data from databanks such as platelet web, i-hop or hprd [23, 182, 86].

Above this, interactions, which were detected by applying string database and interaction prediction tool were considered [215]. In a second step, all possibly detected targets were validated by extensive literature search.

7. Gene expression analysis

The Gene Expression Omnibus (GEO) database [12] was used to find gene expression data sets for experimental validation of expression levels. Experimental published data sets on the search terms "transverse aortic constriction" (TAC) conjugated with "cardiomyocytes" were retrieved. Transverse aortic constriction in mice is a frequently used method for the induction of cardiac hypertrophy and subsequent heart failure. Following a thoracotomy, the transverse aorta is constricted between the innominate and left carotid arteries with a piece of a silk suture [47]. At first, this induces compensated hypertrophy of the heart, in many cases this entails a temporary enhancement of cardiac contractility. But during the further procedure, responding to the chronic hemodynamic overload, the hypertrophy becomes, as known in physiological setting, maladaptive. This leads to cardiac dilatation and heart failure [191, 82].

To get more valid data, datasets containing less than three replicates in each group or having no sham-operated control group were excluded. The appliance of these criteria led to two time series. One of them (GEO series number: GSE 5500) analyses gene expression during seven days after TAC and sham operation respectively. The other series (GEO series number: GSE 18224) exploited 9 weeks after TAC or rather sham operation.

GEO2R [12], a web application for identifying the diffence in gene expression, was used to analyze the two series. By applying the Benjamini and Hochberg correction (false discovery rate) all genes with an adjusted p-value less than 0.05 were considered [15].

8. Experimental

For further validation, especially of the in silico predicted time courses, in vitro experiments were executed by the group of Prof. Dr. Kristina Lorenz, Institut für Pharmakologie und Toxikologie der Universität Würzburg. The in silico model and the intial predicted time courses of the in silico model served as assistance to design the in vitro experiments.

It is accentuated, that the author did not perform the in vitro experiments by himself. Nevertheless, to underline the correctness of the computed results of an in silico model, experimental validation is necessary. For a good comprehension of the results described below, especially the comparison of in vitro and in silico modeling shown in Figure 12.1, the material and methods of the performed experiments are described in the following.

COS7 cells were transfected with plasmids encoding for M_2-muscarinic receptor as an example for a non-hypertrophic signal delivering receptor respectively with plasmids encoding for M_1-muscarinic receptor and EGFR (epidermal growth factor receptor) as examples for hypertrophic signal delivering receptors. COS7 cells are fibroblast-like cell lines derived from monkey kidney tissue used for production of recombinant proteins and to cultivate viruses [75]. In a next step the transfected cells were treated with their agonist, the M_2-muscarinic-transfected cells and M_1-muscarinic-receptor transfected cells with carbachol and the EGFR-transfected cells with epidermal growth factor. Then, antibodies against pERK(TEY) and pERK(Thr188) were given for immunoblotting.

In order to enumerate, following reagents were used and steps were done:

COS7 cells were maintained in Dulbecco's modified Eagle's medium supplemented with 10% (v/v) fetal calf serum, 100 U/ml penicillin, 100 µg/ml streptomycin and 2 mM L-glutamine at 37°C and 7% CO2, respectively. For transient expression in COS7 cells, cDNA constructs Flag-tagged murine ERK 2 was sub-cloned into pcDNA3 vector (Invitrogen). Plasmids encoding the human M_1- and M_2-muscarinic receptors from Missouri S&T cDNA Resource Center were used. Cells were transfected with indicated cDNAs (Flag-tagged wild-type ERK 2, M_1-muscarinic receptors, M_2-muscarinic receptors and/or EGFR) 18 hours after seeding using DEAE-

Dextran method. 36 hours after transfection the experiments were performed. Antibodies to ERK 1/2 (Cell Signaling, 9102), pERK 1/2(TEY) (Cell Signaling, 9101) and pERK1/2(Thr188) (IB – described in [133]) were used for immunoblotting. Immunoblot analyses were performed as described in [133]. Cells were lysed in ice-cold buffer (containing 0.5% (v/v) NP-40, 150 mM NaCl, 25 mM Na4P2O7, 50 mM β-glycerol phosphate disodium salt, 2 mM EDTA, 2 mM EGTA, 25 mM Tris (pH 8.0), 10% (v/v) glycerol, 50 mM NaF, 0.1 mM Na3VO4, 0.002% (w/v) NaN3), which was supplemented with protease inhibitors (10 µg/ml soybean trypsin inhibitor, 1 mM benzamidine, 1 mM phenylmethylsulfonyl fluoride). Before getting lysed, cells were stimulated with the indicated agonists for 5, 10 or 30 minutes. By densitometric analyses immunoblot signals were identified and signals were normalized to unstimulated controls. The analysis included only immunoblots with equal ERK loading.

The experiments itself were not performed by the author, but the analysis and especially comparison with the in silico model were executed by the author. Therefore, it is necessary to understand the exact terms and materials of the experiments.

Part III.

Results

9. A semi-quantitative dynamical model of ERK signaling

Cell Designer model

Figure 9.1 shows the network topology. There are all stimuli and proteins as well as activating/inhibiting reactions involved in the ERK-pathway in cardiomyocytes shown. Cytsosol and nucleus as compartments of the cell, which are relevant for the reproduction of the network are also shown. Cell Designer version 3.5.1. was used to draw the network.

A table with the references for each node and edge is shown in Table 9.1, the network in xml-format can be found in Appendix A.

Table 9.1.: Network assembly: Λ indicates the logical connection AND, $\rightarrow$ indicates activation and -I indicates inhibition.

node	*edge type*	*node*	*reference*	*Edge weight in SQUAD simulation*
angiotensin II	$\rightarrow$	G_q-coupled AT_1- receptor	[133]	5
carbachol	$\rightarrow$	G_i-coupled M_2-receptor	[133]	10
Epac	$\rightarrow$	PKC	[203]	10
ERK 1/2 dim 2P	$\rightarrow$	p90RSK	[133]	0,01
ERK 1/2 dim 2P	$\rightarrow$	p70S6K	[133]	0,01

continues on next page

Table 9.1.: Network assembly: Λ indicates the logical connection AND, → indicates activation and -I indicates inhibition.

node	*edge type*	*node*	*reference*	*Edge weight in SQUAD simulation*
ERK 1/2 dim 2P ⋀Gβγ	→	ERK 1/2 dim 3P	[133]	ERK 1/2 dim 2P –I AND: 100,00; AND –I ERK 1/2 dim 3P: 1,00; Gβγ → ERK 1/2 dim 3P: 100,00
ERK 1/2 dim 3P	→	Elk1	[133]	8
ERK 1/2 dim 3P	→	MSK1	[133]	7
ERK 1/2 dim 3P	→	c-Myc	[133]	6
G_i-coupled M_2-receptor	→	Ras (GTP bound)	[133]	10
G_i-coupled M_2-receptor	→	PKC	[106]	10
G_q-coupled AT_1- receptor	→	Gβγ	[133]	10
G_q-coupled AT_1- receptor	→	Ras (GTP bound)	[133]	1
G_q-coupled AT_1- receptor	→	PKC	[148]	10
GRK2	-I	G_s-coupled β1-adrenergic receptor	[242]	0,1
G_s-coupled β1-adrenergic receptor	→	Ras (GTP bound)	[229]	1

continues on next page

Table 9.1.: Network assembly: Λ indicates the logical connection AND, → indicates activation and -I indicates inhibition.

node	*edge type*	*node*	*reference*	*Edge weight in SQUAD simulation*
G_s-coupled β1-adrenergic receptor	→	Gβγ	[229]	10
G_s-coupled β1-adrenergic receptor	→	Epac	[203]	10
hypertrophic stimulus	→	angiotensin II	[133]	1
hypertrophic stimulus	→	isoproterenol	[229]	10
isoproterenol	→	G_s-coupled β1-adrenergic receptor	[229]	10
MEK 1/2	→	ERK 1/2 dim 2P	[133]	0,001
non-hypertrophic stimulus	→	carbachol	[133]	10
PKC	-I	RKIP	[131]	10
PKC	→	RKIP dim	[131]	10
Raf1	→	MEK 1/2	[133]	1
Ras (GTP bound)	→	Raf1	[133]	10
RKIP	-I	Raf1	[131]	0,01
RKIP dim	-I	GRK2	[131]	30

The signalling cascade in the presented model can be activated in two differing ways: Via carbachol and the G_i-coupled M_2-muscarinic receptor would be an example for a stimulus which induces no hypertrophy. Activation via angiotensin II and the AT_1-receptor or via isoproterenol and the SS_1-adrenergic receptor respectively represent hypertrophy-inducing stimuli. The backloops from stimulus to stimulating protein (carbachol/ angiotensin II/ isoproterenol) are artficial and had to be

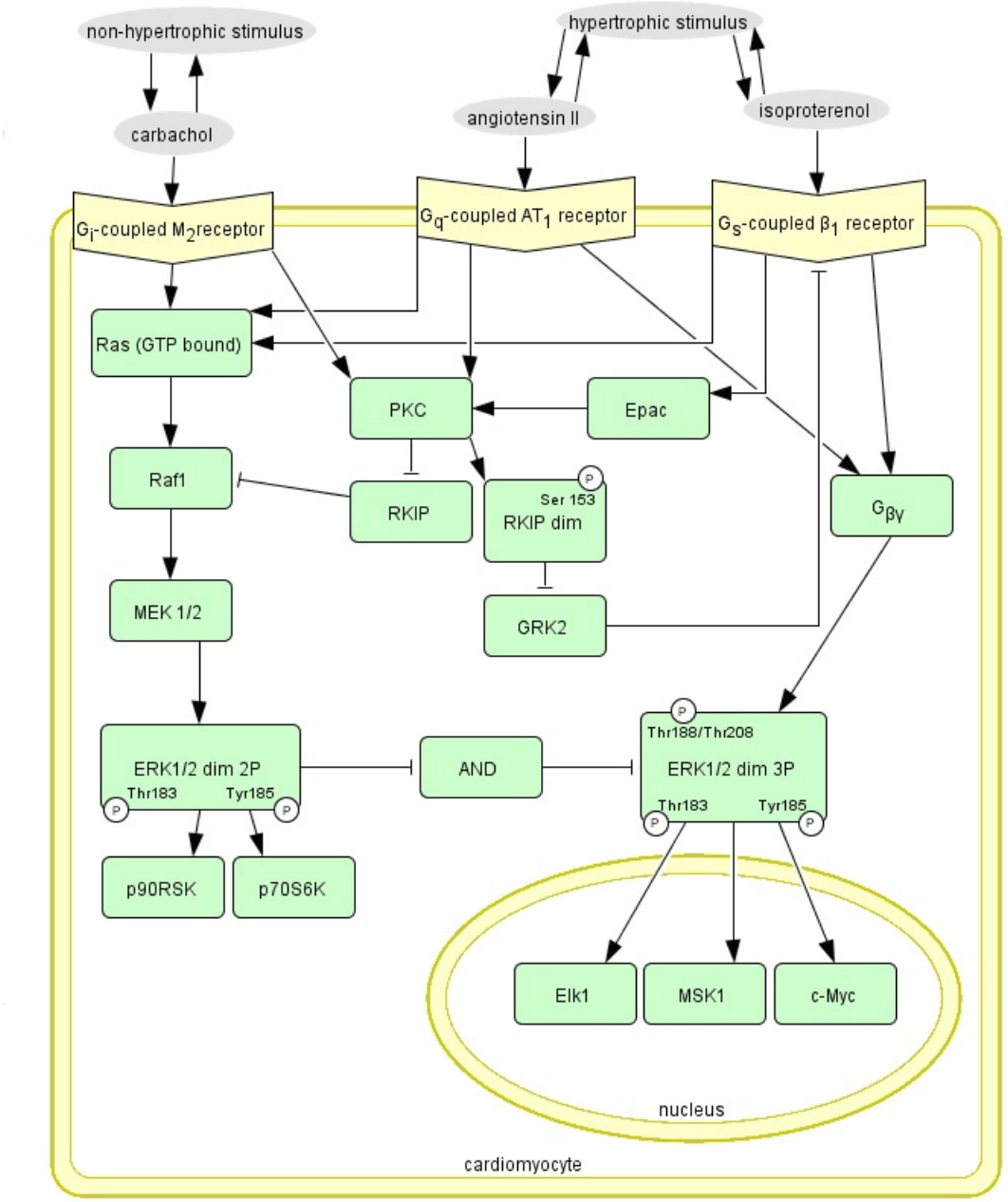

Figure 9.1.: Network topology Cell Designer: The oval shaped, grey coloured symbols indicate stimuli and the stimuli-transferring substances respectively. The v-shaped, yellow coloured symbols show receptors. The squared, green coloured symbols with rounded down angles symbolize proteins and in one case it stands for an artificial node as described below. If there are relevant phosphorylation sites, they are shown by a "P" in a small white circle at the border of the protein-symbol and the phosphorylated amino acid is named beneath the "P". An arrow headed line stands for activation, whereas a bar-headed line stands for inhibition. Furthermore, nucleus and cytosol as important compartments for the model are pictured.

implemented to get the model executable. The AT_1-receptor is a G_q-coupled receptor, whereas the β_1-adrenergic receptor is a G_s-coupled receptor. G-protein coupled receptors in general are receptors in the membrane of cells and endosomes, that practice signaltransmission in the internal of the cell or the endosome via binding of GTP-binding proteins [92]. They are distinguished depending on whether they bind G_s- G_i- or G_q- proteins [189].

After passing several intermediate steps as described in chapter 3 all stimuli lead to ERK 1/2 phosphorylation in the TEY motif at Tyrosin185 and Threonin183. Targets localised in the cytoplasm are phosphorylated by the non-hypertrophic as well as by the hypertrophic stimuli. In the model p90RSK, also known as MAPK-activated protein kinase-1, and P70S6K (Ribosomal protein S6 kinase beta-1) serve as examples. P90RSK supports cell survival, but can either mediate cell growth and proliferation [175, 68]. Without detection of the ecxact mechanism has yet been done, it is known that p90RSK is involved in the development of cancer [36]. After physical exercise, P70S6K participates in the activation of protein synthesis and thereby in the building of muscle [8, 145].

An additional phosphorylation of ERK 1/2 is resulting, when a hypertrophic stimulus is present: Thr208 in ERK1 and Thr188 in ERK2 become phosphorylated. This third phosphorylation is not mediated by the well established cAMP-dependent pathway downstream to activation by G-protein-coupled receptor, but rather by interaction of ERK 1/2 with $G_{\beta\gamma}$ subunits. In 2009 this was shown for G_q-coupled receptor, in 2012 for G_s -coupled receptors [229, 133]. Activation of ERK 1/2 in the TEY motif is necessary for the described interaction. In the presented model this is represented with the artifical node "AND" and two inhibitory edges: AND executes an inhibitory effect on ERK 1/2 dim 3P, when downstream to a non-hypertrophic stimulus ERK 1/2 dim 2P is activated, this inhibitory effect is abrogated because ERK 1/2 dim 2P itself has an inhibitory effect on AND. Nevertheless, in lack of $G_{\beta\gamma}$ beeing present ERK 1/2 dim 3P is not active. If only $G_{\beta\gamma}$ is present, but ERK 1/2 dim 2P is not active, the inhibitory effect of AND on ERK 1/2 dim 3P predominates, ERK 1/2 dim 3P is not activated. Only if both conditions (ERK 1/2 dim 2P activation and presence of $G_{\beta\gamma}$) apply following to a hypertrophic stimulus, ERK 1/2 dim 3P gets phosphorylated and thereby activated. This corresponds to the in vitro found situation.

The now at three sites phoyphorylated ERK (Thr183, Tyr185 and Thr188 in ERK2; respectively Thr183, Tyr185 and Thr208 in ERK1) is then transported to the nucleus where it phosphorylates further targets, which overall lead to hypertrophy. Elk1, c-Myc and MSK1 are identified nuclear targets down to the present

day [134, 133]. Elk1 is a transcription factor, which mediates transcription of diverse proteins. Thereby it takes place in growth signalling and influences calcium metabolism [219, 93]. c-Myc, a well investigated proto-oncogen, typically raises the expression of nearly any type of gene [64]. Within the framework of heart failure, c-Myc expression is up-regulated in response to hypertrophic stimuli (see also Figure 11.1) [181]. Post-mitotic cardiomyocytes are capacitated by c-Myc to reenter the cell cycle. Furthermore, c-Myc increases gene expression of several genes involved in cardiac hypertrophy. Protein synthesis is raised and cell mass is heightened by c-Myc [240]. MSK1 (Mitogen- and stress-activated protein kinase-1) as an AGC kinase of the RSK family is a cytoplasmic serine/threonine kinase involved in stress activated MAPK cascade signaling, EGFR pathway, inflammation via the NF-$\varkappa$B transcription factor and histone modification [210, 46, 35, 228]. ACG kinases in gerneral are kinases regulated by secondary messengers such as cyclic AMP (PKA) or lipids (PKC).

The group of Prof. Dr. Kristina Lorenz, Institut für Pharmakologie und Toxikologie der Universität Würzburg, identified an important feedback loop involving RKIP, Raf1, PKC and GRK2 and taking part in the ERK 1/2 pathway.

GRK2 induces desensitization of G-protein-coupled receptors in general, in our model for example, this would be the the β1-adrenergic receptor. Potentially, GRK2 inhibits further receptor signalling in our model, namely this of M_2-muscarinic receptor and AT_1- receptor [59].

Under standard conditions, RKIP inhibits Raf1 by phosphorylation [132]. But the activation of PKC leads to phosphorylation and in turn dimerization of RKIP, which induces a target switch from Raf1 to GRK2. This leads to an inhibition of GRK2.

The result of those two effects is a double amplification of the signal coming in: It takes the inhibitor of Raf1 off and stopps the inhibition of the activating receptors in our model (β1-adrenergic receptor and probably also M_2-muscarinic receptor and AT_1- receptor [131]. PKC by itself is activated via carbachol (non-hypertrophic stimulus) as well as angiotensin II (hypertrophic stimulus) as well as isoproterenol via Epac.

These multiple associated proteins and interactions were incorporated in Figure 9.1 for the setting of the structure of the network. The underlying Boolean logic, meaning activation versus inhibition, was also considered.

The receptors and their agonists in the model stand as examples for hypertrophic or nonhypertrophic pathway. Beyond the M_2-muscarinic receptor, β1-adrenergic receptor and AT_1- receptor receptor are a few more receptors and their agonists well-

receptor	*receptor type*	*agonist/s (a selection)*	*effect*	*reference*
AT_1- receptor	G_q-coupled receptor	AT II	hypertrophic pathway (shown in Figure 9.1)	[133]
M_1-muscarinic receptor	G_q-coupled receptor	acetylcholine	hypertrophic pathway (shown in Figure 12.1)	[133, 25]
M_2-muscarinic receptor	G_i-coupled receptor	carbachol	nonhypertrophic pathway (shown in Figure 9.1 and Figure 12.1)	[133, 25]
Epidermal-growth-factor receptor = ErbB1-receptor	receptor tyrosine kinase (ErbB family of receptors)	epidermal growth factor	hypertrophic pathway (shown in Figure 12.1)	[25]
ErbB2-receptor = Her2neu-receptor	receptor tyrosine kinase (ErbB family of receptors)	neuregulin1-β1	hypertrophic pathway	[133]
α1-adrenergic receptor	G_q-coupled receptor	phenylephrin 1A	hypertrophic pathway	[133, 229]
α2A-adrenergic receptor	G_i-coupled receptor	adrenalin	nonhypertrophic pathway	[133]
β1-adrenergic receptor	G_s-coupled receptor	isoproterenol, dobutamine	hypertrophic pathway (shown in Figure 9.1)	[229]

Table 9.2.: Receptor, receptor type, agonists, affected pathways and validation references

established and investigated to effect one of the two pathways. Table 9.2 shows the different receptors, effected pathways, their physiological relevance and validation references. There is either preference for non-hypertrophic, mitogenic signals or preference for hypertrophic signals. In general one could suppose, that G_q-, G_i- and ErbB-coupled receptors belong to the hypertrophic family of receptors, whereas G_s-coupled receptors rather stimulate the non-hypertrophic pathway.

SQUAD simulation

The software SQUAD (standardized quantitative dynamics [49]) was used for dynamic simulations and the identification of steady states. By using different exponential functions, the software generates cellular states between no activation and full activation, even in lack of precise informations about the underlying kinetic. Thereby it combines discrete and continuous modeling techniques as described above. In the presented network, the calculation is made for all nodes: the directly affected receptors (G_i-coupled M_2-muscarinic receptor, G_q-coupled AT_1- receptor, G_s-coupled β1-adrenergic receptor) as well as all subsequent network nodes and their resulting activation levels.

In vitro and vivo, a target can react more or less powerful to an incoming signal. This can be reflected in weighting the edges in an in silico model. To produce operability of the model and to reflect the in vitro experiments in COS7 cells as mentioned below in chapter 12 a few modifications had to be made in weighting the edges: For instance the ERK 1/2 dim 2P-AND-edge had to be set quite high, whereas the MEK1/2-ERK 1/2 dim 2P-edge had to bet set quite low. This adjustments are done in a trial and error manner, especially for precise adjustment to the in vitro found time courses in COS7 cells. For all exact values see Table 9.1 and Appendix A.

Beyond adjustment of the weight of edges SQUAD allows the modification of various parameters as described in chapter 5, but only the weight of some edges had to be modificated to produce operability and to resemble the situation observed in the COS7 cell experiments (shown in Figure 12.1).

Western blot/ line graph

The following data show the calculation and comparison of the network responses for stimulation of the ERK pathway by a non-hypertrophic stimulus (carbachol via the M_2-receptor) and two hypertrophic stimuli (angiotensin II via the AT_1- receptor and isoproterenol via the β1-adrenergic receptor). Upon entering a stimulus, the software environment computes the resulting activation for all subsequent nodes. Thereby it allows an accurate modelling of time courses and activation levels of nodes (usually standing for proteins) in the hypertrophic and non hypertrophic cascade of the cardiomyocyte.

Several graphic forms of presentation of the deliverables are available. Figure 9.2 presents the results of the network as a virtual Western blot whereas Figure 9.3 presents the results as a line graph.

In a Virtual Western blot concentration predictions for network nodes are com-

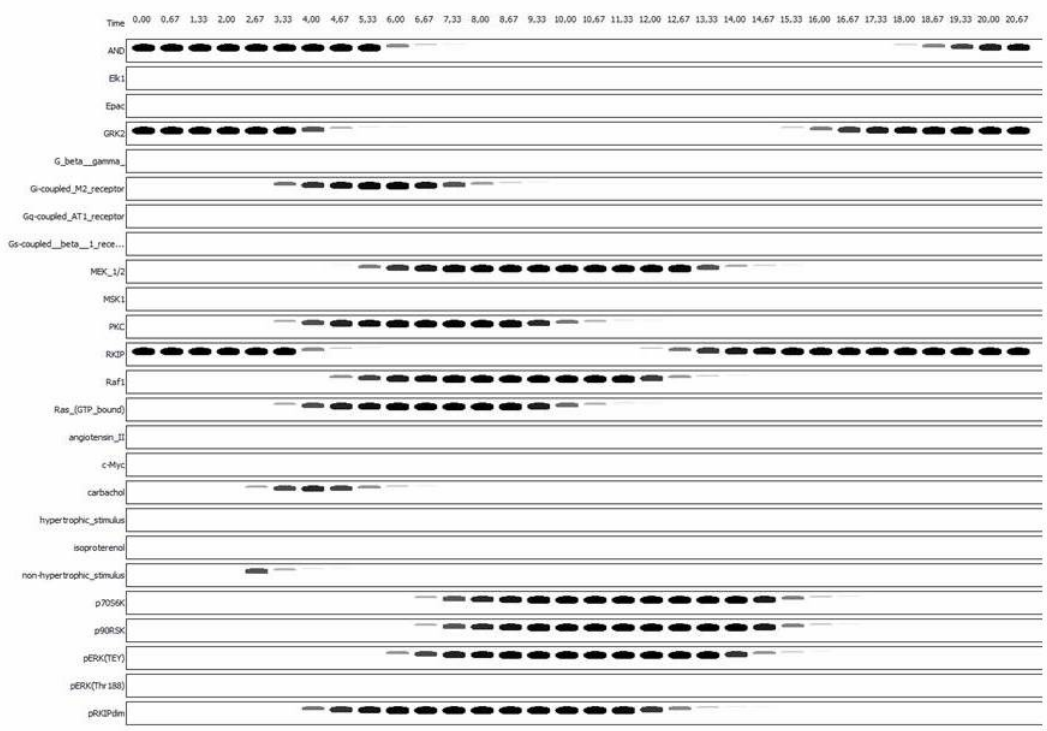

(a) Virtual Western blot which shows simulation of ERK-pathway after a non-hypertrophic stimulus: Each column shows a node, concentration predictions (and thereby activation levels) are applied on a time line. Deep dark blots stand for high concentrations, whereas greyish color notes indicate lower concentrations corrsponding to their intensity.

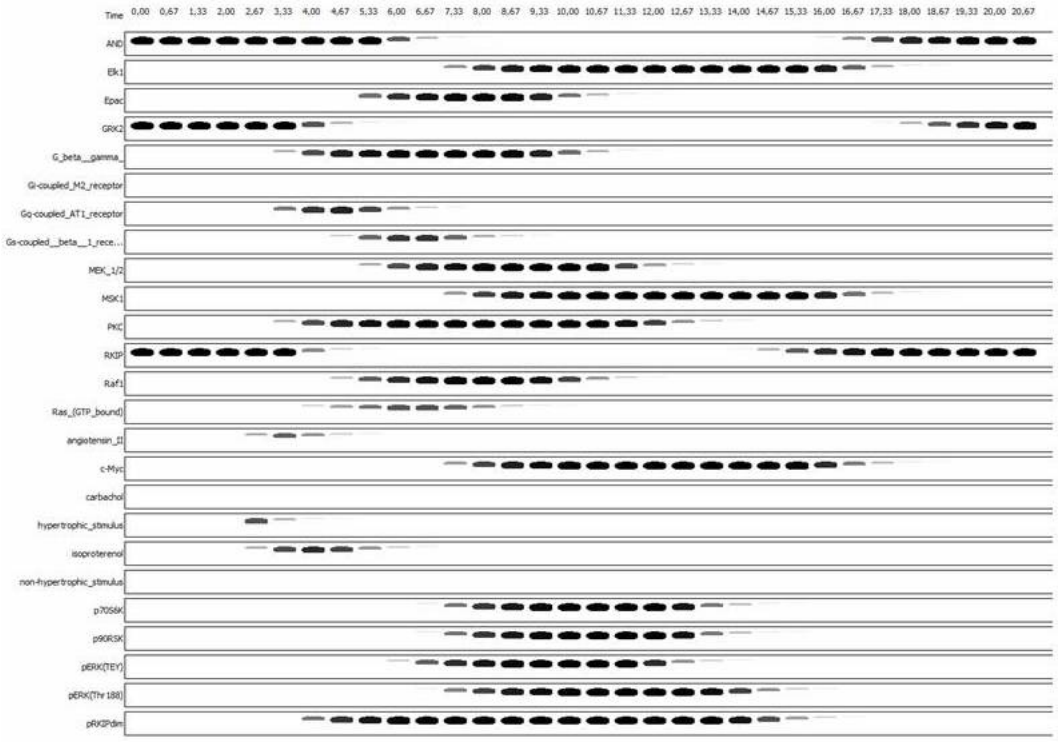

(b) Virtual Western blot which shows simulation of ERK-pathway after an hypertrophic stimulus

Figure 9.2.: SQUAD simulations

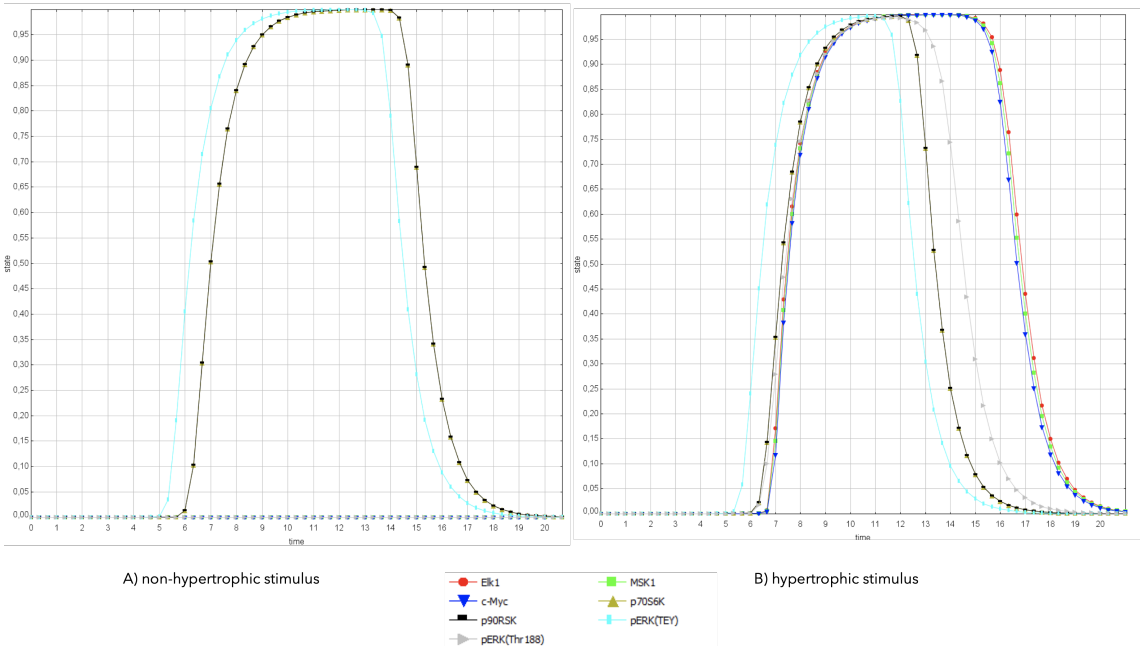

Figure 9.3.: SQUAD readout as a line graph: Time on horizontal axis is plotted versus state (activation level) on vertical axis. For clear arrangement relevant nodes (different phosphorylation states of ERK and targets of ERK) were chosen. Maximum value of state is 1, indicating a high activation level, minimum value is 0, indicating a low activation level. Several nodes of the model were chosen. A) shows the readouts after a non-hypertrophic stimulus, B) shows the readouts after an hypertrophic stimulus.

puted over a time lapse. A high concentration prediction indicates a high activation level, whereas a low concentration prediction indicates no activation. In the Virtual Western blot showing simulation of ERK-pathway after a non-hypertrophic stimulus (Figure 9.2 (a)) ERK becomes phosphorylated twice (on Thr183 and Tyr185 in the TEY-motif, represented as pERK(TEY)), ERK is localized in the cytoplasm and phosphorylates cytosolic targets (particularly p90RSK, p70S6k). There are no blots detectable in the columns of the nucleosolic targets Elk1, MSK1 and c-Myc.

In the Virtual Western blot showing simulation of ERK-pathway after a hypertrophic stimulus (Figure 9.2 (b)) ERK becomes additionally phosphorylated on a third position (ERK 2 at Thr188 or ERK 1 at Thr208, shown as pERK(Thr188). As a result ERK is relocated to the nucleus where it phosphorylates additional nucleosolic targets (particularly Elk1, MSK1, c-Myc). Concluding all targets of ERK (cytosolic as well as nucleosolic) show high activation levels.

The line graph (Figure 9.3) demonstrates the chronological connection well: In presence of a non-hypertrophic stimulus, firstly the double-phosphorylated ERK (pERK(TEY)) reaches a high activation level, then the cytosolic targets (p90RSK and p70S6K) reach high activation levels. Both lines are overlapping in the graph and thereby it is only one line visible. In presence of a hypertrophic stimulus, after activating the cytosolic targets, ERK becomes phosphorylated additionally in third position, pERK(Thr188) reaches high activation levels, and in series the nucleosolic targets become activated. Since ERK has to switch the cell compartement (cytosol to nucleus) before activating the nucleosolic targets, the time elapsing between activation of pEKR(Thr188) and activating its nucleosolic targets versus activation of pERK(TEY) and activating its cytoslic targets is significantly larger.

Steady states

Another interesting question are the steady states of the simulation. Commonly, a steady state is a mode, where variables stay fixed as time proceeds, a flux balance is existing.

SQUAD can be used to identify steady states. It uses a Boolean modelling technique to describe all the steady states of a network only based on the topology, without having kinetic data [49]. SQUAD systematically samples all the systems states by an intelligent heuristic, more precisely using a Reduced Order Binary Decision Diagram algorithm [72]. Each of the N modelled nodes can either be ON, OFF or intermediate (state 1, state 0, 0<state>1) as described above. The outcome of this are more than 2^Npossible combinations. SQUAD checks all these combinations to find out the stable ones.

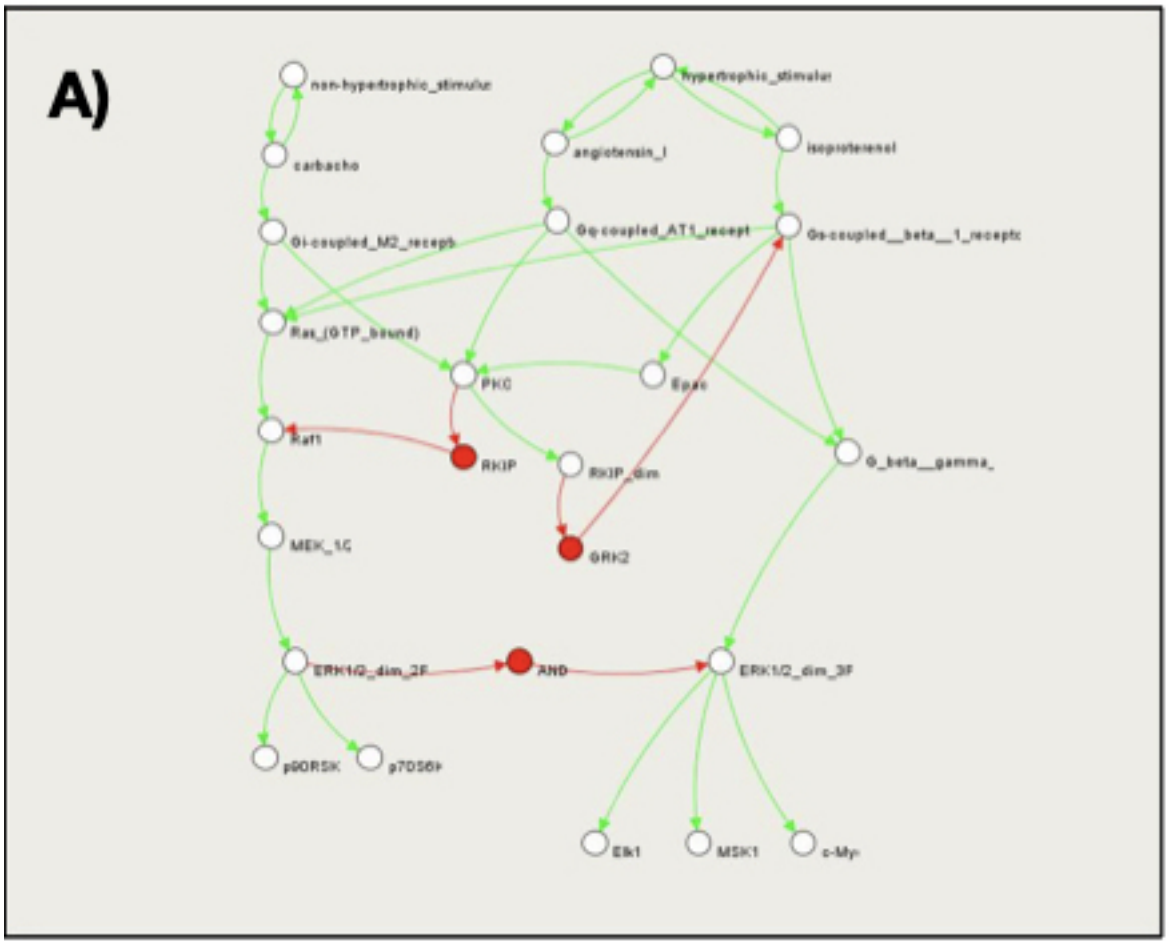

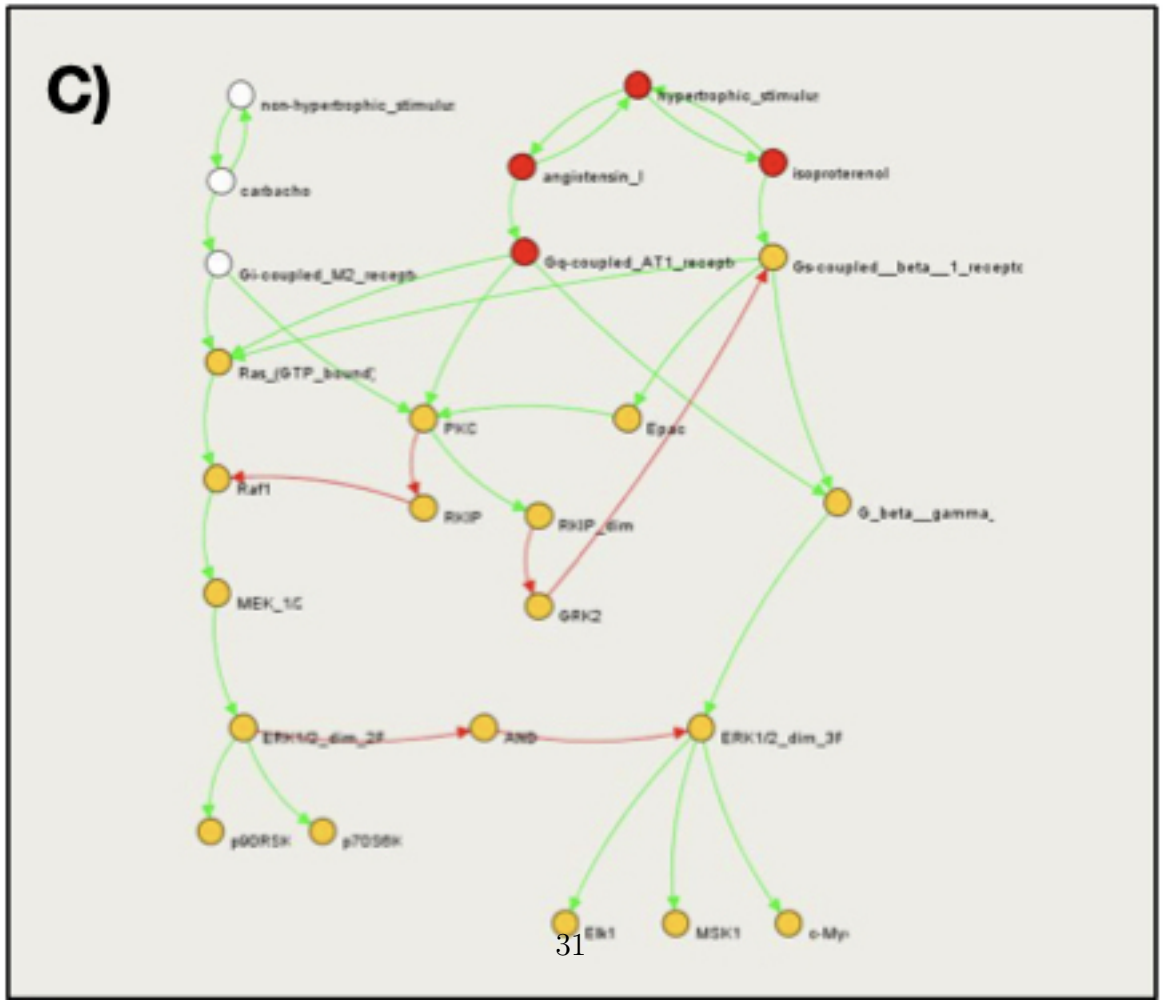

Figure 9.4 : Steady states: A white dot indicates inactivation (state = 0), a red dot

Basically, there are four system states to be considered: Firstly, there is full activation of either the non-hypertrophic or secondly the hypertrophic cascade. Thirdly, there is no activation. The fourth potentially steady state is when the non-hypertrophic as well as the hypertrophic stimulus are active (in vivo this would be a strong stress stimulus affecting the cardiomyocyte). PKC is activated, at least partially in the three active cases and promotes the RKIP switch from Raf1 to GRK2.

In the presented CellDesigner model there are backward activations from carbachol, angiotensin II and isoproterenol to either the non-hypertrophic or rather the hypertrophic stimulus integrated.

Without having the backward activation from carbachol, angiotensin II and isoproterenol to their corresponding stimulus, SQUAD simulation only shows one steady state for the cardiac hypertrophy network (basal conditions, RKIP is completely active and inhibits Raf1). For the three other steady states, these self-enforcing loops are necessary. Otherwise, a single hyper- or non-hypertrophic pulse would turn the system into a hypertrophic steady state. This does not correlate to the situation observed in the experiments in COS7 cells, and therefore, it has to be decided to integrate these self-enforcing loops.

For the presented network with self-enforcing loops, four steady states are computed. Figure 9.4 shows these four steady states. In Figure 9.4 A) no stimulus is active, RKIP, GRK2 and the artificial node AND reach full activation, whereas all other nodes are completely inactive. Figure 9.4 B) shows the steady state, when a non-hypertrophic stimulus is active. Carbachol and the M_2-muscarinic receptor reach full activation, whereas the downstream nodes including the cytosolic targets of pERK(TEY) reach partial activation. pERK(Thr188) and the nucleosolic targets stay inactive. The M_2-muscarinic receptor activates PKC and RKIP switches its target in parts from Raf1 to GRK2, but yet there is no feedback mechanism computed, because it is only a guess, that GRK2 could also intensify the signal of M_2-muscarinic receptor, but it is not proven so far, and therefore it is not modelled. Figure 9.4 C) shows the steady state, when a hypertrophic stimulus is present. Angiotensin II, isoproterenol and the AT_1- receptor are fully active, all downstream targets including the cytosolic as well as the nucleosolic targets of pERK(TEY) and pERK(Thr188) are partially active. Because all three receptors activate PKC and the M_2-muscarinic receptor is not active, furthermore RKIP performs no full target switch from Raf1 to GRK2 and thereby, the β1-adrenergic receptor is not fully active, because it is still partially inhibited from GRK2. Figure 9.4 D) shows the steady state, when both stimuli, the hypertrophic and the non-hypertrophic stimuli,

		hypertrophic stimulus	*non-hypertrophic stimulus*
with feedback-loop	constant pulse	0,27	0,29
	single pulse	0,32	0,4
without feedback loop	constant pulse	0,24	0,27
	single pulse	0,32	0,4

Table 9.3.: Thresholds for downstream-target activation

are present. All downstream nodes including the cytosolic as well as the nucleosolic targets of pERK(TEY) and pERK(Thr188) reach full activation. RKIP performs a complete target switch, GRK2 is completely inactivated and thereby the inhibition of β1-adrenergic receptor is completely abrogated. The above described feedback mechanism is fully active.

In general, these four computed steady states depict the situation in vivo well. With regard to the feedback loop, and especially that there is only a full target switch when both stimuli are present, there is yet no in vivo or in vitro data. But presumably, the computed situation is similar to an in vitro or in vivo situation and could be target of further research.

Thresholds

Thresholds for the activation of the downstream targets of pERK(TEY) and pERK(Thr188) were also computed. This means, the strength of the incoming signal that is necessary to activate the downstream targets were computed. This was done for the non-hypertrophic as well as the hypertrophic stimulus, and for a single-pulse as well as a constant pulse. Also, the situation was computed with and without the feedback-loop via RKIP. The examinations can be found in Table 9.3

In each setting, the threshold for a single pulse was higher then the one for a constant pulse. This goes along with the situation found in vivo, usually a single pulse has less effect than a constant pulse with the same strength. This could be, besides the third phosphorylation of ERK, another turning point in the switch from a physiological to a maladaptive answer in the cardiomyocyte.

The comparison between the cascade with and without the feedback loop is only a theoretical experiment, because in vivo the feedback mechanism is always present and yet there is no manner investigated to block this whole mechanism. The required strength of a single pulse stays uneffected by computing the threshold without the feedback loop. The required strength for a constant pulse is less for the hypertrophic as well as the non-hypertrophic stimulus, when the cascade is computed without the

feedback loop. At first glance, this stands in contrast to the above described double-signal-amplificational effect of the target switch from RKIP from Raf1 to GRK2. To be specific, one could suppose that signal amplification means a lower required signal strength to get the downstream targets activated.

But different reasons are thinkable and have to be considered in this case: Firstly, as described above, it is proven, that all three receptors (M_2-muscarinic receptor, AT_1- receptor and β1-adrenergic receptor) activate PKC and thereby enable the target switch from RKIP. But yet it is an assumption, that GRK2 in turn inhibits all three receptors when activated, but this is only proven for the beta1 receptor and thereby only modelled for this receptor. So this could be an improvement for the model after further investigation for a more accurate representation of the situation found in vivo. Secondly, it is thinkable, that signal amplification rather means a lower threshold for activation, but a longer lasting answer to a stimulus.

CNA simulation

CNA topology

CNA [107, 109] was alternatively used to modelize the cascade to examine the same network with another software. CNA was used because it advantageously allows the different implementation of the dynamic interpolation between node states.

As described in chapter 5, the nodes in CNA simualtions can not only reach the state entirely ON or OFF as common Booelan models, but also intermediate states. But in contrast to SQUAD simulations, they can not reach mutliple states, but rather predefined states, the CNA simulation is not infinitely variable. The network topology is shown in Figure 9.5. It is similar to the introduced, with CellDesigner created topology for SQUAD simulations, but there are a few differences. With CNA, each node and interaction has to be defined with an Boolean logic, the artificial node AND is thereby not necessary in contrast to SQUAD. The backward activation from carbachol, angiotensin II and isoproterenol to their corresponding stimulus is also not necessary in CNA simulation.

Figure 9.5 provides the CNA network topology, a special focus is set on the feedback loops.

A reaction can be defined with the logical operators AND or NOT. A + indicates an AND, whereas a prefixed ! indicates a NOT. For example $A + B = C$ means, if A and B are active, C becomes activated. $A+!B + C = D$ means, if A and C are active and B is not active, D becomes activated.

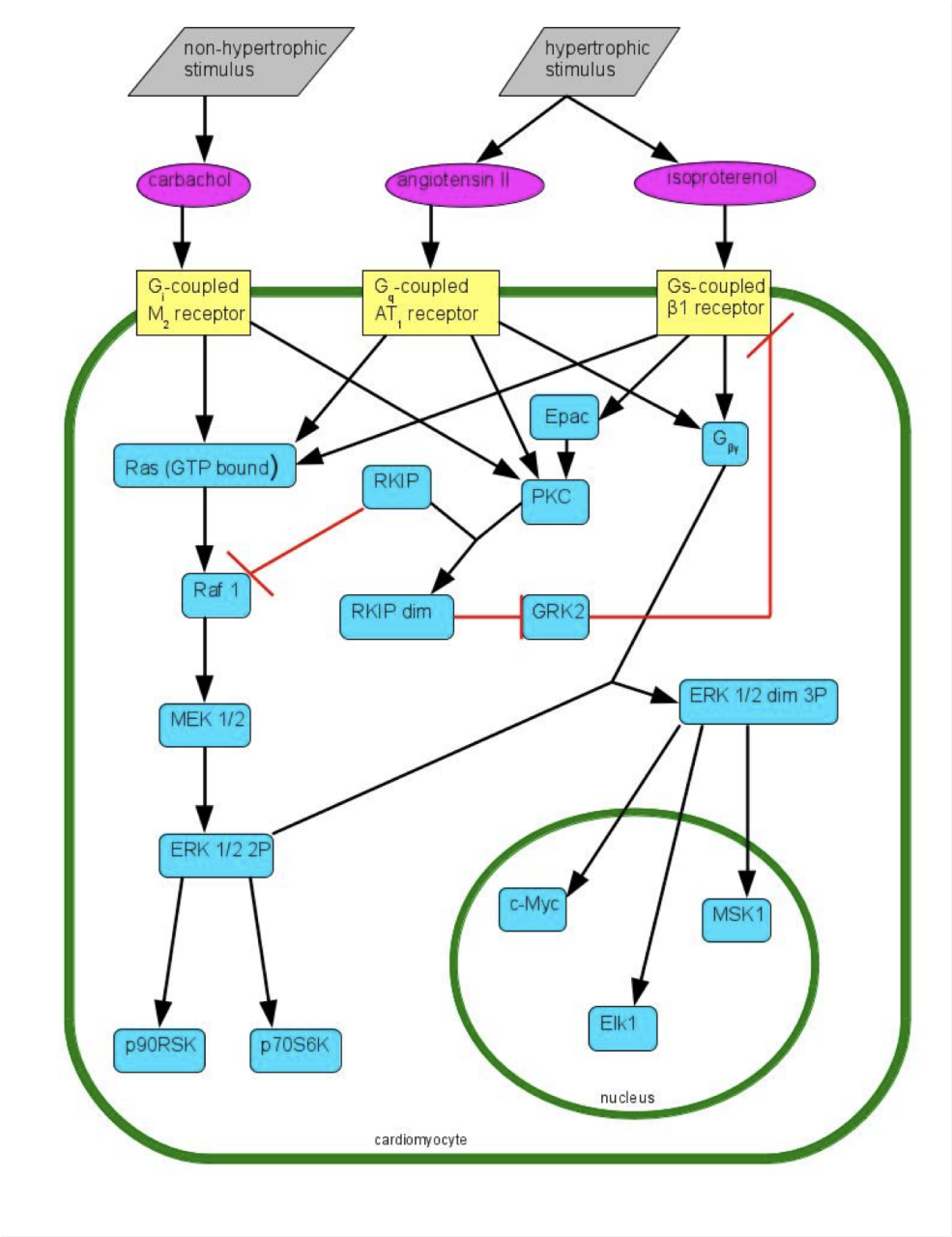

Figure 9.5.: CNA topology: The grey colored rhombs show the two different stimuli. The oval shaped magenta colored symbols indicate the stimuli transferring substances. The squared, yellow colored symbols show the three different receptors. The squared, blue coloured symbols with rounded down angles symbolize the proteins taking part downstream receptor activation. An arrow headed line (in black) stands for activation, whereas an bar-headed line (in red) stands for inhibition. If an activating edge has two starting points, both are necessary for activation of the target. Nucleus and cytosol as fundamental compartments for the model are illustrated also.

Various discrete activation levels can be defined. In the instant case, this was important because the aim was to investigate different levels of activation of hypertrophic or non-hypertrophic stimulating pathways. For the presented network, the state 0, 1 and 2 were defined. 0 stands for no activation, 1 for a weak activation level and 2 for a high activation level of the hypertrophic and non-hypertrophic pathways. There are only the three described activation levels and no intermediate states.

CNA simulation

In contrast to the continuous model technique via SQUAD, the discrete simulation model technique via CNA allows a more convenient analysis of feedback loops. This concerns the feedback loops via RKIP, Raf1 and GRK2 basically. RKIP becomes phosphorylated via PKC after activation of PKC via all three receptors in the model, RKIP then forms a homo-dimer. In turn, instead of Raf1 before forming the dimer, the RKIP dimer inhibits GRK2. This switch leads to signal amplification in two ways: GRK2 does not inhibit its target receptor anymore and Raf1 is not inhibited anymore, it does not weaken the downstream signals anymore.

In CNA simulation, both signals (hypertrophic and non-hypertrophic signal) as well as a combination of both can be modelled. Moreover, a situation where isolated edges or nodes are deactivated can be modelled. On the one hand, this can serve to illustrate the effect of a situation found in vitro, for instance a feedback loop. On the other hand, it can serve to disclose potential pharmaceutical points of contact.

If there is a hypertrophic stimulus as shown in Figure 9.6, both the non-hypertrophic (namely p90RSK and p70S6K) and the hypertrophic (namely c-Myc, Elk1 and MSK1) targets reach activation level 2. PKC phosphorylates RKIP, which then builds a dimer. Under basic conditions, RKIP is active and reaches level 1, now it reaches level 0. In turn, instead of Raf1 before dimerization, GRK2 becomes inhibited by the now dimerized RKIP and GRK2 reaches level 0. A bifocal signal amplification as described above results: Firstly, GRK2 does not inhibit its target receptors (G_s-coupled β1-adrenergic receptor in the simulation) anymore and secondly, Raf1 is fully active (value 2) because it is not inhibited furthermore.

When there is no stimulus, as shown in Figure 9.7 the cytosolic as well as nucleosolic targets are not activated (level 0 = basal conditions). RKIP inhibits Raf1, RKIPdim is not built because PKC is not activated and GRK2 inhibits its target (Gs-coupled beta 1 receptor) because it is not inhibited by RKIPdim.

In case there is a non-hypertrophic stimulus as shown in Figure 9.8 only the cytosolic, non-hypertrophic targets reach level 2. The nucleosolic targets possess the value 0. They are not activated. PKC is activated, so that RKIP builds a

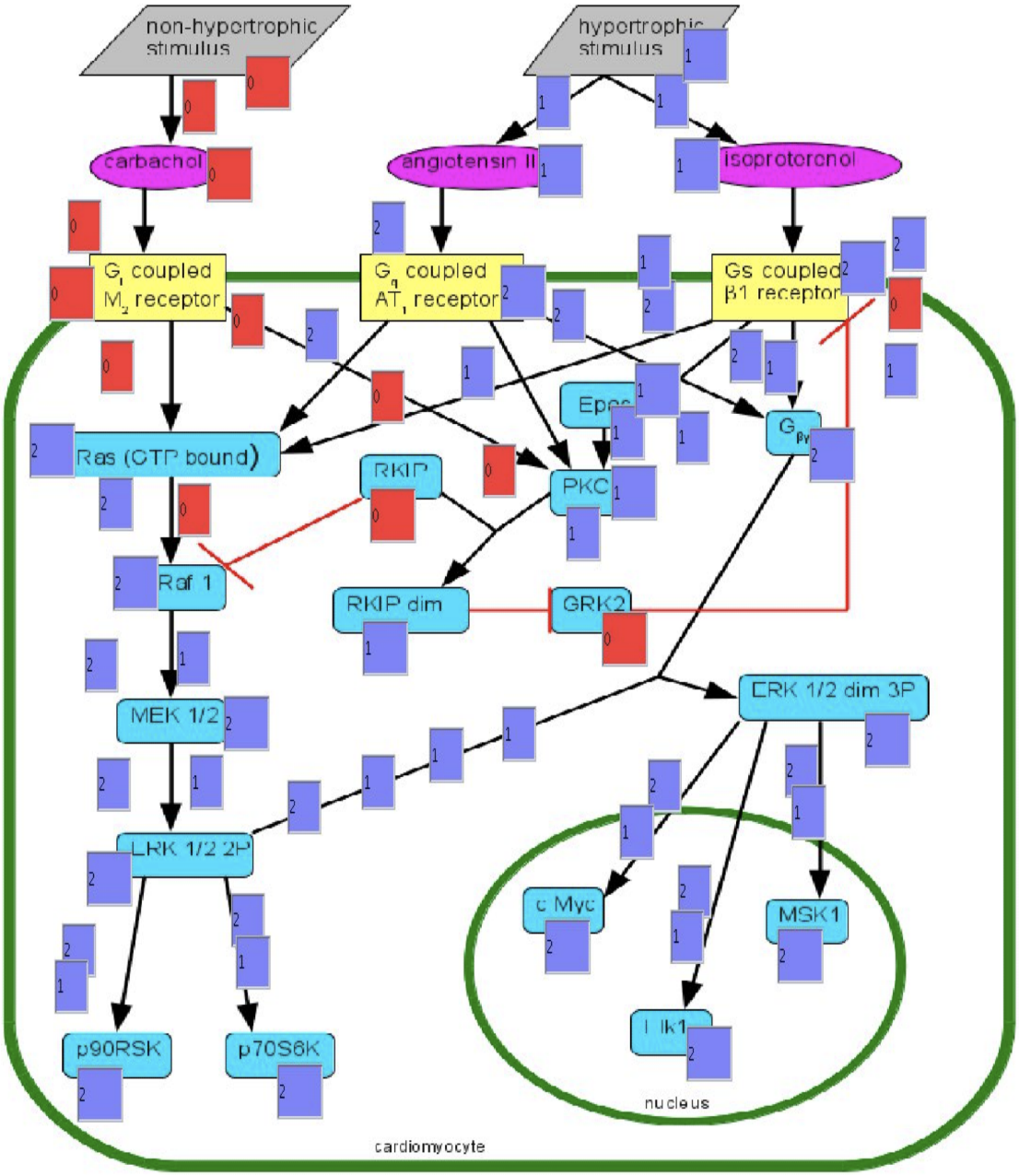

Figure 9.6.: CNA simulation: hypertrophic stimulusThe small squares represent values of nodes and edges. A red square indicates the level 0, whereas a violet square indicates values < 0 until 2. All downstream targets reach high activation levels (value 2). RKIP inhibits GRK2.

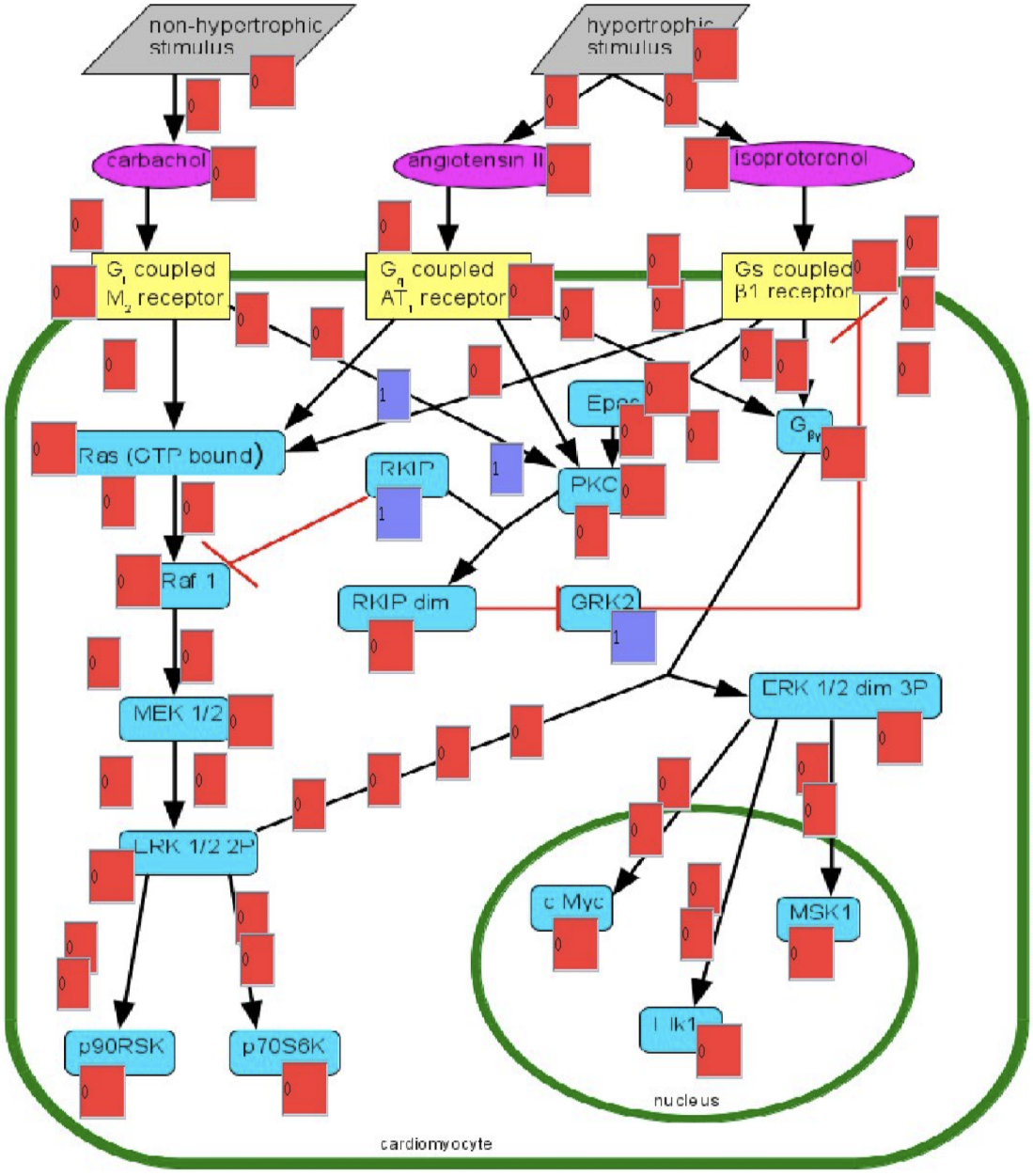

Figure 9.7.: CNA simulation: no stimulusAll downstream targets show the value 0 if there is no stimulus. RKIP inhibits Raf1.

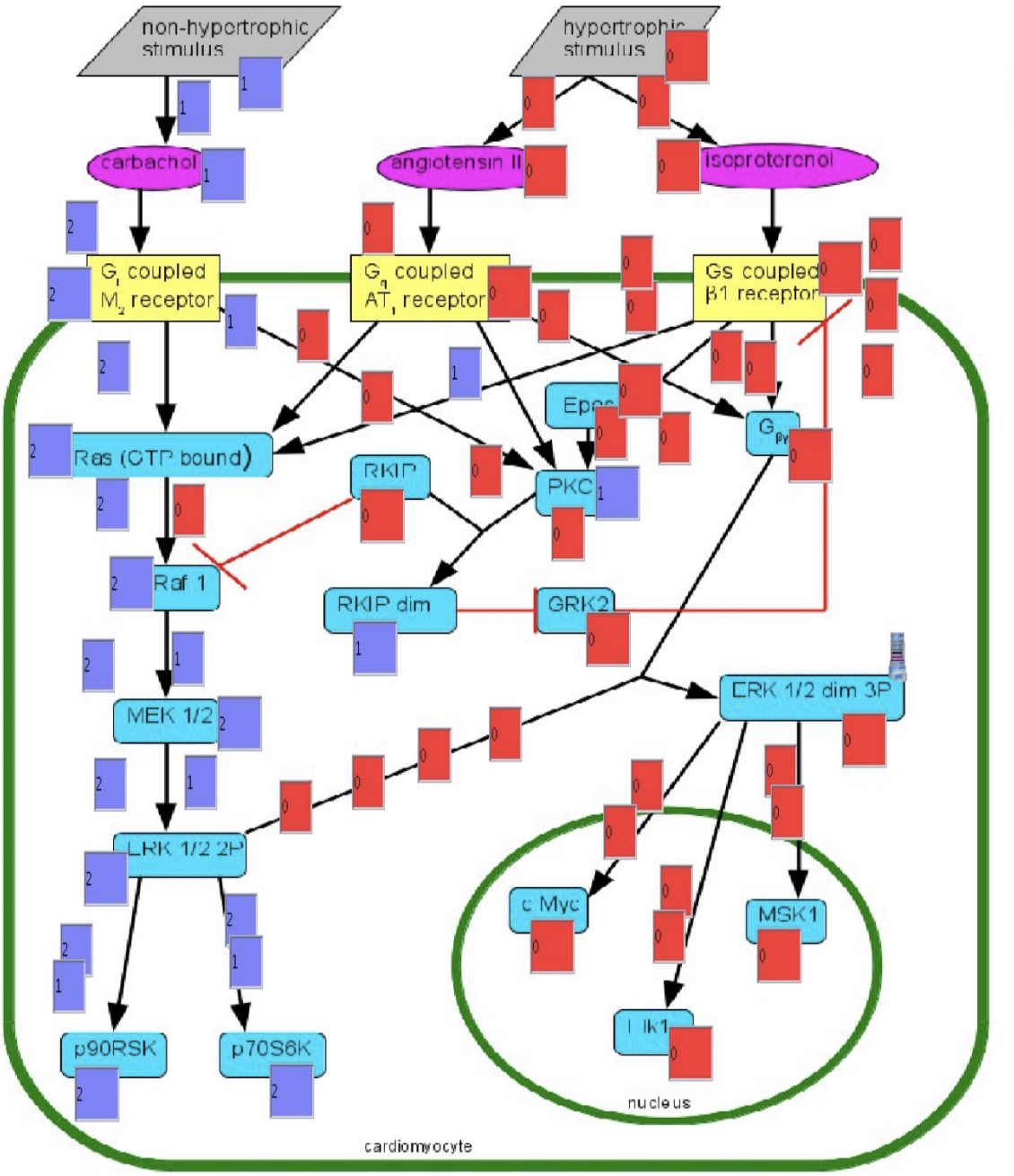

Figure 9.8.: CNA simulation: non-hypertrophic stimulus: The cytosolic targets become fully activated (level 2). RKIP inhibits GRK2.

dimer and provides its target switch: Raf1 is not inhibited through RKIP anymore, whereas now GRK2 is inhibited by RKIPdim. Its target G_s-coupled β1-adrenergic receptor is not inhibited anymore by GRK2. In the present case, this takes no effect on the cascade, but as described above, GRK2 probably also inhibits other receptors, but this is only to be suggested and has to be proven in further experiments. In case GRK2 would effect G_i-coupled M_2-receptor as well as the G_s-coupled β1-adrenergic receptor, it would lead to an intensification of the signals by taking off the inhibitory effect.

The situation when both stimuli are present was modelled with the involved feedback loops, which reflects the situation found in vitro. Furthermore, as an example of a blockade of a connection, the situation without RKIP loosing its inhibitory effect of Raf1 was modelled.

Figure 9.9 shows a simulation when both stimuli are present and the feedback loops are active. PKC inhibits RKIP, so that Raf1 is not inhibited anymore. GRK2 is inhibited by RKIPdim and loses its inhibitory effect on G_s-coupled β1-adrenergic receptor. The described amplification of the signals results. Both, the hypertrophic as well as the non-hypertrophic targets are strongly activated (level 2).

Figure 9.10 shows a simulation, when both stimuli are given, but the inhibitory effect from RKIP to Raf1 persists. Raf1 weakens the signal on its downstream targets. The activation levels of the hypertrophic and the non-hypertrophic targets merely reach a weak activation level (level 1). There is no signal amplification.

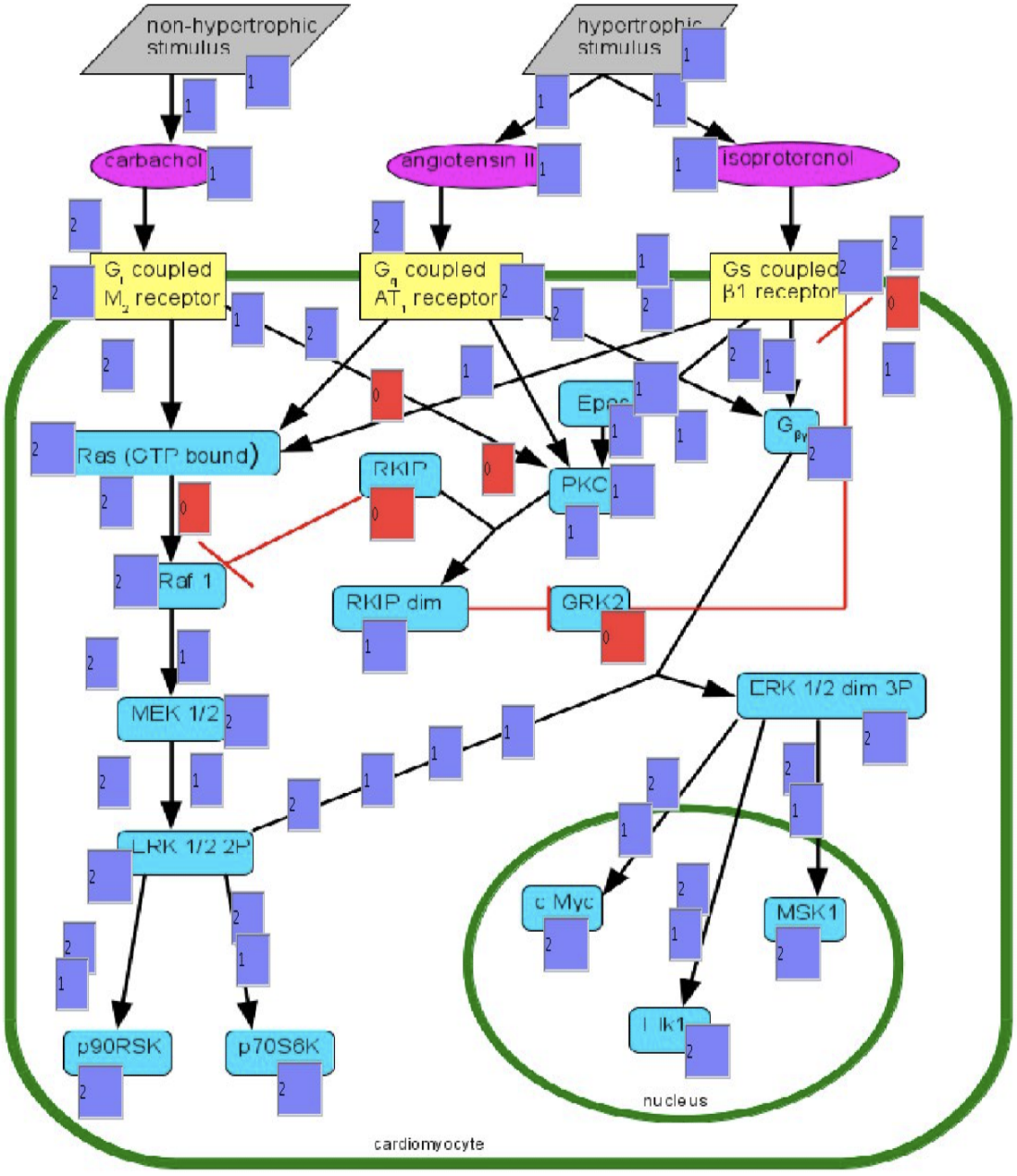

Figure 9.9.: CNA simulation: both stimuli with feedback loopsAll downstream targets reach high activation levels (value 2). RKIP inhibits GRK2. Raf1 is not inhibited.

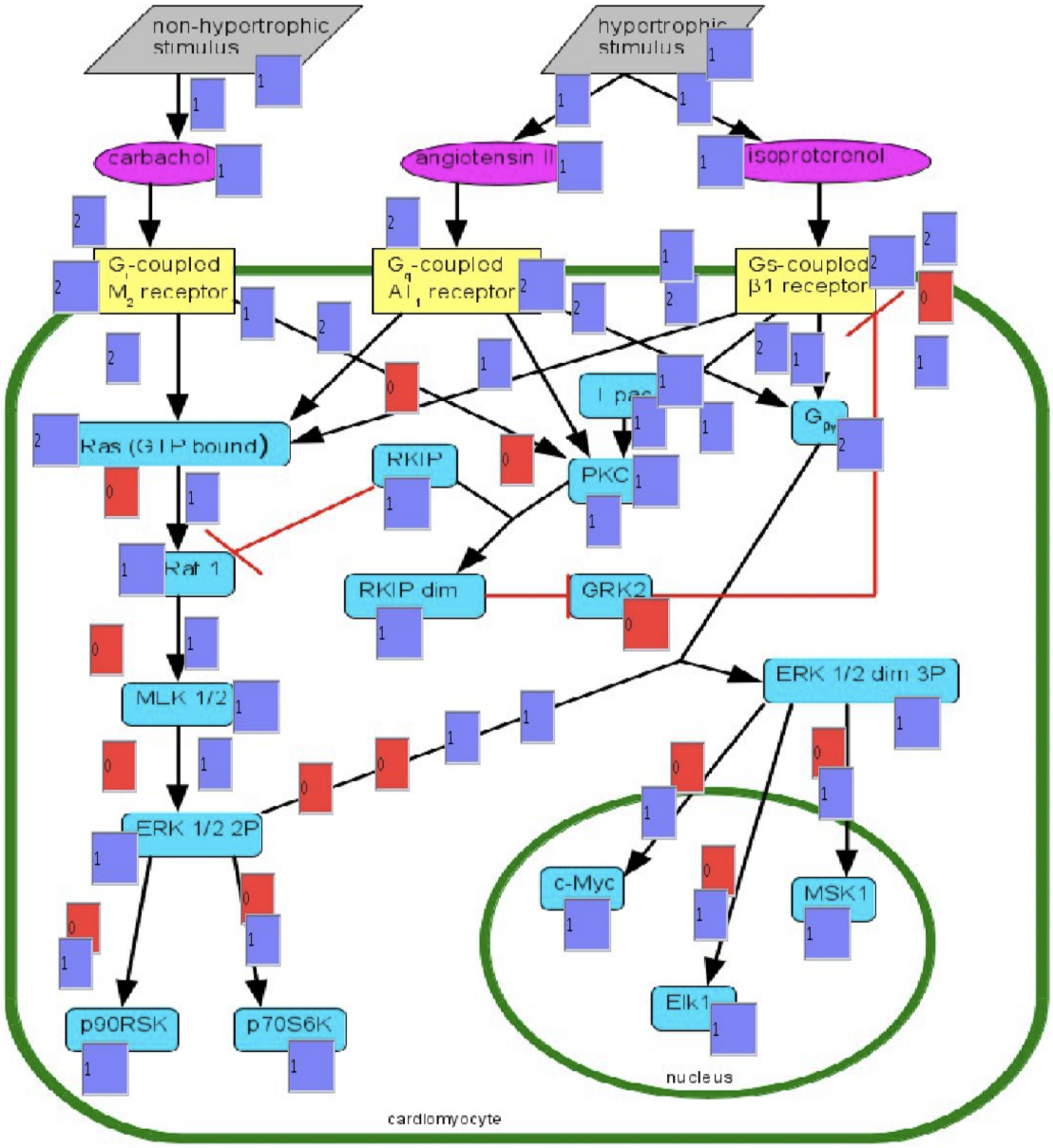

Figure 9.10.: CNA simulation: both stimuli, Raf1-feedback turned offAll downstream targets reach only intermediate activation levels (value 1).

10. New predicted targets of ERK 1/2

Further target proteins of ERK were searched by using established data bases and validating through ample literature as described in material and methods. For a whole overview of all found and validated interaction see Table B.1. Broader investigations compromised not only the targets and its effect, but also localization of the target in the cell, the ERK isoform which is involved and the cell type, in which the interaction was found. These additional informations can be found also in Table B.1 in the appendix. In chapter 11 gene expression analysis were observed, the new predicted target proteins which were found during them and their adjusted p-values are noted in Table 11.1, in Table 11.2 as well in the column "additional information" in Table B.1.

By incorporation of all these achieved results, there are a few very promising targets, which could be of great interest for further investigation and they will be described in detail in the following paragraph.

Besides the already existing targets in the cascade of ERK 1/2 Caspase 8, GRB2-associated-binding protein 2, Mxi-2, SMAD2, FHL2 and SPIN90 are interesting targets, which are worthy turning attention to. All of them are involved in either cardiomyocyte differentiation, cardiac hypertrophy or in triggering apoptosis, respectively in several of them.

FHL2 (Four and a half LIM domains protein 2) antagonizes ERK 1/2 mediated cardiac hypertrophy by inhibiting transcriptional coupling. It is located in the nucleus [168, 183]. In general, it is a protein which serves as a repressor, for instance it is down-regulated during transformation of normal myoblasts to rhabdomyosarcoma. Associated diseases with FHL2 are Familial Isolated Dilated Cardiomyopathy and Hemophagocytic Lymphohistiocytosis [227, 223].

Caspase 8 is known as a pro-apoptotic factor, ERK 1/2 can inhibit Caspase-8 induced apoptosis in ovarian and breast cancer cell lines [141]. Besides, the interaction of Caspase 8 with p38MAPK is well established: For instance in neutrophils apoptosis can be hindered by p38MAPK, because it inhibits Caspase 8 [3]. Caspase

8 can mediate p38α MAPK-dependent apoptosis induced by palmitic acid in cardiomyocytes as well [166]. If ERK 1/2 interacts in cardiomyocytes with Caspase 8, this could be of great interest to examine and a potential therapeutic target.

GRB2-associated-binding protein 2 (GAB2) is well established in t-lymphocytes. It acts downstream of several membrane receptors including cytokine, antigen, hormone, cell matrix and growth factor receptors. Thereby it regulates multiple signaling pathways, including for example osteoclast differentiation, allergic response and hematopoiesis [231, 26]. In connection with ERK, it has to be indicated, that ERK-mediated phosphorylation of GAB2 regulates via intermediate steps the fine tuning of proliferative answer [5].

Mxi-2, which is a splice isoform of p38MAPK, enhances the activity of ERK in matters of activation of nuclear targets by facilitating nuclear translocation of ERK. Mxi-2 thereby regulates activation of nuclear targets as Elk1 or HIF1 [201, 38]. It does not effect cytosolic targets and therefore it could play a crucial role in the balance between ERK 1/2 nuclear and cytoplasmic signals [37].

SMAD2 (Mothers against decapentaplegic homolog 2) regulates multiple cellular actions, such as cell proliferation, apoptosis, and differentiation by mediating the signal of the transforming growth factor TGF-β [188]. ERK transduces Ras signal to SMAD2 and this inhibits SMAD2 transcriptional activity. This has been shown for lymphatic endothelial cells and for tumor cells [91, 113]. Diseases associated with SMAD2 mutations are for instance arterial aneurysms and dissections [151]. Moreover, it was shown that SMAD2 and c-Myc, one of the three nuclear targets in the presented cascade, interact also. C-Myc interacts directly with SMAD2 and thereby the TGF-β-mediated induction of the CDK inhibitor p15(Ink4B) can be inhibited which is one step that takes part in cell growth and cancer development [63]. Because of these multiple possibilities of interaction with proteins known for taking part in developing heart failure, the interaction of SMAD2 with ERK has to be investigated further.

Nck and SPIN90 are binding partners, this plays an essential role in the formation of sarcomeres during differentiation of cardiomyocytes. Via cell adhesion activated PDGF activates ERK 1, which in turn phosphorylates and thereby activates SPIN90. This mechanism is of essential importance for solid cell adhesion in cardiomyocytes[127]. Moreover, it has been shown that SPIN90 knockdown tempers the formation and movement of endosomal vesicles in the early stages of epidermal growth factor receptor endocytosis[167]. From this it follows that SPIN90 is a central target because of its role in the structure building of cardiomyocytes.

11. Gene expression Analysis

By analysis of gene expression data in heart failure of cardiomyocytes, expression levels for the components of the cascade under non-hypertrophic and hypertrophic conditions can be reviewed. As described in chapter 7, it has been reverted to pre-existing gene expression data sets. As they had three replicates and solid time series on murine cardiomyocyte gene expression response, only two studies were selected to achieve high quality results. One of these two, GEO series number GSE 5500, analyses gene expression during 7 days after TAC (transverse aortic constriction) respectively sham operation, whereas the other series, GSE 18224, analyses 9 weeks after TAC respectively sham operation.

Not only the genes encoding for proteins in the ERK cascade but also all differentially expressed genes were analyzed. The outcomes of both studies were matched to identify genes, which are altered in both studies to achieve more significance. An overview of these genes, that are altered in both experiments can be found in Table 11.1. These findings show, that other pathways besides the ERK-cascade are affected by TAC.

Table 11.1.: Genes altered in GSE 5500 as well as in GSE 18224: GSE analyses 7 days after TAC, whereas GSE 18224 analyses 9 weeks after TAC. Genes with an adjusted p-value less than 0.05 after the false discovery rate were included. Beyond that, the first 250 spots from each experiment were used for the comparison.

Gene symbol	*Gene title*	*Gene ID*	*Adj. p-value GSE 5500*	*Adjusted p-value GSE 18224*
1500009L16 Rik	RIKEN cDNA 1500009L16 gene	1452840_at	0.028608	5.73e-05
Ano10	anoctamin 10	1426672_at	0.026066	5.15e-05
Bgn	biglycan	1437889_x_at	0.016966	7.30e-05

continues on next page

Table 11.1.: Genes altered in GSE 5500 as well as in GSE 18224: GSE analyses 7 days after TAC, whereas GSE 18224 analyses 9 weeks after TAC. Genes with an adjusted p-value less than 0.05 after the false discovery rate were included. Beyond that, the first 250 spots from each experiment were used for the comparison.

Gene symbol	*Gene title*	*Gene ID*	*Adj. p-value GSE 5500*	*Adjusted p-value GSE 18224*
Bgn	biglycan	1448323_a_at	0.028369	3.35e-04
Bgn	biglycan	1416405_at	0.047221	3.55e-04
Cilp	cartilage intermediate layer protein, nucleotide pyrophosphohydrolase	1457296_at	0.003647	6.29e-05
Col1a1	collagen, type I, alpha 1	1423669_at	0.046904	1.14e-03
Col5a2	collagen, type V, alpha 2	1450625_at	0.00327	1.03e-03
Col8a1	collagen, type VIII, alpha 1	1455627_at	0.002963	3.04e-04
Col8a1	collagen, type VIII, alpha 1	1418440_at	0.002963	9.61e-05
Col8a1	collagen, type VIII, alpha 1	1418441_at	0.007573	6.30e-04
Col8a1	collagen, type VIII, alpha 1	1447819_x_at	0.009684	5.21e-04
Ctgf	connective tissue growth factor	1416953_at	0.026312	8.38e-04
Fbn1	fibrillin 1	1460208_at	0.043775	7.75e-04
Frzb	frizzled-related protein	1448424_at	0.024229	1.20e-03
Ift122	intraflagellar transport 122	1427239_at	0.018931	5.78e-04
Kcnv2	potassium channel, subfamily V, member 2	1440537_at	0.034454	5.39e-04
Lgals4	lectin, galactose binding, soluble 4	1451336_at	0.017818	5.39e-04
Ltbp2	latent transforming growth factor beta binding protein 2	1418061_at	0.018931	3.35e-04
Meox1	mesenchyme homeobox 1	1417595_at	0.015167	8.37e-04
Mfap5	microfibrillar associated protein 5	1418454_at	0.007776	1.23e-03

continues on next page

Table 11.1.: Genes altered in GSE 5500 as well as in GSE 18224: GSE analyses 7 days after TAC, whereas GSE 18224 analyses 9 weeks after TAC. Genes with an adjusted p-value less than 0.05 after the false discovery rate were included. Beyond that, the first 250 spots from each experiment were used for the comparison.

Gene symbol	*Gene title*	*Gene ID*	*Adj. p-value GSE 5500*	*Adjusted p-value GSE 18224*
Mybpc2	myosin binding protein C, fast-type	1455736_at	0.010186	1.51e-04
Myh7	myosin, heavy polypeptide 7, cardiac muscle, beta	1448553_at	0.001554	4.22e-07
Nppa	natriuretic peptide type A	1456062_at	0.021041	6.19e-04
Srpx2	sushi-repeat-containing protein, X-linked 2	1427919_at	0.048266	1.28e-03
Synpo	synaptopodin	1434089_at	0.004904	6.23e-04
Thbs1	thrombospondin 1	1421811_at	0.007776	1.03e-03
Tmsb10	thymosin, beta 10	1417219_s_at	0.043459	1.27e-03
Vcan	versican	1421694_a_at	0.037309	1.20e-03

Many structural proteins, components of the extracellular matrix and signaling transducing proteins are affected, for example different types of collagens and biglycans. Biglycan is a small leucine-rich repeat proteoglycan (SLRP) and can be found in diverse extracellular matrix tissues, amongst others bone, cartilage and tendon[224]. In the heart, biglycan has been shown to regulate collagen fibril diameters in tendon. There is a relation between biglycan and cardiac extra-cellular remodeling, but yet the exact mechanisms have not been proven [16, 246].

Collagens are the major structural proteins in the extracellular matrix in all connective tissues. Due to the wide appearance of connective tissue in the body, for instance in tendons, ligaments and skin, collagens make around 30 percent of the content of the whole body protein. It consists of triple-helices of elongated fibrils formed by amino acids wound together [50]. In heart failure, it has been shown, that collagens pass through diverse changes. For example there are changes in the degree of cross-linking as well as the types of collagens and their proportions to each other [45, 76]. It is scientific consensus, that collagens accumulate in cases of pathological

Gene symbol	Gene ID	Gene title	Adjusted p-value
Cnksr1	1455399_at	Connector enhancer of kinase suppressor of Ras 1	5.73e-05
Elk1	1446390_at	ELK1, member of ETS oncogene family	5.09e-03
Myc	1424942_a_at	Myelocytomatosis oncogene	1.89e-02
Prkcd	1422847_a_at	Protein kinase C, delta	1.31e-02
Prkce	1452878_at	Protein kinase C, epsilon	3.36e-02
Rab27b	1417214_at	RAB27b, member RAS oncogene family	1.24e-03
Rab31	1416165_at	RAB31, member RAS oncogene family	1.20e-03
Rab3a	1422589_at	RAB3A, member RAS oncogene family	5.39e-04
Raf1	1420090_at	v-Raf-leukemia viral oncogene 1	2.70e-02
Rps6ka5	1440343_at	Ribosomal protein S6 kinase, polypeptide 5 = MSK1	1.43e-02

Table 11.2.: Genes, that appear in the ERK-cascade or rather stand in proximate correlation to genes in ERK-cascade and are altered in GSE 18224: Adjusted p-value was at least 0.05, evaluation occurred 9 weeks after TAC. Some genes (for example the ras oncogene family) appear in different isoforms in the cascade. .

hypertrophy [17, 100].

Frizzle related protein is a modulator of the important Wnt signaling pathway and has inhibitory effects on the Wnt pathway in general [22]. Frizzle related proteins reach the highest level in heart, but it can be found also in other tissue. It plays roles during cardiac embryogenesis as well as in cardiac remodeling, not only in mice after TAC, but also in human heart failure its expression level is increased [6, 205].

Of special interest is myosin-binding protein c, because it is identified to be target of MAPK (see also Table B.1). Already in 1996, it has been shown that MAPK-dependent state of phosphorylation modifies the cellular function of c-Myb [230]. Regrettably, it is not in the focus of investigation furthermore, so the exact underlying mechanisms are not definitely clear at the moment.

In summary, these results show that changes in the ultrastructure of the cardiomyocyte are the final result of both gene expression experiments.

Table 11.2 shows altered genes, that appear in the presented ERK-cascade and are significantly altered in the gene expression data set GSE 18224, the larger of both experiments. In the matched results of both experiments, there were no altered genes from ERK-cascade that complied with the criteria for inclusion.

mRNA expression levels for several proteins that are involved in the ERK-cascade could be verified, whether the genes were down- or up-regulated was analyzed accessorily Figure 11.1.

The nuclear targets of ERK were regulated in different directions: Myc mRNA was up-regulated whereas Elk1 mRNA and MSK1 (Rps6ka5 in Figure 11.1) mRNA were down-regulated. mRNAs for two isoforms of Protein kinase C showed also significant, but appropriate regulation directions: whereas Protein kinase C-δ (Prkcd in Figure 11.1) was up-regulated, Protein kinase C-ε (Prkce in Figure 11.1) was down-regulated. Raf1 was down-regulated after TAC. These data support the knowledge base, that mRNA expression levels do not necessarily correlate with protein activation via phosphorylation and that gene expression underlies complex processes.

Two bystanders not explicitly considered in the ERK-simulation have to be termed additionally. Connector enhancer of kinase suppressor of Ras 1 (Cnksr1), a regulatory protein influencing Ras1, whose knockdown partially blocks the MAPK pathway, showed significant expression levels [62]. RAB27b, another RAS regulatory protein, showed also significant altered expression levels, but its role in ERK-cascade respectively heart failure is not well investigated [187].

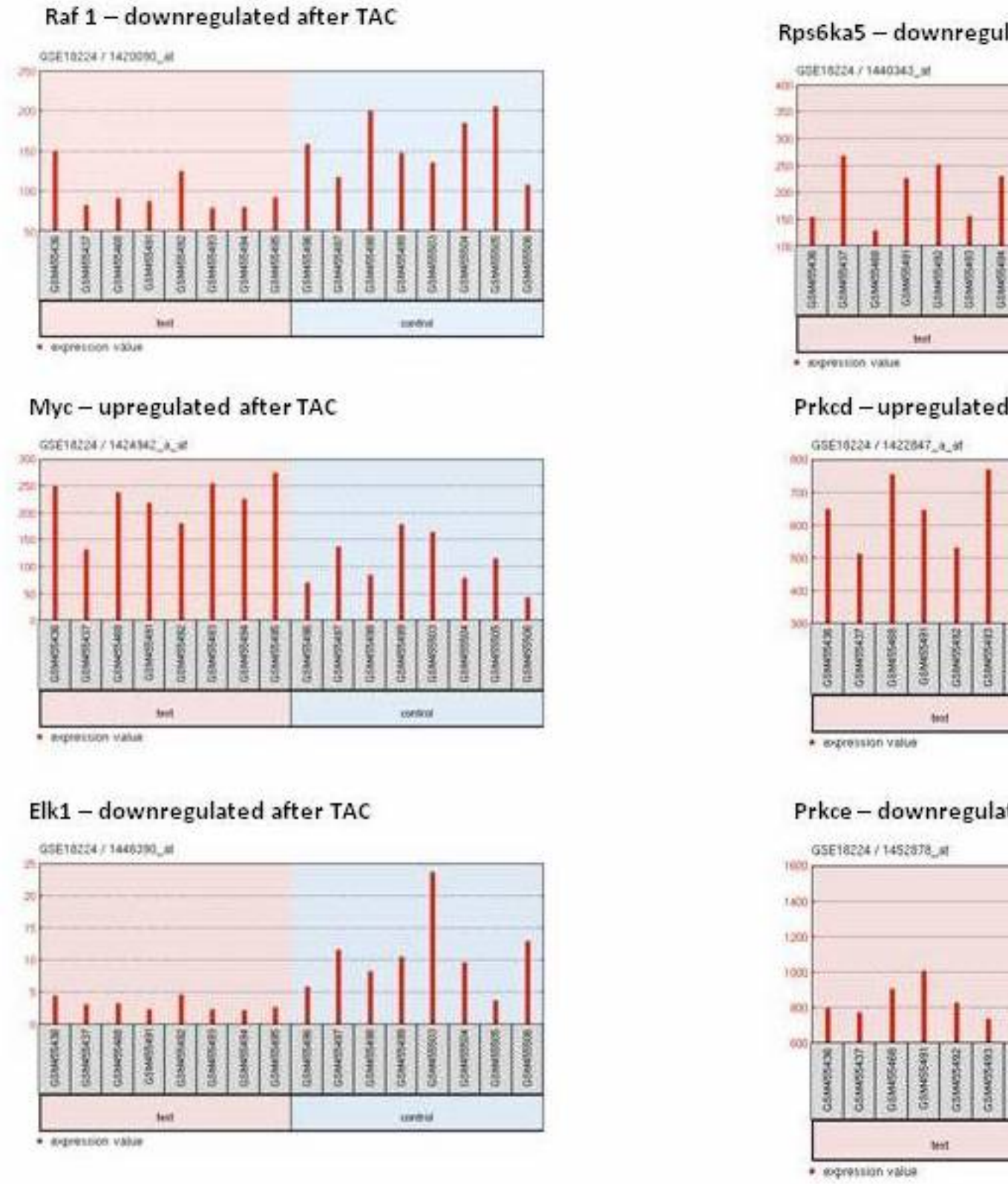

Figure 11.1.: Genexpression Data GSE 18224: Regulation directions (down- versus upregulation)

12. Comparison with in vitro results

For confirmation of the in silico predicted results the group of Prof. Kristina Lorenz executed in vitro experiments with COS7 cells as described in chapter 8. The comparison of these in-vitro experiments with the simulation were performed by the author.

This experimental validation included time-dependent and agonist-dependent ERK 1/2 phosphorylation in Western Blot and following densitometric quantification. Three agonists and four time points chosen. From previous experiments, kinetic data, for example the time point when ERK stabilizes at a maximum, is known [133], so the phosphorylation in ERK 1 respectively ERK 2 was measured by two phospho-antibodies in time courses of 0, 5, 10 and 30 minutes after stimulation with the appropriate agonist, because these time points cover an adequate time range of phosphorylation. Two agonists representing the hypertrophic pathway (carbachol as agonist for M_1-muscarinic receptor and epidermal growth factor as agonist for EGFR) and one agonist representing the non-hypertrophic pathway (carbachol as agonist for M_2-muscarinic receptor) served as examples. As showed in Table 9.2 all six, the three chosen agonists in the in vitro experiments as well as the three examples chosen in the in silico model (carbachol via M_2-muscarinic receptor, angiotensin II via AT_1- receptor and isoproterenol via β1-adrenergic receptor) serve as representatives for many other known agonists effecting the non-hypertrophic or hypertrophic pathway.

Figure 12.1 shows a comparison of the in silico and in vitro results. The three columns A), B) and C) show results for A) the M_1-muscarinic receptor, B) the M_2-muscarinic receptor and C) the EGF receptor. The first line shows concentrations of pERK(Thr 188) after stimulation with the appropriate agonist at the chosen time points as a bar chart, whereas the second line shows concentrations of pERK(TEY) after stimulation at the same time points. The third line shows Western blot measuring results for ERK, pERK(Thr188) as well as pERK(TEY). The fourth line shows the corresponding results of the in silico model: A) and C) are

compared with the measuring-results for hypertrophic stimuli, B) is compared with the measuring-results for non-hypertrophic stimuli in a line graph. pERK(Thr188) is represented as red graph with dots in the course of the graph, pERK(TEY) is represented as green graph with squares in the course of the graph.

A strong third ERK phosphorylation (pERK(Thr188)) and thereby activation of the hypertrophic pathway in Figure 12.1 A) (M_1-muscarinic receptor) and Figure 12.1 C) (EGF receptor) is shown in the in silico experiments. The phosphorylation signal increases over time. In the phosphorylation level of the M_2-receptor shown in Figure 12.1 B) which is primarily leading to the non-hypertrophic pathway and activation of cytosolic targets, there is no increase in phosphorylation level of pERK(Thr 188).

The second line shows the TEY motif phosphorylation (pERK(TEY)) and time course for the cytosolic, non-hypertrophic pathway which shows a strong activation for all three stimuli. This activation increases faster than the activation of pERK(Thr188). As described in section 5 and shown in Figure 9.3 and by knowing that ERK has to be phosphorylated in TEYmotif before the third phosphorylation in Thr188 can occur, the faster increase of pERK(TEY) phosphorylation level is a logical consequence. A peak of the phosphorylation of pERK(TEY) signal arises at 10 minutes, and after this the values show a decrease again. It must be pointed out, that the measurement points are not straight-lined.

Unlike the in silico simulation, all in vitro experiments show basal rates of both phosphorylation states of ERK around 1 ng/ml. In Figure 12.1 B) pERK(Thr188) shows this value over all time courses, whereas all other measurements show this value only at time point 0. In SQUAD simulation, basal ERK levels are arranged on the baseline. In vivo, one can act on the assumption, that there are certain concentrations of all phosphorylation states at all times detectable. For the present aim, the changes of values under particular conditions are of greater interest and for a clear presentation it was abstained from modeling basal levels off the baseline in the in silico model.

By using a concatenated e-function, SQUAD simulation allows an almost linear increase of pERK(TEY) in Figure 12.1 A-C) and pERK(Thr188) in Figure 12.1 A) and C) until the values approximate to the maximum level. The values start to increase at time step 3 and stabilize at 80% activation at time-step 6, yielding a plateau around time-step 8. After reaching and stabilizing this maximum level, the values decrease again and approximate to the basal level. The decrease of pERK(TEY) is shown in Figure 12.1. The decrease of pERK(Thr188) is not shown in the chosen time interval to permit a comparison with the in vitro results, in which

the decrease of pERK(Thr188) is not also shown. In Figure 9.3 the decrease of pERK(Thr188) is visible and shows similar kinetics to the decrease of pERK(TEY).

Each time-step in the in silico model corresponds to about 5 min of time measured in the in vitro experiments. Whereas the in vitro experiments show values for the measurement points only, the in silico model allows predictions for all time points.

Naturally there are several limitations by design, causing the in silico model to differ to the experimental data: As the in silico-simulation via SQUAD uses default e-functions and concatenations of them, only exponential activations or decays, respectively concatenations of them, are precisely modelled. As demonstrated above, for the phosphorylation kinetics of pERK(Thr188) and pERK(TEY) the agreement is passable.

In modelling signaling phosphorylation cascades and their inhibition, the software SQUAD was tested in several other cellular environments. Including for example liver cells, stem cells, dendritic cells, platelets and in these systems good kinetic agreement was found as well [153, 178].

With CNA simulation, which uses besides the typical Boolean modelling multi-valued logical networks [108, 107, 109], the adjustment to the in vitro experiments succeeds not as well. For comparison, when a hypertrophic stimulus occurs in the CNA model, this leads directly to high activation (level 2) for pERK(Thr188). As described above, in the CNA model three different values were used: 0, 1, 2 for no, intermediate and high activation. As CNA provides only a discrete state simulation the rapid activation is not visible as it is in SQUAD or in the in silico experiment but rather the terminal point is shown.

The comparison of time courses as well as thresholds (shown in Table 9.3) shows that the SQUAD model captures the information also in a qualitative manner: If a stimulus occurs only for a short time period, the effect is different from the effect of a continously active stimulus. This can be found also in vivo: Whereas short sympathetic stress situation does not lead to cardiac hypertrophy, continuous sympathetic overdrive leads to cardiac hypertrophy and sickness in turn.

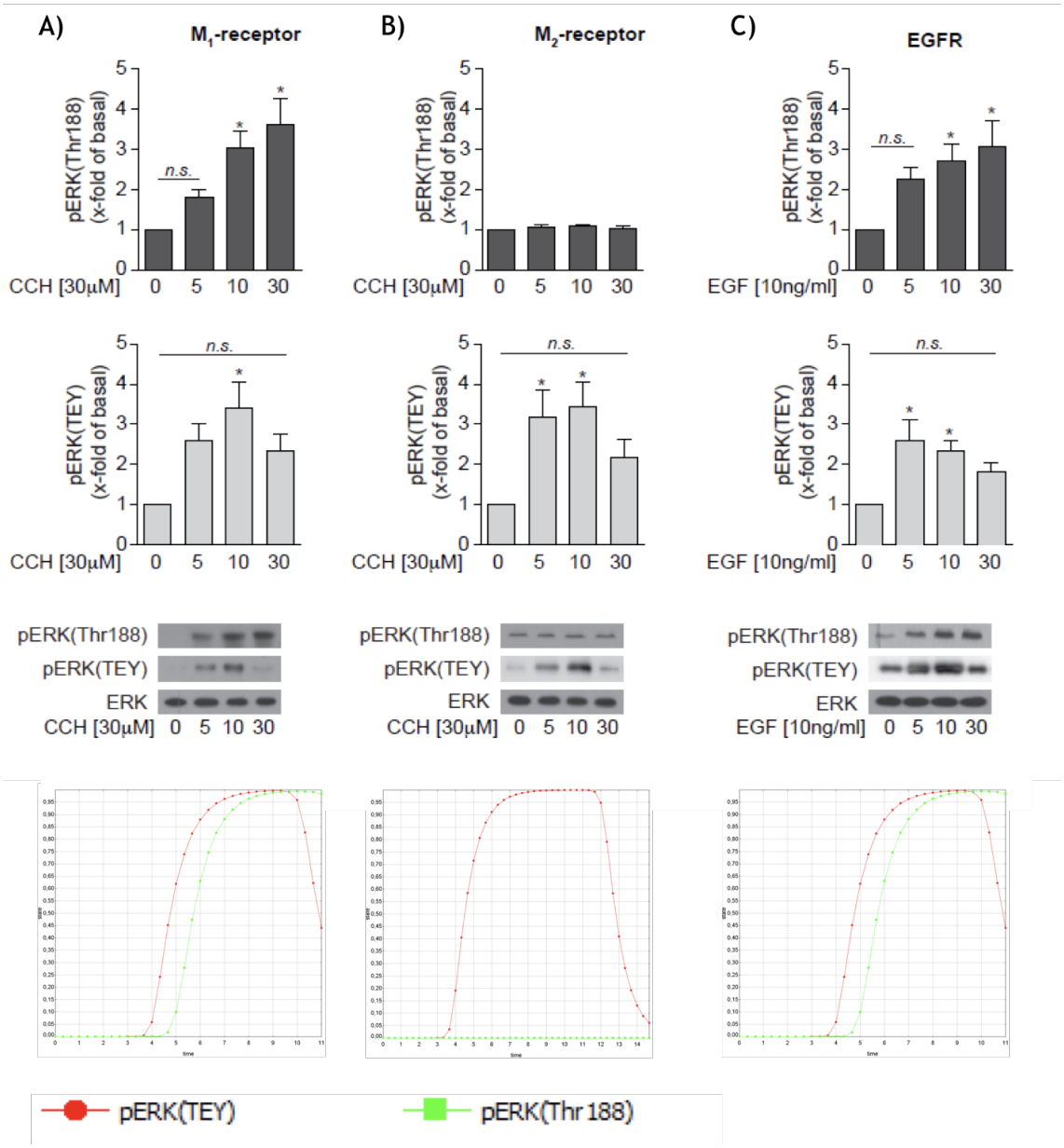

Figure 12.1.: Experimental analysis compared with SQUAD readouts: COS7 cells were transfected with plasmids encoding for A) M1-muscarinic receptor B) M2- muscarinic receptor or C) epidermal growth factor (EGF) receptor., comparison with SQUAD readouts with A) and C) as examples for hypertrophic stimuli as well as B) as example for a non-hypertrophic stimulus. Receptors were treated with A) carbachol (CCH; 30 µM), B) carbachol (CCH; 30 µM) or C) epidermal growth factor (EGF; 10 ng/ml) for 5, 10 or 30 minutes. Immunoblot analyses with Western blots antibodies directed against in TEY motif (twice) phosphorylated Erk 2 [pErk(TEY)] or (thrice) phosphorylated Thr188 [pErk(Thr188)]. n=4-11 experiments; $P < 0.05$ versus unstimulated control. The corresponding in silico-predicted courses can be found in the last column.

Part IV.

Discussion

13. First integrative biological model of ERK-pathway in cardiomyocyte

Numerous studies demonstrated, that ERK 1/2 is a major player in mediating cardiac hypertrophy and that an additional phosphorylation at Thr188 in ERK 2 can cause cardiac hypertrophy be switching from cytosolic to nucleosolic targets [200, 27, 28, 73, 133, 134, 70]. This thesis introduces an integrative biological view on the ERK 1/2 cascade in cardiomyocytes for the first time. A special significance lies on the additional phosphorylation site. The third phosphorylation of already double phosphorylated ERK in general seems to be an interesting mechanism. Other tissues and cells also showed a third phosphorylation, for example platelets. As platelets are anucleated, there is no discrimation between cytosolic and nucleosolic targets, but rather between cytoskeletal and non-cytoskeletal activation of the platelet [153].

The thesis includes several perceptions: Firstly a regulatory network of the ERK-cascade in the cardiomyocyte in form of a first semi-quantitative model on all events for this important signaling cascade and bioinformatical analysis of it. In this connection, structural as well as dynamical cellular functions are considered. Secondly, because experimental data are necessary for the validation of a model, corresponding in vitro experiments, realized by Prof. Kristina Lorenz, especially with regard on time courses, are presented. In collection, a first normalized and validated model which provides time-resolved data was established.

Thirdly genomic analysis in form of gene expression analysis are investigated, to verify involved components as well as to detect potential components, that could be of interest for further investigation of cardiac hypertrophy. Moreover, further targets of ERK 1/2 were investigated with the same destination.

The aim of system biology is always, to become an extensive comprehension of all regulatory processes. Oftentimes, not every single process is entirely examined and suppositions are necessary to establish a complex model, without having hard evidence for every single step. For example, the assumption, that Epac activates

PKC could be wrong, novel experiments, indeed in cardiomyocytes but at least on nociceptive sensory neurons, rather suggest that Epac activates Ras [24, 206]. Nevertheless, these suppositions are necessary, but when they are proven to be wrong, they offer an entry for improvements of a model.

Moreover, separate from the point that one often has to deal with a lack of information, system biology is an integrative science, combining parts of biology, mathematics as well as physics, the mathematical-analytical part is not the main focus and comparative easy accessible computational methods and heuristics are necessary. For instance, in the present case at the outset, the current level of information included only information about the network topology (nodes and connections of them), but nearly all kinetic constants for a full dynamic simulation were unknown. A complex mathematical analysis is not possible without having kinetic parameters. The semi-quantitative model advocated in this thesis uses as foundation logical connections between the involved components, regarding occurrence and mode of action. To get dynamical information the software SQUAD and CellNetAnalyzer (CNA) were used. After having computed predictions of time courses, in vitro experiments were performed. The computed predictions hereby assisted to establish the base for the design of the in vitro experiments. After having in vitro time courses, in turn the in silico model was adjusted. So the soft spots of both sciences can be balanced.

Furthermore, by using different software, in this case SQUAD and CNA, the respective weakness can be partial eliminated. SQUAD modelling allows no exact estimation of steady states. In this case, achieving steady states was only possible because of computing backward activation from carbachol, angiotensin II and isoproterenol to their corresponding stimulus. One reason could be, that SQUAD indeed quickly, but therefore efficiently samples steady states using a fast heuristic [202]. Therefore, SQUAD generates limitations in for instance modelling complex inhibition scenarios [153]. Nonetheless, a big benefit of SQUAD is the rapid setup of a dynamic model using concatenated e-functions for interpolation. In the presented case, the via SQUAD generated kinetic data agreed well with the in vitro results.

However, CNA simulation delivered exact results for four steady states (hypertrophic stimulus, non-hypertrophic stimulus, simultaneous hypertrophic and non-hypertrophic stimulus, no stimulus) which agree with physiological observations (for this see Table 9.2) as well as good results for inhibiting feedback loops (see also Figure 9.6 - Figure 9.10). On the other hand, using CNA, only stepwise activation is possible (in this case state 0,1,2) which allows neither exact prediction of time courses nor reaching the targets multiple values. So in conclusion, both models accorded with each other in key parts and completed each other.

The system biological approach allows a wide view on the ERK 1/2 cascade in cardiomyocytes especially in development of heart failure, but although ERK is definitely a key player in this process, it is not the only mediator. Current research of cardiac hypertrophy and heart failure in turn incorporates beyond ERK-cascade calsarcins [67], growth factors as TGFβ and IGF [89, 147], mTOR [157], the role of inflammation and thereby IL-6, NF-ϰb [56, 85, 116] as well as the role of calcium [156]. The gene expression data experiments showed also changes in the ultrastructure of the cardiomyocyte as mainly conclusion of the experiments presented in chapter 11.

A model, which concerns all these factors is, due to the immense importance of this clinical picture and its increasing incidence, definitely desirable, but exceeds the extent of a single doctoral thesis.

14. Insights into cardiomyocyte signaling

The SQUAD network, with its logical heuristic, works in a manner, that the hypertrophic stimuli (in the presented case ATII via AT_1- receptor and isoproterenol via β1-adrenergic receptor) can reach all five targets (cytosolic as well was nucleosolic) whenever they are present. Carbachol via M_2-receptor as an example for a non-hypertrophic stimulus causes no hypertrophy by only activating the cytosolic targets, when it is activated singularly. Unfortunately, the other two receptors dominate the system.

This has to be investigated further in vitro and in vivo, but many findings indicate that this behavior occurs in these cases as well. As the cytosolic targets have protecting effects, an aim of an (pharmacological) intervention could be to respect this fact and intervent either at the beginning of the cascade or at the final path of the hypertrophic cascade, but not on the common part of the cascade.

The inhibition of the third ERK-phosphorylation is object of investigations on molecular level [131, 132, 48]. These experiments include also data for RKIP inhibition, which was in silico modelled in Figure 9.10.

The SQUAD model allows also a differentiation between different hypertrophic stimuli: As an example, if both hypertrophic stimuli (angiotensin II and isoproterenol) appear, a weaker and shorter lasting activation of AT_1- receptor and a stronger and longer lasting activation of β1-adrenergic receptor occurs. This accords to in vitro found results and the GRK2-negative feedback loop [131].

The threshold dependent behavior of the modelled ERK-cascade shown in Table 9.3 is also a newly investigated mechanism. Other in silico models uncovered also threshold-dependent behavior, for example for platelets and SRc-phosphorylation [153].

The simulation allows predictions about time scales and thereby not only quantitative, but also qualitative insights: A faster activation of the cytosolic targets occurs in comparison to the activation of nucleosolic targets (see also Figure 9.2 and Figure 9.3). In synopsis with the experimental data and the gene expression

analysis, a fast appearance of the non-hypertrophic effects in the space of minimum minutes as well as a rather slow process of the hypertrophic effects were proven. Slow process means, that effects appear in the range of many hours to several weeks.

15. Predictions about pharmacological targets

Along with flanking measures like alcohol abstinence or adjusted physical activity and in some cases invasive measures like cardioversion or pacemaker-implantation, the standard medical therapy includes follwing drug classes: ACE inhibitors, angiotensin receptor blockers, β-blockers, mineralocorticoid receptor antagonists and diuretics. In special patient populations these drugs become complemented with digitalis glykosids, oral anticoagulants or platelet aggregation inhibitors [245, 9]. The only two of these substances, which addresses ERK cascade in parts are β-blockers and AT_1-receptor antagonists, but they do not act very specific and affect not only the hypertrophic but also the adaptive effects. Besides they have multiple side effects and the model shows multiple more potential target points.

Nearly all of the mentioned drugs treat symptoms or risk factors. The ERK cascade is very suitable as target for drugs as it seems to promote the switch from a protective to a maladaptive answer [133]. Unfortunately, there is yet no drug established in clinical use except the mentioned β-blockers and AT_1-receptor antagonists, which addresses ERK cascade, but the development of those drugs is an object of research in preclinical studies. Up to now Pimasertib an orally bio-available small-molecule inhibitor of ERK 1/2 and selumetinib, primiarily developed for the treatment of neurofibromatosis 1, are promising [199, 121]. Yet, there is no drug known, which intervenes in the process of the third phosphorylation of ERK 1/2 and thereby targets to physiological-to-maladaptive-step specifically.

The presented ERK-model enables the user to predict on further potential pharmacological targets which could influence cardiac hypertrophy and enables to model pharmacological scenarios with different receptor stimulation combinations. A more mathematical ERK-model, published by Breitenbach et al. 2019 [24] which uses the here presented network topology, enables to model optimal pharmacological intervention points, combined effects of activation and inhibiting as well as further thresholds.

The entire network analysis and the analysis of further targets provide several

intervention options:

As already mentioned, the third ERK phosphorylation leads to cardiac hypertrophy via activating nuclear targets. Therefore, either preventing the third phosphorylation or blocking the nuclear targets could be a possible approach. More promising appears the blockade of the third phosphorylation, as there are probably multiple more nuclear targets beyond the two mentioned which mediate cardiac hypertrophy (see also Table B.1).

Another interesting target point of medicinal therapy is the GRK2-RKIP-feedback loop. As mentioned, dimerized RKIP inhibits GRK2, whereas non-dimerized RKIP inhibits Raf1. This effect amplifies an incoming stimulus und could be used as a pharmacological target. Moreover, Raf1 is known to be cardioprotective, which underscores the importance of this feedback loop.

Another way to prevent cardiac hypertrophy could be, to prevent activation of hypertrophy mediating genes, which is part of research at this moment [135].

The assembly of downstream targets of ERK shown in Table B.1 hints for a better understanding of the tissue transformation that is involved in hypertrophy and includes further potential pharmacological targets.

16. Perspective for further research

As already mentioned, the thesis presented in this model acted as a base for a more mathematical model of the ERK cascade in cardiomyocytes [24]. This new model uses the presented model as base and that it describes the proceedings in cardiomyocytes correctly to establish a model, which can simulate external stimuli. Although, the road to drugs applicable in clinical use targeting the ERK cascade is still long, this model does the next step as it allows to simulate external stimuli to the cell and make them visible. Moreover, a combination of different external stimuli can be simulated.

In contrast to the model presented in this thesis, the new model did not focus on exact kinetic predictions. A next step could be to establish a model, which includes both, the possibility to calculate several external stimuli combinations and simultaneously, accurate time courses. Such complex simulations will necessitate further in vitro experiments, firstly to receive data about time courses and secondly, to validate predicted courses as it was done in this thesis.

A great amount of research data in the last few years underlines the assumption, that ERK 1/2 are promising targets in the treatment of heart failure. Especially, the additional phosphorylation of ERK at Thr188 seems to be an interesting target point. After publishing results presented in this work, it was shown that interference with ERK-dimerization, a condition for the phosphorylation of ERK at Thr188, decreases cardiac hypertrophy without causing harmful cardiac effects. The nuclear ERK 1/2-signaling and cardiomyocyte hypertrophy could be prevented by inhibiting the third ERK phosphorylation at Thr188 by an inhibitory peptide. Auspicious effects like cytosolic survival signaling were not affected by this inhibitory peptide [221]. As it has been shown, that MAPK/ERK activation and in turn signaling is crucial for cardiac regeneration, for example in zebrafish experiments [196, 128], it appears necessary to assess the ERK cascade at a later point to prevent negative effects while allowing positive effects.

Not withstanding that this third phosphorylation seems very promising, it is not

the only possible target point in treating heart failure. It has been shown that novel EGFR inhibitors weaken angiotensin II, a cardiac hypertrophy [177]. ERK is known to act downstream of EGFR and is one example for an hypertrophic stimuli in the here presented in vitro experiments shown in Figure 12.1. But angiotensin II is no typical known interacting partner of EGFR. The underlying mechanisms are not investigated in this case as well as the influence on harmful effects.

Surprisingly, not only an increased ERK activation in cardiomyocytes, but also in non-myocytes has been shown to drive hypertrophy in Marfan mice [193]. This could be a hint, to not focus only on the ERK effects on cardiomyocytes, but also on other cell types. Building on the results of this thesis and the insights on the still open questions of the right approach to treat cardiomyocytes and prevent cardiac hypertrophy, a general in silico method to calculate optimal pharmacological stimuli for the ERK cardiomyocyte signalling network was developed [24].

Summing up, we are bound to recognize, that in the current state there is no drug established, which addresses the ERK cascade specifically to treat heart insufficiency. But as it is furthermore subject of many studies, it is to be expected that in future drugs affecting the ERK cascade can be established and thereby heart failure can be treated causally.

Part V.

Summary

ERK 1/2 are known key players in the pathophysiology of heart failure, but the members of the ERK cascade, in particular Raf1, can also protect the heart from cell death and ischemic injury. An additional autophosphorylation (ERK 1 at Thr208, ERK 2 at Thr188) empowers ERK 1/2 translocation to the nucleus and phosphorylation of nuclear targets which take part in the development of cardiac hypertrophy. Thereby, targeting this additional phosphorylation is a promising pharmacological approach.

In this thesis, an in silico model of ERK cascade in the cardiomyocyte is introduced. The model is a semi-quantitive model and its behavior was tested with different softwares (SQUAD and CellNetAnalyzer). Different phosphorylation states of ERK 1/2 as well as different stimuli can be reproduced. The different types of stimuli include hypertrophic as well as non-hypertrophic stimuli. With the introduced in silico-model time courses and synergistic as well as antagonistic receptor stimuli combinations can be predicted. The simulated time courses were experimentally validated. SQUAD was mainly used to make predictions about time courses and thresholds, whereas CNA was used to analyze steady states and feedback loops.

Furthermore, new targets of ERK 1/2 which partially contribute, also in the formation of cardiac hypertrophy, were identified and the most promising of them were illuminated. Important further targets are Caspase 8, GAB2, Mxi-2, SMAD2, FHL2 and SPIN90.

Cardiomyocyte gene expression data sets were analyzed to verify involved components and to find further significantly altered genes after induced hypertrophy with TAC (transverse aortic constriction). Changes in the ultrastructure of the cardiomyocyte are the final result of induced hypertrophy.

Summing up all these findings, both, the third ERK phosphorylation as well as the RKIP-feedback loop are promising pharmacological target points.

Bibliography

[1] W. David Merryman Alison K. Schroer, Larisa M. Ryzhova. Network modeling approach to predict myo?broblast differentiation. *Cellular and Molecular Bioengineering*, 2014.

[2] L. A. Allan, N. Morrice, S. Brady, G. Magee, S. Pathak, and P. R. Clarke. Inhibition of caspase-9 through phosphorylation at thr 125 by erk mapk. *Nat Cell Biol*, 5(7):647–54, 2003.

[3] M. Alvarado-Kristensson, F. Melander, K. Leandersson, L. Ronnstrand, C. Wernstedt, and T. Andersson. p38-mapk signals survival by phosphorylation of caspase-8 and caspase-3 in human neutrophils. *J Exp Med*, 199(4):449–58, 2004.

[4] Yaman Arkun. Dynamic modeling and analysis of the cross-talk between insulin/akt and mapk/erk signaling pathways. *PloS one*, 11:e0149684, 2016.

[5] M. Arnaud, C. Crouin, C. Deon, D. Loyaux, and J. Bertoglio. Phosphorylation of grb2-associated binder 2 on serine 623 by erk mapk regulates its association with the phosphatase shp-2 and decreases stat5 activation. *J Immunol*, 173(6):3962–71, 2004.

[6] E T Askevold, P Aukrust, S H Nymo, I G Lunde, O J Kaasbøll, S Aakhus, G Florholmen, I K Ohm, M E Strand, H Attramadal, A Fiane, C P Dahl, A V Finsen, L E Vinge, G Christensen, A Yndestad, L Gullestad, R Latini, S Masson, L Tavazzi, GISSI-HF Investigators, and T Ueland. The cardiokine secreted frizzled-related protein 3, a modulator of wnt signalling, in clinical and experimental heart failure. *Journal of internal medicine*, 275:621–630, June 2014.

[7] J Avruch, A Khokhlatchev, J M Kyriakis, Z Luo, G Tzivion, D Vavvas, and X F Zhang. Ras activation of the raf kinase: tyrosine kinase recruitment of the map kinase cascade. *Recent progress in hormone research*, 56:127–155, 2001.

[8] N. Babchia, A. Calipel, F. Mouriaux, A. M. Faussat, and F. Mascarelli. The pi3k/akt and mtor/p70s6k signaling pathways in human uveal melanoma cells: interaction with b-raf/erk. *Invest Ophthalmol Vis Sci*, 51(1):421–9, 2010.

[9] Bundesaerztekammer (BAEK), Kassenaerztliche Bundesvereinigung (KBV), and Arbeitsgemeinschaft der Wissenschaftlichen Medizinischen Fachgesellschaften (AWMF). Nationale versorgungsleitlinie chronische herzinsuffizienz Ű kurzfassung, 2. auflage. 2017.

[10] M. C. Balasu, L. N. Spiridon, S. Miron, C. T. Craescu, A. J. Scheidig, A. J. Petrescu, and S. E. Szedlacsek. Interface analysis of the complex between erk2 and ptp-sl. *PLoS One*, 4(5):e5432, 2009.

[11] Albert-László Barabási and Zoltán N Oltvai. Network biology: understanding the cell's functional organization. *Nature reviews. Genetics*, 5:101–113, February 2004.

[12] T. Barrett, S. E. Wilhite, P. Ledoux, C. Evangelista, I. F. Kim, M. Tomashevsky, K. A. Marshall, K. H. Phillippy, P. M. Sherman, M. Holko, A. Yefanov, H. Lee, N. Zhang, C. L. Robertson, N. Serova, S. Davis, and A. Soboleva. Ncbi geo: archive for functional genomics data sets–update. *Nucleic Acids Res*, 41(Database issue):D991–5, 2013.

[13] C. Bartholomeusz, D. Rosen, C. Wei, A. Kazansky, F. Yamasaki, T. Takahashi, H. Itamochi, S. Kondo, J. Liu, and N. T. Ueno. Pea-15 induces autophagy in human ovarian cancer cells and is associated with prolonged overall survival. *Cancer Res*, 68(22):9302–10, 2008.

[14] N. Belmonte, B. W. Phillips, F. Massiera, P. Villageois, B. Wdziekonski, P. Saint-Marc, J. Nichols, J. Aubert, K. Saeki, A. Yuo, S. Narumiya, G. Ailhaud, and C. Dani. Activation of extracellular signal-regulated kinases and creb/atf-1 mediate the expression of ccaat/enhancer binding proteins beta and -delta in preadipocytes. *Mol Endocrinol*, 15(11):2037–49, 2001.

[15] Yoaf Benjamini and Yosef Hochberg. Controlling the false discovery rate: a practical and powerful approach to multiple testing. *Journal of the Royal Statistical Society*, 57(Series B):289–300, 1995.

[16] Erika Bereczki and Miklós Sántha. The role of biglycan in the heart. *Connective tissue research*, 49:129–132, 2008.

[17] B. C. Bernardo, K. L. Weeks, L. Pretorius, and J. R. McMullen. Molecular distinction between physiological and pathological cardiac hypertrophy: experimental findings and therapeutic strategies. *Pharmacol Ther*, 128(1):191–227, 2010.

[18] Robert Besancon. *The Encyclopedia of Physics*. Number P. 406. Springer Science & Business Media, p. 406, 2013.

[19] Antoine Besnard, Beatriz Galan-Rodriguez, Peter Vanhoutte, and Jocelyne Caboche. Elk-1 a transcription factor with multiple facets in the brain. *Frontiers in neuroscience*, 5:35, 2011.

[20] Nils Blüthgen and Stefan Legewie. Systems analysis of mapk signal transduction. *Essays in biochemistry*, 45:95–107, 2008.

[21] Richard Bonneau. Learning biological networks: from modules to dynamics. *Nature chemical biology*, 4:658–664, November 2008.

[22] Paola Bovolenta, Pilar Esteve, Jose Maria Ruiz, Elsa Cisneros, and Javier Lopez-Rios. Beyond wnt inhibition: new functions of secreted frizzled-related proteins in development and disease. *Journal of cell science*, 121:737–746, March 2008.

[23] D. Boyanova, S. Nilla, I. Birschmann, T. Dandekar, and M. Dittrich. Plateletweb: a systems biologic analysis of signaling networks in human platelets. *Blood*, 119(3):e22–34, 2012.

[24] Tim Breitenbach, Kristina Lorenz, and Thomas Dandekar. How to steer and control erk and the erk signaling cascade exemplified by looking at cardiac insufficiency. *International journal of molecular sciences*, 20, May 2019.

[25] Alexandra Brietz, Kristin Verena Schuch, Gaby Wangorsch, Kristina Lorenz, and Thomas Dandekar. Analyzing erk 1/2 signalling and targets. *Mol. BioSyst.*, 12:2436–2446, 2016.

[26] Tilman Brummer, Mark Larance, Maria Teresa Herrera Abreu, Ruth J Lyons, Paul Timpson, Christoph H Emmerich, Emmy D G Fleuren, Gillian M Lehrbach, Daniel Schramek, Michael Guilhaus, David E James, and Roger J Daly. Phosphorylation-dependent binding of 14-3-3 terminates signalling by the gab2 docking protein. *The EMBO journal*, 27:2305–2316, September 2008.

[27] O F Bueno, L J De Windt, K M Tymitz, S A Witt, T R Kimball, R Klevitsky, T E Hewett, S P Jones, D J Lefer, C F Peng, R N Kitsis, and J D Molkentin. The mek1-erk1/2 signaling pathway promotes compensated cardiac hypertrophy in transgenic mice. *The EMBO journal*, 19:6341–6350, December 2000.

[28] O. F. Bueno and J. D. Molkentin. Involvement of extracellular signal-regulated kinases 1/2 in cardiac hypertrophy and cell death. *Circ Res*, 91(9):776–81, 2002.

[29] Anh L Bui, Tamara B Horwich, and Gregg C Fonarow. Epidemiology and risk profile of heart failure. *Nature reviews. Cardiology*, 8:30–41, January 2011.

[30] Statistisches Bundesamt. Todesursachenstatistik. *Statistisches Bundesamt, Fachserie 12, Reihe 4*.

[31] T. J. Burkholder. Stretch-induced erk2 phosphorylation requires pla2 activity in skeletal myotubes. *Biochem Biophys Res Commun*, 386(1):60–4, 2009.

[32] A. Byron, J. D. Humphries, S. E. Craig, D. Knight, and M. J. Humphries. Proteomic analysis of alpha4beta1 integrin adhesion complexes reveals alpha-subunit-dependent protein recruitment. *Proteomics*, 12(13):2107–14, 2012.

[33] A. M. Cacace, N. R. Michaud, M. Therrien, K. Mathes, T. Copeland, G. M. Rubin, and D. K. Morrison. Identification of constitutive and ras-inducible phosphorylation sites of ksr: implications for 14-3-3 binding, mitogen-activated protein kinase binding, and ksr overexpression. *Mol Cell Biol*, 19(1):229–40, 1999.

[34] S. Cagnol, E. Van Obberghen-Schilling, and J. C. Chambard. Prolonged activation of erk1,2 induces fadd-independent caspase 8 activation and cell death. *Apoptosis*, 11(3):337–46, 2006.

[35] O. L. Carpenter and S. Wu. Regulation of msk1-mediated nf-kappab activation upon uvb irradiation. *Photochem Photobiol*, 2013.

[36] A. Carriere, H. Ray, J. Blenis, and P. P. Roux. The rsk factors of activating the ras/mapk signaling cascade. *Front Biosci*, 13:4258–75, 2008.

[37] Berta Casar, Javier Rodríguez, Gilad Gibor, Rony Seger, and Piero Crespo. Mxi2 sustains erk1/2 phosphorylation in the nucleus by preventing erk1/2 binding to phosphatases. *The Biochemical journal*, 441:571–578, January 2012.

[38] Berta Casar, Victoria Sanz-Moreno, Mustafa N Yazicioglu, Javier Rodríguez, María T Berciano, Miguel Lafarga, Melanie H Cobb, and Piero Crespo. Mxi2 promotes stimulus-independent erk nuclear translocation. *The EMBO journal*, 26:635–646, February 2007.

[39] C. J. Caunt and C. A. McArdle. Erk phosphorylation and nuclear accumulation: insights from single-cell imaging. *Biochem Soc Trans*, 40(1):224–9, 2012.

[40] Y Chai, G Chipitsyna, J Cui, B Liao, S Liu, K Aysola, M Yezdani, E S Reddy, and V N Rao. c-fos oncogene regulator elk-1 interacts with brca1 splice variants brca1a/1b and enhances brca1a/1b-mediated growth suppression in breast cancer cells. *Oncogene*, 20:1357–1367, March 2001.

[41] Z Chen, T B Gibson, F Robinson, L Silvestro, G Pearson, B Xu, A Wright, C Vanderbilt, and M H Cobb. Map kinases. *Chemical reviews*, 101:2449–2476, August 2001.

[42] E. Chevet, H. N. Wong, D. Gerber, C. Cochet, A. Fazel, P. H. Cameron, J. N. Gushue, D. Y. Thomas, and J. J. Bergeron. Phosphorylation by ck2 and mapk enhances calnexin association with ribosomes. *EMBO J*, 18(13):3655–66, 1999.

[43] M. Cormont, J. F. Tanti, A. Zahraoui, E. Van Obberghen, and Y. Le Marchand-Brustel. Rab4 is phosphorylated by the insulin-activated extracellular-signal-regulated kinase erk1. *Eur J Biochem*, 219(3):1081–5, 1994.

[44] P. S. Costello, R. H. Nicolas, Y. Watanabe, I. Rosewell, and R. Treisman. Ternary complex factor sap-1 is required for erk-mediated thymocyte positive selection. *Nat Immunol*, 5(3):289–98, 2004.

[45] David J Crossman, Isuru D Jayasinghe, and Christian Soeller. Transverse tubule remodelling: a cellular pathology driven by both sides of the plasmalemma? *Biophysical reviews*, 9:919–929, December 2017.

[46] M. Deak, A. D. Clifton, L. M. Lucocq, and D. R. Alessi. Mitogen- and stress-activated protein kinase-1 (msk1) is directly activated by mapk and sapk2/p38, and may mediate activation of creb. *EMBO J*, 17(15):4426–41, 1998.

[47] A. C. deAlmeida, R. J. van Oort, and X. H. Wehrens. Transverse aortic constriction in mice. *J Vis Exp*, (38), 2010.

[48] K. Deiss, C. Kisker, M. J. Lohse, and K. Lorenz. Raf kinase inhibitor protein (rkip) dimer formation controls its target switch from raf1 to g protein-coupled receptor kinase (grk) 2. *J Biol Chem*, 287(28):23407–17, 2012.

[49] A. Di Cara, A. Garg, G. De Micheli, I. Xenarios, and L. Mendoza. Dynamic simulation of regulatory networks using squad. *BMC Bioinformatics*, 8:462, 2007.

[50] Gloria A Di Lullo, Shawn M Sweeney, Jarmo Korkko, Leena Ala-Kokko, and James D San Antonio. Mapping the ligand-binding sites and disease-associated mutations on the most abundant protein in the human, type i collagen. *The Journal of biological chemistry*, 277:4223–4231, February 2002.

[51] E. Diaz-Rodriguez, J. C. Montero, A. Esparis-Ogando, L. Yuste, and A. Pandiella. Extracellular signal-regulated kinase phosphorylates tumor necrosis factor alpha-converting enzyme at threonine 735: a potential role in regulated shedding. *Mol Biol Cell*, 13(6):2031–44, 2002.

[52] M. Donsmark, J. Langfort, C. Holm, T. Ploug, and H. Galbo. Contractions activate hormone-sensitive lipase in rat muscle by protein kinase c and mitogen-activated protein kinase. *J Physiol*, 550(Pt 3):845–54, 2003.

[53] M. Donsmark, J. Langfort, C. Holm, T. Ploug, and H. Galbo. Regulation and role of hormone-sensitive lipase in rat skeletal muscle. *Proc Nutr Soc*, 63(2):309–14, 2004.

[54] Werner Dubitzky, Olaf Wolkenhauer, et al. *Encyclopedia of Systems Biology*. Springer New York, p. 1680-1681, 2013.

[55] F Ebner and M Reiter. The alteration by propranolol of the inotropic and bathmotropic effects of dihydro-ouabain on guinea-pig papillary muscle. *Naunyn-Schmiedeberg's archives of pharmacology*, 307:99–104, June 1979.

[56] Yasemin Erten, Murat Tulmac, Ulver Derici, Hatice Pasaoglu, Kadriye Altok Reis, Musa Bali, Turgay Arinsoy, Atiye Cengel, and Sukru Sindel. An association between inflammatory state and left ventricular hypertrophy in hemodialysis patients. *Renal failure*, 27:581–589, 2005.

[57] J. Eswaran, J. P. von Kries, B. Marsden, E. Longman, J. E. Debreczeni, E. Ugochukwu, A. Turnbull, W. H. Lee, S. Knapp, and A. J. Barr. Crystal structures and inhibitor identification for ptpn5, ptprr and ptpn7: a family of

human mapk-specific protein tyrosine phosphatases. *Biochem J*, 395(3):483–91, 2006.

[58] H.-W. Baenkler et al. *Kurzlehrbuch Innere Medizin*. Georg Thieme Verlag KG, 2007.

[59] Tama Evron, Tanya L Daigle, and Marc G Caron. Grk2: multiple roles beyond g protein-coupled receptor desensitization. *Trends in pharmacological sciences*, 33:154–164, March 2012.

[60] M. Fabbro, B. B. Zhou, M. Takahashi, B. Sarcevic, P. Lal, M. E. Graham, B. G. Gabrielli, P. J. Robinson, E. A. Nigg, Y. Ono, and K. K. Khanna. Cdk1/erk2- and plk1-dependent phosphorylation of a centrosome protein, cep55, is required for its recruitment to midbody and cytokinesis. *Dev Cell*, 9(4):477–88, 2005.

[61] E. J. Faivre and C. A. Lange. Progesterone receptors upregulate wnt-1 to induce epidermal growth factor receptor transactivation and c-src-dependent sustained activation of erk1/2 mitogen-activated protein kinase in breast cancer cells. *Mol Cell Biol*, 27(2):466–80, 2007.

[62] H. Farhan, M. W. Wendeler, S. Mitrovic, E. Fava, Y. Silberberg, R. Sharan, M. Zerial, and H. P. Hauri. Mapk signaling to the early secretory pathway revealed by kinase/phosphatase functional screening. *J Cell Biol*, 189(6):997–1011, 2010.

[63] Xin-Hua Feng, Yao-Yun Liang, Min Liang, Weiguo Zhai, and Xia Lin. Direct interaction of c-myc with smad2 and smad3 to inhibit tgf-beta-mediated induction of the cdk inhibitor p15(ink4b). *Molecular cell*, 9:133–143, January 2002.

[64] S. N. Finver, K. Nishikura, L. R. Finger, F. G. Haluska, J. Finan, P. C. Nowell, and C. M. Croce. Sequence analysis of the myc oncogene involved in the t(8;14)(q24;q11) chromosome translocation in a human leukemia t-cell line indicates that putative regulatory regions are not altered. *Proc Natl Acad Sci U S A*, 85(9):3052–6, 1988.

[65] J. Font de Mora and M. Brown. Aib1 is a conduit for kinase-mediated growth factor signaling to the estrogen receptor. *Mol Cell Biol*, 20(14):5041–7, 2000.

[66] C. Forcet, E. Stein, L. Pays, V. Corset, F. Llambi, M. Tessier-Lavigne, and P. Mehlen. Netrin-1-mediated axon outgrowth requires deleted in colorectal cancer-dependent mapk activation. *Nature*, 417(6887):443–7, 2002.

[67] N Frey, J A Richardson, and E N Olson. Calsarcins, a novel family of sarcomeric calcineurin-binding proteins. *Proceedings of the National Academy of Sciences of the United States of America*, 97:14632–14637, December 2000.

[68] M. Frodin and S. Gammeltoft. Role and regulation of 90 kda ribosomal s6 kinase (rsk) in signal transduction. *Mol Cell Endocrinol*, 151(1-2):65–77, 1999.

[69] Matsuoka Y. Jouraku A. Morohashi M. Kikuchi N. Kitano H. Funahashi, A. Celldesigner 3.5: A versatile modeling tool for biochemical networks. *Proceedings of the IEEE*, 96:1254–1265, 2008.

[70] Simona Gallo, Annapia Vitacolonna, Alessandro Bonzano, Paolo Comoglio, and Tiziana Crepaldi. Erk: A key player in the pathophysiology of cardiac hypertrophy. *International journal of molecular sciences*, 20, May 2019.

[71] J. Garcia, Y. Ye, V. Arranz, C. Letourneux, G. Pezeron, and F. Porteu. Iex-1: a new erk substrate involved in both erk survival activity and erk activation. *EMBO J*, 21(19):5151–63, 2002.

[72] A. Garg, I. Xenarios, L. Mendoza, and DeMicheli G. *An Efficient Method for Dynamic Analysis of Gene Regulatory Networks and in silico Gene Perturbation Experiments. In: Research in Computational Molecular Biology. RECOMB 2007.*, volume 4453 of *Lecture Notes in Computer Science*. Springer, Berlin, Heidelberg, 2007.

[73] Nancy Gerits, Sergiy Kostenko, and Ugo Moens. In vivo functions of mitogen-activated protein kinases: conclusions from knock-in and knock-out mice. *Transgenic research*, 16:281–314, June 2007.

[74] Shouryadipta Ghosh, Kenneth Tran, Lea M D Delbridge, Anthony J R Hickey, Eric Hanssen, Edmund J Crampin, and Vijay Rajagopal. Insights on the impact of mitochondrial organisation on bioenergetics in high-resolution computational models of cardiac cell architecture. *PLoS computational biology*, 14:e1006640, December 2018.

[75] Y Gluzman. Sv40-transformed simian cells support the replication of early sv40 mutants. *Cell*, 23:175–182, January 1981.

[76] Arantxa González, Begoña López, Susana Ravassa, Gorka San José, and Javier Díez. The complex dynamics of myocardial interstitial fibrosis in heart failure. focus on collagen cross-linking. *Biochimica et biophysica acta. Molecular cell research*, 1866:1421–1432, September 2019.

[77] Luca Grieco, Laurence Calzone, Isabelle Bernard-Pierrot, François Radvanyi, Brigitte Kahn-Perlès, and Denis Thieffry. Integrative modelling of the influence of mapk network on cancer cell fate decision. *PLoS computational biology*, 9:e1003286, October 2013.

[78] M. H. Han, W. S. Lee, A. Nagappan, H. J. Kim, C. Park, G. Y. Kim, S. H. Hong, N. D. Kim, G. Kim, C. H. Ryu, S. C. Shin, and Y. H. Choi. Polyphenols from korean prostrate spurge euphorbia supina induce apoptosis through the fas-associated extrinsic pathway and activation of erk in human leukemic u937 cells. *Oncol Rep*, 2016.

[79] H. Hao, V. M. Muniz-Medina, H. Mehta, N. E. Thomas, V. Khazak, C. J. Der, and J. M. Shields. Context-dependent roles of mutant b-raf signaling in melanoma and colorectal carcinoma cell growth. *Mol Cancer Ther*, 6(8):2220–9, 2007.

[80] I. S. Harris, S. Zhang, I. Treskov, A. Kovacs, C. Weinheimer, and A. J. Muslin. Raf-1 kinase is required for cardiac hypertrophy and cardiomyocyte survival in response to pressure overload. *Circulation*, 110(6):718–23, 2004.

[81] J. Hayakawa, C. Depatie, M. Ohmichi, and D. Mercola. The activation of c-jun nh2-terminal kinase (jnk) by dna-damaging agents serves to promote drug resistance via activating transcription factor 2 (atf2)-dependent enhanced dna repair. *J Biol Chem*, 278(23):20582–92, 2003.

[82] Joerg Heineke and Jeffery D Molkentin. Regulation of cardiac hypertrophy by intracellular signalling pathways. *Nature reviews. Molecular cell biology*, 7:589–600, August 2006.

[83] T. J. Hemesath, E. R. Price, C. Takemoto, T. Badalian, and D. E. Fisher. Map kinase links the transcription factor microphthalmia to c-kit signalling in melanocytes. *Nature*, 391(6664):298–301, 1998.

[84] Z. Herincs, V. Corset, N. Cahuzac, C. Furne, V. Castellani, A. O. Hueber, and P. Mehlen. Dcc association with lipid rafts is required for netrin-1-mediated axon guidance. *J Cell Sci*, 118(Pt 8):1687–92, 2005.

[85] Stephane Heymans, Maarten F Corsten, Wouter Verhesen, Paolo Carai, Rick E W van Leeuwen, Kevin Custers, Tim Peters, Mark Hazebroek, Lauran Stöger, Erwin Wijnands, Ben J Janssen, Esther E Creemers, Yigal M Pinto, Dirk Grimm, Nina Schürmann, Elena Vigorito, Thomas Thum, Frank Stassen, Xiaoke Yin, Manuel Mayr, Leon J de Windt, Esther Lutgens, Kristiaan Wouters, Menno P J de Winther, Serena Zacchigna, Mauro Giacca, Marc van Bilsen, Anna-Pia Papageorgiou, and Blanche Schroen. Macrophage microrna-155 promotes cardiac hypertrophy and failure. *Circulation*, 128:1420–1432, September 2013.

[86] R. Hoffmann and A. Valencia. A gene network for navigating the literature. *Nat Genet*, 36(7):664, 2004.

[87] Paulien Hogeweg. The roots of bioinformatics in theoretical biology. *PLoS computational biology*, 7:e1002021, March 2011.

[88] Michael Huerta, Florence Haseltine, and Yuan Liu. Nih working definition of bioinformatics and computational biology. 07 2000.

[89] J J Hunter and K R Chien. Signaling pathways for cardiac hypertrophy and failure. *The New England journal of medicine*, 341:1276–1283, October 1999.

[90] Jianhua Huo, Feng Wei, Chengzhong Cai, Beverly Lyn-Cook, and Li Pang. Sex-related differences in drug-induced qt prolongation and torsades de pointes: A new model system with human ipsc-cms. *Toxicological sciences : an official journal of the Society of Toxicology*, 167:360–374, February 2019.

[91] T. Ichise, N. Yoshida, and H. Ichise. Fgf2-induced ras-mapk signalling maintains lymphatic endothelial cell identity by upregulating endothelial-cell-specific gene expression and suppressing tgfbeta signalling through smad2. *J Cell Sci*, 127(Pt 4):845–57, 2014.

[92] Roshanak Irannejad, Jin C Tomshine, Jon R Tomshine, Michael Chevalier, Jacob P Mahoney, Jan Steyaert, Søren G F Rasmussen, Roger K Sunahara, Hana El-Samad, Bo Huang, and Mark von Zastrow. Conformational biosensors reveal gpcr signalling from endosomes. *Nature*, 495:534–538, March 2013.

[93] R. Janknecht, W. H. Ernst, V. Pingoud, and A. Nordheim. Activation of ternary complex factor elk-1 by map kinases. *EMBO J*, 12(13):5097–104, 1993.

[94] Z I Januskevicius, P V Zabela, D I Zemaitytė, B I Liutkevich, and A P Audickienė. [comparison of antiarrhythmic and chronotropic effect of obsidan and isoptine in extrasystole]. *Kardiologiia*, 16:20–26, April 1976.

[95] J. Jiang, P. Mohan, and C. A. Maxwell. The cytoskeletal protein rhamm and erk1/2 activity maintain the pluripotency of murine embryonic stem cells. *PLoS One*, 8(9):e73548, 2013.

[96] Karoline Horgmo Jæger, Verena Charwat, Bérénice Charrez, Henrik Finsberg, Mary M Maleckar, Samuel Wall, Kevin E Healy, and Aslak Tveito. Improved computational identification of drug response using optical measurements of human stem cell derived cardiomyocytes in microphysiological systems. *Frontiers in pharmacology*, 10:1648, 2019.

[97] Karoline Horgmo Jæger, Andrew G Edwards, Andrew McCulloch, and Aslak Tveito. Properties of cardiac conduction in a cell-based computational model. *PLoS computational biology*, 15:e1007042, May 2019.

[98] Jun Hyuk Kang, Ho-Sung Lee, Yun-Won Kang, and Kwang-Hyun Cho. Systems biological approaches to the cardiac signaling network. *Briefings in bioinformatics*, 17:419–428, May 2016.

[99] S. Kang, S. Dong, A. Guo, H. Ruan, S. Lonial, H. J. Khoury, T. L. Gu, and J. Chen. Epidermal growth factor stimulates rsk2 activation through activation of the mek/erk pathway and src-dependent tyrosine phosphorylation of rsk2 at tyr-529. *J Biol Chem*, 283(8):4652–7, 2008.

[100] Y. J. Kang. Cardiac hypertrophy: a risk factor for qt-prolongation and cardiac sudden death. *Toxicol Pathol*, 34(1):58–66, 2006.

[101] K. Kato, A. Utani, N. Suzuki, M. Mochizuki, M. Yamada, N. Nishi, H. Matsuura, H. Shinkai, and M. Nomizu. Identification of neurite outgrowth promoting sites on the laminin alpha 3 chain g domain. *Biochemistry*, 41(35):10747–53, 2002.

[102] Clinton D Kemp and John V Conte. The pathophysiology of heart failure. *Cardiovascular pathology : the official journal of the Society for Cardiovascular Pathology*, 21:365–371, 2012.

[103] Y. Keshet and R. Seger. The map kinase signaling cascades: a system of hundreds of components regulates a diverse array of physiological functions. *Methods Mol Biol*, 661:3–38, 2010.

[104] D. W. Kim and B. H. Cochran. Extracellular signal-regulated kinase binds to tfii-i and regulates its activation of the c-fos promoter. *Mol Cell Biol*, 20(4):1140–8, 2000.

[105] D. W. Kim and B. H. Cochran. Jak2 activates tfii-i and regulates its interaction with extracellular signal-regulated kinase. *Mol Cell Biol*, 21(10):3387–97, 2001.

[106] S. Kim, T. Bondeva, and P. G. Nelson. Activation of protein kinase c isozymes in primary mouse myotubes by carbachol. *Brain Res Dev Brain Res*, 137(1):13–21, 2002.

[107] S. Klamt, J. Saez-Rodriguez, and E. D. Gilles. Structural and functional analysis of cellular networks with cellnetanalyzer. *BMC Syst Biol*, 1:2, 2007.

[108] S. Klamt, J. Stelling, M. Ginkel, and E. D. Gilles. Fluxanalyzer: exploring structure, pathways, and flux distributions in metabolic networks on interactive flux maps. *Bioinformatics*, 19(2):261–9, 2003.

[109] S. Klamt and A. von Kamp. An application programming interface for cellnetanalyzer. *Biosystems*, 105(2):162–8, 2011.

[110] S. Kojima, M. Okuno, R. Matsushima-Nishiwaki, S. L. Friedman, and H. Moriwaki. Acyclic retinoid in the chemoprevention of hepatocellular carcinoma (review). *Int J Oncol*, 24(4):797–805, 2004.

[111] Walter Kolch, Muffy Calder, and David Gilbert. When kinases meet mathematics: the systems biology of mapk signalling. *FEBS letters*, 579:1891–1895, March 2005.

[112] D. Konstantinidis, G. Koliakos, K. Vafia, P. Liakos, C. Bantekas, V. Trachana, and M. Kaloyianni. Inhibition of the na+-h+ exchanger isoform-1 and the extracellular signal-regulated kinase induces apoptosis: a time course of events. *Cell Physiol Biochem*, 18(4-5):211–22, 2006.

[113] M Kretzschmar, J Doody, I Timokhina, and J Massagué. A mechanism of repression of tgfbeta/ smad signaling by oncogenic ras. *Genes & development*, 13:804–816, April 1999.

[114] J. Krueger, F. L. Chou, A. Glading, E. Schaefer, and M. H. Ginsberg. Phosphorylation of phosphoprotein enriched in astrocytes (pea-15) regulates extracellular signal-regulated kinase-dependent transcription and cell proliferation. *Mol Biol Cell*, 16(8):3552–61, 2005.

[115] A. Kumagai, H. Namba, S. Takakura, E. Inamasu, V. A. Saenko, A. Ohtsuru, and S. Yamashita. No evidence of araf, craf and met mutations in braft1799a negative human papillary thyroid carcinoma. *Endocr J*, 53(5):615–20, 2006.

[116] Johanna Kuusisto, Vesa Kärjä, Petri Sipola, Ivana Kholová, Keijo Peuhkurinen, Pertti Jääskeläinen, Anita Naukkarinen, Seppo Ylä-Herttuala, Kari Punnonen, and Markku Laakso. Low-grade inflammation and the phenotypic expression of myocardial fibrosis in hypertrophic cardiomyopathy. *Heart (British Cardiac Society)*, 98:1007–1013, July 2012.

[117] J. M. Kyriakis and J. Avruch. Protein kinase cascades activated by stress and inflammatory cytokines. *Bioessays*, 18(7):567–77, 1996.

[118] John M Kyriakis and Joseph Avruch. Mammalian mapk signal transduction pathways activated by stress and inflammation: a 10-year update. *Physiological reviews*, 92:689–737, April 2012.

[119] Anuradha Lala and Akshay S Desai. The role of coronary artery disease in heart failure. *Heart failure clinics*, 10:353–365, April 2014.

[120] P. Langlais, C. Wang, L. Q. Dong, C. A. Carroll, S. T. Weintraub, and F. Liu. Phosphorylation of grb10 by mitogen-activated protein kinase: identification of ser150 and ser476 of human grb10zeta as major phosphorylation sites. *Biochemistry*, 44(24):8890–7, 2005.

[121] Chen Li, Zhongxiu Chen, Hao Yang, Fangbo Luo, Lihong Chen, Huawei Cai, Yajiao Li, Guiying You, Dan Long, Shengfu Li, Qiuping Zhang, and Li Rao. Selumetinib, an oral anti-neoplastic drug, may attenuate cardiac hypertrophy via targeting the erk pathway. *PloS one*, 11:e0159079, 2016.

[122] J. H. Li, X. R. Huang, H. J. Zhu, M. Oldfield, M. Cooper, L. D. Truong, R. J. Johnson, and H. Y. Lan. Advanced glycation end products activate smad signaling via tgf-beta-dependent and independent mechanisms: implications for diabetic renal and vascular disease. *FASEB J*, 18(1):176–8, 2004.

[123] R. Li, Z. Gong, C. Pan, D. D. Xie, J. Y. Tang, M. Cui, Y. F. Xu, W. Yao, Q. Pang, Z. G. Xu, M. Y. Li, X. Yu, and J. P. Sun. Metal-dependent protein phosphatase 1a functions as an extracellular signal-regulated kinase phosphatase. *FEBS J*, 280(11):2700–11, 2013.

[124] X. Li, V. G. Brunton, H. R. Burgar, L. M. Wheldon, and J. K. Heath. Frs2-dependent src activation is required for fibroblast growth factor receptor-induced phosphorylation of sprouty and suppression of erk activity. *J Cell Sci*, 117(Pt 25):6007–17, 2004.

[125] Q. Liang, R. J. Wiese, O. F. Bueno, Y. S. Dai, B. E. Markham, and J. D. Molkentin. The transcription factor gata4 is activated by extracellular signal-regulated kinase 1- and 2-mediated phosphorylation of serine 105 in cardiomyocytes. *Mol Cell Biol*, 21(21):7460–9, 2001.

[126] W. X. Liao, L. Feng, H. Zhang, J. Zheng, T. R. Moore, and D. B. Chen. Compartmentalizing vegf-induced erk2/1 signaling in placental artery endothelial cell caveolae: a paradoxical role of caveolin-1 in placental angiogenesis in vitro. *Mol Endocrinol*, 23(9):1428–44, 2009.

[127] C. S. Lim, S. H. Kim, J. G. Jung, J. K. Kim, and W. K. Song. Regulation of spin90 phosphorylation and interaction with nck by erk and cell adhesion. *J Biol Chem*, 278(52):52116–23, 2003.

[128] Peiyun Liu and Tao P Zhong. Mapk/erk signalling is required for zebrafish cardiac regeneration. *Biotechnology letters*, 39:1069–1077, July 2017.

[129] R. S. Lo, D. Wotton, and J. Massague. Epidermal growth factor signaling via ras controls the smad transcriptional co-repressor tgif. *EMBO J*, 20(1-2):128–36, 2001.

[130] A. Locatelli and C. A. Lange. Met receptors induce sam68-dependent cell migration by activation of alternate extracellular signal-regulated kinase family members. *J Biol Chem*, 286(24):21062–72, 2011.

[131] K. Lorenz, M. J. Lohse, and U. Quitterer. Protein kinase c switches the raf kinase inhibitor from raf-1 to grk-2. *Nature*, 426(6966):574–9, 2003.

[132] K. Lorenz, E. Schmid, and K. Deiss. Rkip: a governor of intracellular signaling. *Crit Rev Oncog*, 19(6):489–96, 2014.

[133] K. Lorenz, J. P. Schmitt, E. M. Schmitteckert, and M. J. Lohse. A new type of erk1/2 autophosphorylation causes cardiac hypertrophy. *Nat Med*, 15(1):75–83, 2009.

[134] K. Lorenz, J. P. Schmitt, M. Vidal, and M. J. Lohse. Cardiac hypertrophy: targeting raf/mek/erk1/2-signaling. *Int J Biochem Cell Biol*, 41(12):2351–5, 2009.

[135] K. Lorenz, K. Stathopoulou, E. Schmid, P. Eder, and F. Cuello. Heart failure-specific changes in protein kinase signalling. *Pflugers Arch*, 466(6):1151–62, 2014.

[136] M. Maekawa, E. Nishida, and T. Tanoue. Identification of the anti-proliferative protein tob as a mapk substrate. *J Biol Chem*, 277(40):37783–7, 2002.

[137] M. Majka, J. Ratajczak, M. A. Kowalska, and M. Z. Ratajczak. Binding of stromal derived factor-1alpha (sdf-1alpha) to cxcr4 chemokine receptor in normal human megakaryoblasts but not in platelets induces phosphorylation of mitogen-activated protein kinase p42/44 (mapk), elk-1 transcription factor and serine/threonine kinase akt. *Eur J Haematol*, 64(3):164–72, 2000.

[138] M. Majumdar, J. Meenakshi, S. K. Goswami, and K. Datta. Hyaluronan binding protein 1 (habp1)/c1qbp/p32 is an endogenous substrate for map kinase and is translocated to the nucleus upon mitogenic stimulation. *Biochem Biophys Res Commun*, 291(4):829–37, 2002.

[139] H. Makkonen, T. Jaaskelainen, T. Pitkanen-Arsiola, M. Rytinki, K. K. Waltering, M. Matto, T. Visakorpi, and J. J. Palvimo. Identification of ets-like transcription factor 4 as a novel androgen receptor target in prostate cancer cells. *Oncogene*, 27(36):4865–76, 2008.

[140] M. Malmlof, E. Roudier, J. Hogberg, and U. Stenius. Mek-erk-mediated phosphorylation of mdm2 at ser-166 in hepatocytes. mdm2 is activated in response to inhibited akt signaling. *J Biol Chem*, 282(4):2288–96, 2007.

[141] Ranadip Mandal, Monika Raab, Yves Matthess, Sven Becker, Rainald Knecht, and Klaus Strebhardt. perk 1/2 inhibit caspase-8 induced apoptosis in cancer cells by phosphorylating it in a cell cycle specific manner. *Molecular oncology*, 8:232–249, March 2014.

[142] M. C. Martin, L. A. Allan, E. J. Mancini, and P. R. Clarke. The docking interaction of caspase-9 with erk2 provides a mechanism for the selective inhibitory phosphorylation of caspase-9 at threonine 125. *J Biol Chem*, 283(7):3854–65, 2008.

[143] MATLAB and Inc. Natick Massachusetts United States Statistics Toolbox Release 2012b, The MathWorks.

[144] John J V McMurray, Stamatis Adamopoulos, Stefan D Anker, Angelo Auricchio, Michael Böhm, Kenneth Dickstein, Volkmar Falk, Gerasimos Filippatos,

Cândida Fonseca, Miguel Angel Gomez-Sanchez, Tiny Jaarsma, Lars Køber, Gregory Y H Lip, Aldo Pietro Maggioni, Alexander Parkhomenko, Burkert M Pieske, Bogdan A Popescu, Per K Rønnevik, Frans H Rutten, Juerg Schwitter, Petar Seferovic, Janina Stepinska, Pedro T Trindade, Adriaan A Voors, Faiez Zannad, Andreas Zeiher, and ESC Committee for Practice Guidelines. Esc guidelines for the diagnosis and treatment of acute and chronic heart failure 2012: The task force for the diagnosis and treatment of acute and chronic heart failure 2012 of the european society of cardiology. developed in collaboration with the heart failure association (hfa) of the esc. *European heart journal*, 33:1787–1847, July 2012.

[145] C. Medeiros, M. J. Frederico, G. da Luz, J. R. Pauli, A. S. Silva, R. A. Pinho, L. A. Velloso, E. R. Ropelle, and C. T. De Souza. Exercise training reduces insulin resistance and upregulates the mtor/p70s6k pathway in cardiac muscle of diet-induced obesity rats. *J Cell Physiol*, 226(3):666–74, 2011.

[146] D. Medgyesi, R. Sarkozi, G. Koncz, K. Arato, G. Varadi, G. K. Toth, and G. Sarmay. Functional consequences of a mapk docking site on human fcgammariib. *Immunol Lett*, 92(1-2):83–90, 2004.

[147] Mandeep R Mehra, Patricia A Uber, and Gary S Francis. Heart failure therapy at a crossroad: are there limits to the neurohormonal model? *Journal of the American College of Cardiology*, 41:1606–1610, May 2003.

[148] M. Meier and G. L. King. Protein kinase c activation and its pharmacological inhibition in vascular disease. *Vasc Med*, 5(3):173–85, 2000.

[149] L. Mendoza and I. Xenarios. A method for the generation of standardized qualitative dynamical systems of regulatory networks. *Theor Biol Med Model*, 3:13, 2006.

[150] Mark Merchant, John Moffat, Gabriele Schaefer, Jocelyn Chan, Xi Wang, Christine Orr, Jason Cheng, Thomas Hunsaker, Lily Shao, Stephanie J Wang, Marie-Claire Wagle, Eva Lin, Peter M Haverty, Sheerin Shahidi-Latham, Hai Ngu, Margaret Solon, Jeffrey Eastham-Anderson, Hartmut Koeppen, Shih-Min A Huang, Jacob Schwarz, Marcia Belvin, Daniel Kirouac, and Melissa R Junttila. Combined mek and erk inhibition overcomes therapy-mediated pathway reactivation in ras mutant tumors. *PloS one*, 12:e0185862, 2017.

[151] Dimitra Micha, Dong-Chuan Guo, Yvonne Hilhorst-Hofstee, Fop van Kooten, Dian Atmaja, Eline Overwater, Ferdy K Cayami, Ellen S Regalado, René

van Uffelen, Hanka Venselaar, Sultana M H Faradz, Gerrit Vriend, Marjan M Weiss, Erik A Sistermans, Alessandra Maugeri, Dianna M Milewicz, Gerard Pals, and Fleur S van Dijk. Smad2 mutations are associated with arterial aneurysms and dissections. *Human mutation*, 36:1145–1149, December 2015.

[152] M. Mischnik, D. Boyanova, K. Hubertus, J. Geiger, N. Philippi, M. Dittrich, G. Wangorsch, J. Timmer, and T. Dandekar. A boolean view separates platelet activatory and inhibitory signalling as verified by phosphorylation monitoring including threshold behaviour and integrin modulation. *Mol Biosyst*, 9(6):1326–39, 2013.

[153] M. Mischnik, S. Gambaryan, H. Subramanian, J. Geiger, C. Schutz, J. Timmer, and T. Dandekar. A comparative analysis of the bistability switch for platelet aggregation by logic ode based dynamical modeling. *Mol Biosyst*, 10(8):2082–9, 2014.

[154] S. Miyamoto, H. Teramoto, J. S. Gutkind, and K. M. Yamada. Integrins can collaborate with growth factors for phosphorylation of receptor tyrosine kinases and map kinase activation: roles of integrin aggregation and occupancy of receptors. *J Cell Biol*, 135(6 Pt 1):1633–42, 1996.

[155] K. Mizutani, H. Ito, I. Iwamoto, R. Morishita, T. Deguchi, Y. Nozawa, T. Asano, and K. I. Nagata. Essential roles of erk-mediated phosphorylation of vinexin in cell spreading, migration and anchorage-independent growth. *Oncogene*, 26(50):7122–31, 2007.

[156] Francesco Moccia, Francesco Lodola, Ilaria Stadiotti, Chiara Assunta Pilato, Milena Bellin, Stefano Carugo, Giulio Pompilio, Elena Sommariva, and Angela Serena Maione. Calcium as a key player in arrhythmogenic cardiomyopathy: Adhesion disorder or intracellular alteration? *International journal of molecular sciences*, 20, August 2019.

[157] Jeffery D Molkentin. Parsing good versus bad signaling pathways in the heart: role of calcineurin-nuclear factor of activated t-cells. *Circulation research*, 113:16–19, June 2013.

[158] P. Monje, M. J. Marinissen, and J. S. Gutkind. Phosphorylation of the carboxyl-terminal transactivation domain of c-fos by extracellular signal-regulated kinase mediates the transcriptional activation of ap-1 and cellular transformation induced by platelet-derived growth factor. *Mol Cell Biol*, 23(19):7030–43, 2003.

[159] A. Motegi, J. Fujimoto, M. Kotani, H. Sakuraba, and T. Yamamoto. Alk receptor tyrosine kinase promotes cell growth and neurite outgrowth. *J Cell Sci*, 117(Pt 15):3319–29, 2004.

[160] Dariush Mozaffarian, Emelia J Benjamin, Alan S Go, Donna K Arnett, Michael J Blaha, Mary Cushman, Sarah de Ferranti, Jean-Pierre Després, Heather J Fullerton, Virginia J Howard, Mark D Huffman, Suzanne E Judd, Brett M Kissela, Daniel T Lackland, Judith H Lichtman, Lynda D Lisabeth, Simin Liu, Rachel H Mackey, David B Matchar, Darren K McGuire, Emile R Mohler, Claudia S Moy, Paul Muntner, Michael E Mussolino, Khurram Nasir, Robert W Neumar, Graham Nichol, Latha Palaniappan, Dilip K Pandey, Mathew J Reeves, Carlos J Rodriguez, Paul D Sorlie, Joel Stein, Amytis Towfighi, Tanya N Turan, Salim S Virani, Joshua Z Willey, Daniel Woo, Robert W Yeh, Melanie B Turner, American Heart Association Statistics Committee, and Stroke Statistics Subcommittee. Heart disease and stroke statistics–2015 update: a report from the american heart association. *Circulation*, 131:e29–322, January 2015.

[161] V. Muralidharan-Chari, J. Clancy, C. Plou, M. Romao, P. Chavrier, G. Raposo, and C. D'Souza-Schorey. Arf6-regulated shedding of tumor cell-derived plasma membrane microvesicles. *Curr Biol*, 19(22):1875–85, 2009.

[162] Michael Mutlak and Izhak Kehat. Extracellular signal-regulated kinases 1/2 as regulators of cardiac hypertrophy. *Frontiers in pharmacology*, 6:149, 2015.

[163] D. H. Nguyen, A. D. Catling, D. J. Webb, M. Sankovic, L. A. Walker, A. V. Somlyo, M. J. Weber, and S. L. Gonias. Myosin light chain kinase functions downstream of ras/erk to promote migration of urokinase-type plasminogen activator-stimulated cells in an integrin-selective manner. *J Cell Biol*, 146(1):149–64, 1999.

[164] L. Nie, M. Xu, A. Vladimirova, and X. H. Sun. Notch-induced e2a ubiquitination and degradation are controlled by map kinase activities. *EMBO J*, 22(21):5780–92, 2003.

[165] T. Noguchi, M. Tsuda, H. Takeda, T. Takada, K. Inagaki, T. Yamao, K. Fukunaga, T. Matozaki, and M. Kasuga. Inhibition of cell growth and spreading by stomach cancer-associated protein-tyrosine phosphatase-1 (sap-1) through dephosphorylation of p130cas. *J Biol Chem*, 276(18):15216–24, 2001.

[166] Charles C Oh, John Lee, Karen D'Souza, Weiyang Zhang, Raymond Q Migrino, Kent Thornburg, and Peter Reaven. Activator protein-1 and caspase 8 mediate p38? mapk-dependent cardiomyocyte apoptosis induced by palmitic acid. *Apoptosis : an international journal on programmed cell death*, 24:395–403, June 2019.

[167] Hyejin Oh, Hwan Kim, Kyung-Hwun Chung, Nan Hyung Hong, Baehyun Shin, Woo Jin Park, Youngsoo Jun, Sangmyung Rhee, and Woo Keun Song. Spin90 knockdown attenuates the formation and movement of endosomal vesicles in the early stages of epidermal growth factor receptor endocytosis. *PloS one*, 8:e82610, 2013.

[168] Ryuji Okamoto, Yuxin Li, Kensuke Noma, Yukio Hiroi, Ping-Yen Liu, Masaya Taniguchi, Masaaki Ito, and James K Liao. Fhl2 prevents cardiac hypertrophy in mice with cardiac-specific deletion of rock2. *FASEB journal : official publication of the Federation of American Societies for Experimental Biology*, 27:1439–1449, April 2013.

[169] Ana Isabel Oliveira, Sandra I Anjo, Joana Vieira de Castro, Sofia C Serra, António J Salgado, Bruno Manadas, and Bruno M Costa. Crosstalk between glial and glioblastoma cells triggers the "go-or-grow" phenotype of tumor cells. *Cell communication and signaling : CCS*, 15:37, October 2017.

[170] R. J. Orton, O. E. Sturm, V. Vyshemirsky, M. Calder, D. R. Gilbert, and W. Kolch. Computational modelling of the receptor-tyrosine-kinase-activated mapk pathway. *Biochem J*, 392(Pt 2):249–61, 2005.

[171] D. M. Ouwens, N. D. de Ruiter, G. C. van der Zon, A. P. Carter, J. Schouten, C. van der Burgt, K. Kooistra, J. L. Bos, J. A. Maassen, and H. van Dam. Growth factors can activate atf2 via a two-step mechanism: phosphorylation of thr71 through the ras-mek-erk pathway and of thr69 through ralgds-src-p38. *EMBO J*, 21(14):3782–93, 2002.

[172] H. Oya, A. Yokoyama, I. Yamaoka, R. Fujiki, M. Yonezawa, M. Y. Youn, I. Takada, S. Kato, and H. Kitagawa. Phosphorylation of williams syndrome transcription factor by mapk induces a switching between two distinct chromatin remodeling complexes. *J Biol Chem*, 284(47):32472–82, 2009.

[173] E. Padmini, V. Uthra, and S. Lavanya. Effect of hsp70 and 90 in modulation of jnk, erk expression in preeclamptic placental endothelial cell. *Cell Biochem Biophys*, 64(3):187–95, 2012.

[174] G. Pearson, F. Robinson, T. Beers Gibson, B. E. Xu, M. Karandikar, K. Berman, and M. H. Cobb. Mitogen-activated protein (map) kinase pathways: regulation and physiological functions. *Endocr Rev*, 22(2):153–83, 2001.

[175] G. Pearson, F. Robinson, T. Beers Gibson, B. E. Xu, M. Karandikar, K. Berman, and M. H. Cobb. Mitogen-activated protein (map) kinase pathways: regulation and physiological functions. *Endocr Rev*, 22(2):153–83, 2001.

[176] S. F. Pedersen, B. V. Darborg, M. Rasmussen, J. Nylandsted, and E. K. Hoffmann. The na+/h+ exchanger, nhe1, differentially regulates mitogen-activated protein kinase subfamilies after osmotic shrinkage in ehrlich lettre ascites cells. *Cell Physiol Biochem*, 20(6):735–50, 2007.

[177] Kesong Peng, Xinqiao Tian, Yuanyuan Qian, Melissa Skibba, Chunpeng Zou, Zhiguo Liu, Jingying Wang, Zheng Xu, Xiaokun Li, and Guang Liang. Novel egfr inhibitors attenuate cardiac hypertrophy induced by angiotensin ii. *Journal of cellular and molecular medicine*, 20:482–494, March 2016.

[178] N. Philippi, D. Walter, R. Schlatter, K. Ferreira, M. Ederer, O. Sawodny, J. Timmer, C. Borner, and T. Dandekar. Modeling system states in liver cells: survival, apoptosis and their modifications in response to viral infection. *BMC Syst Biol*, 3:97, 2009.

[179] J. A. Pitcher, J. J. Tesmer, J. L. Freeman, W. D. Capel, W. C. Stone, and R. J. Lefkowitz. Feedback inhibition of g protein-coupled receptor kinase 2 (grk2) activity by extracellular signal-regulated kinases. *J Biol Chem*, 274(49):34531–4, 1999.

[180] L. I. Plotkin, S. C. Manolagas, and T. Bellido. Transduction of cell survival signals by connexin-43 hemichannels. *J Biol Chem*, 277(10):8648–57, 2002.

[181] P. S. Pollack, S. R. Houser, R. Budjak, and B. Goldman. c-myc gene expression is localized to the myocyte following hemodynamic overload in vivo. *J Cell Biochem*, 54(1):78–84, 1994.

[182] T. S. Prasad, K. Kandasamy, and A. Pandey. Human protein reference database and human proteinpedia as discovery tools for systems biology. *Methods Mol Biol*, 577:67–79, 2009.

[183] N. H. Purcell, D. Darwis, O. F. Bueno, J. M. Muller, R. Schule, and J. D. Molkentin. Extracellular signal-regulated kinase 2 interacts with and is nega-

tively regulated by the lim-only protein fhl2 in cardiomyocytes. *Mol Cell Biol*, 24(3):1081–95, 2004.

[184] X. Qian, L. Esteban, W. C. Vass, C. Upadhyaya, A. G. Papageorge, K. Yienger, J. M. Ward, D. R. Lowy, and E. Santos. The sos1 and sos2 ras-specific exchange factors: differences in placental expression and signaling properties. *EMBO J*, 19(4):642–54, 2000.

[185] Z. Qin, M. DeFee, J. S. Isaacs, and C. Parsons. Extracellular hsp90 serves as a co-factor for mapk activation and latent viral gene expression during de novo infection by kshv. *Virology*, 403(1):92–102, 2010.

[186] C. Quevedo, M. Salinas, and A. Alcazar. Initiation factor 2b activity is regulated by protein phosphatase 1, which is activated by the mitogen-activated protein kinase-dependent pathway in insulin-like growth factor 1-stimulated neuronal cells. *J Biol Chem*, 278(19):16579–86, 2003.

[187] J S Ramalho, T Tolmachova, A N Hume, A McGuigan, C Y Gregory-Evans, C Huxley, and M C Seabra. Chromosomal mapping, gene structure and characterization of the human and murine rab27b gene. *BMC genetics*, 2:2, 2001.

[188] G J Riggins, S Thiagalingam, E Rozenblum, C L Weinstein, S E Kern, S R Hamilton, J K Willson, S D Markowitz, K W Kinzler, and B Vogelstein. Mad-related genes in the human. *Nature genetics*, 13:347–349, July 1996.

[189] Philippe Riou, Svend Kjær, Ritu Garg, Andrew Purkiss, Roger George, Robert J Cain, Ganka Bineva, Nicolas Reymond, Brad McColl, Andrew J Thompson, Nicola O'Reilly, Neil Q McDonald, Peter J Parker, and Anne J Ridley. 14-3-3 proteins interact with a hybrid prenyl-phosphorylation motif to inhibit g proteins. *Cell*, 153:640–653, April 2013.

[190] D. A. Ritt, I. O. Daar, and D. K. Morrison. Ksr regulation of the raf-mek-erk cascade. *Methods Enzymol*, 407:224–37, 2006.

[191] H A Rockman, R S Ross, A N Harris, K U Knowlton, M E Steinhelper, L J Field, J Ross, and K R Chien. Segregation of atrial-specific and inducible expression of an atrial natriuretic factor transgene in an in vivo murine model of cardiac hypertrophy. *Proceedings of the National Academy of Sciences of the United States of America*, 88:8277–8281, September 1991.

[192] G. Roth, J. Kotzka, L. Kremer, S. Lehr, C. Lohaus, H. E. Meyer, W. Krone, and D. Muller-Wieland. Map kinases erk1/2 phosphorylate sterol regulatory element-binding protein (srebp)-1a at serine 117 in vitro. *J Biol Chem*, 275(43):33302–7, 2000.

[193] Rosanne Rouf, Elena Gallo MacFarlane, Eiki Takimoto, Rahul Chaudhary, Varun Nagpal, Peter P Rainer, Julia G Bindman, Elizabeth E Gerber, Djahida Bedja, Christopher Schiefer, Karen L Miller, Guangshuo Zhu, Loretha Myers, Nuria Amat-Alarcon, Dong I Lee, Norimichi Koitabashi, Daniel P Judge, David A Kass, and Harry C Dietz. Nonmyocyte erk1/2 signaling contributes to load-induced cardiomyopathy in marfan mice. *JCI insight*, 2, August 2017.

[194] P. P. Roux, S. A. Richards, and J. Blenis. Phosphorylation of p90 ribosomal s6 kinase (rsk) regulates extracellular signal-regulated kinase docking and rsk activity. *Mol Cell Biol*, 23(14):4796–804, 2003.

[195] P. P. Roux, D. Shahbazian, H. Vu, M. K. Holz, M. S. Cohen, J. Taunton, N. Sonenberg, and J. Blenis. Ras/erk signaling promotes site-specific ribosomal protein s6 phosphorylation via rsk and stimulates cap-dependent translation. *J Biol Chem*, 282(19):14056–64, 2007.

[196] Nicole Rubin, Michael R Harrison, Michael Krainock, Richard Kim, and Ching-Ling Lien. Recent advancements in understanding endogenous heart regeneration-insights from adult zebrafish and neonatal mice. *Seminars in cell & developmental biology*, 58:34–40, October 2016.

[197] C. Ruppert, K. Deiss, S. Herrmann, M. Vidal, M. Oezkur, A. Gorski, F. Weidemann, M. J. Lohse, and K. Lorenz. Interference with erk(thr188) phosphorylation impairs pathological but not physiological cardiac hypertrophy. *Proc Natl Acad Sci U S A*, 110(18):7440–5, 2013.

[198] Karen A Ryall, David O Holland, Kyle A Delaney, Matthew J Kraeutler, Audrey J Parker, and Jeffrey J Saucerman. Network reconstruction and systems analysis of cardiac myocyte hypertrophy signaling. *The Journal of biological chemistry*, 287:42259–42268, December 2012.

[199] Valentina Sala, Simona Gallo, Stefano Gatti, Enzo Medico, Elisa Vigna, Daniela Cantarella, Lara Fontani, Massimo Natale, James Cimino, Mara Morello, Paolo Maria Comoglio, Antonio Ponzetto, and Tiziana Crepaldi. Cardiac concentric hypertrophy promoted by activated met receptor is mitigated

in vivo by inhibition of erk1,2 signalling with pimasertib. *Journal of molecular and cellular cardiology*, 93:84–97, April 2016.

[200] Valentina Sala, Simona Gallo, Christian Leo, Stefano Gatti, Bruce D Gelb, and Tiziana Crepaldi. Signaling to cardiac hypertrophy: insights from human and mouse rasopathies. *Molecular medicine (Cambridge, Mass.)*, 18:938–947, September 2012.

[201] Victoria Sanz-Moreno, Berta Casar, and Piero Crespo. p38alpha isoform mxi2 binds to extracellular signal-regulated kinase 1 and 2 mitogen-activated protein kinase and regulates its nuclear activity by sustaining its phosphorylation levels. *Molecular and cellular biology*, 23:3079–3090, May 2003.

[202] R. Schlatter, N. Philippi, G. Wangorsch, R. Pick, O. Sawodny, C. Borner, J. Timmer, M. Ederer, and T. Dandekar. Integration of boolean models exemplified on hepatocyte signal transduction. *Brief Bioinform*, 13(3):365–76, 2012.

[203] M. Schmidt, F. J. Dekker, and H. Maarsingh. Exchange protein directly activated by camp (epac): a multidomain camp mediator in the regulation of diverse biological functions. *Pharmacol Rev*, 65(2):670–709, 2013.

[204] R. Seger and E. G. Krebs. The mapk signaling cascade. *FASEB J*, 9(9):726–35, 1995.

[205] Vincent F M Segers, Dirk L Brutsaert, and Gilles W De Keulenaer. Cardiac remodeling: Endothelial cells have more to say than just no. *Frontiers in physiology*, 9:382, 2018.

[206] Behzad Shariati, Eric L Thompson, Grant D Nicol, and Michael R Vasko. Epac activation sensitizes rat sensory neurons through activation of ras. *Molecular and cellular neurosciences*, 70:54–67, January 2016.

[207] A. Shimamura, B. A. Ballif, S. A. Richards, and J. Blenis. Rsk1 mediates a mek-map kinase cell survival signal. *Curr Biol*, 10(3):127–35, 2000.

[208] E. Y. Shin, K. S. Shin, C. S. Lee, K. N. Woo, S. H. Quan, N. K. Soung, Y. G. Kim, C. I. Cha, S. R. Kim, D. Park, G. M. Bokoch, and E. G. Kim. Phosphorylation of p85 beta pix, a rac/cdc42-specific guanine nucleotide exchange factor, via the ras/erk/pak2 pathway is required for basic fibroblast growth factor-induced neurite outgrowth. *J Biol Chem*, 277(46):44417–30, 2002.

[209] F. D. Sigoillot, J. A. Berkowski, S. M. Sigoillot, D. H. Kotsis, and H. I. Guy. Cell cycle-dependent regulation of pyrimidine biosynthesis. *J Biol Chem*, 278(5):3403–9, 2003.

[210] L. Smerdova, J. Smerdova, M. Kabatkova, J. Kohoutek, D. Blazek, M. Machala, and J. Vondracek. Upregulation of cyp1b1 expression by inflammatory cytokines is mediated by the p38 map kinase signal transduction pathway. *Carcinogenesis*, 35(11):2534–43, 2014.

[211] V E Smith and A M Katz. Inotropic and lusitropic abnormalities in the genesis of heart failure. *European heart journal*, 4 Suppl A:7–17, January 1983.

[212] R. F. Sood, S. Arbabi, S. Honari, and N. S. Gibran. Missense variant in mapk inactivator ptpn5 is associated with decreased severity of post-burn hypertrophic scarring. *PLoS One*, 11(2):e0149206, 2016.

[213] V Y Stefanovsky, G Pelletier, R Hannan, T Gagnon-Kugler, L I Rothblum, and T Moss. An immediate response of ribosomal transcription to growth factor stimulation in mammals is mediated by erk phosphorylation of ubf. *Molecular cell*, 8:1063–1073, November 2001.

[214] M. Suzuki, H. Makinoshima, S. Matsumoto, A. Suzuki, S. Mimaki, K. Matsushima, K. Yoh, K. Goto, Y. Suzuki, G. Ishii, A. Ochiai, K. Tsuta, T. Shibata, T. Kohno, H. Esumi, and K. Tsuchihara. Identification of a lung adenocarcinoma cell line with ccdc6-ret fusion gene and the effect of ret inhibitors in vitro and in vivo. *Cancer Sci*, 104(7):896–903, 2013.

[215] D. Szklarczyk, A. Franceschini, M. Kuhn, M. Simonovic, A. Roth, P. Minguez, T. Doerks, M. Stark, J. Muller, P. Bork, L. J. Jensen, and C. von Mering. The string database in 2011: functional interaction networks of proteins, globally integrated and scored. *Nucleic Acids Res*, 39(Database issue):D561–8, 2011.

[216] K. Taketa, T. Matsumura, M. Yano, N. Ishii, T. Senokuchi, H. Motoshima, Y. Murata, S. Kim-Mitsuyama, T. Kawada, H. Itabe, M. Takeya, T. Nishikawa, K. Tsuruzoe, and E. Araki. Oxidized low density lipoprotein activates peroxisome proliferator-activated receptor-alpha (pparalpha) and ppargamma through mapk-dependent cox-2 expression in macrophages. *J Biol Chem*, 283(15):9852–62, 2008.

[217] Abdonas Tamosiunas, Dalia Luksiene, Migle Baceviciene, Gailute Bernotiene, Ricardas Radisauskas, Vilija Malinauskiene, Daina Kranciukaite-Butylkiniene,

Dalia Virviciute, Anne Peasey, and Martin Bobak. Health factors and risk of all-cause, cardiovascular, and coronary heart disease mortality: findings from the monica and hapiee studies in lithuania. *PloS one*, 9:e114283, 2014.

[218] Edit Tanai and Stefan Frantz. Pathophysiology of heart failure. *Comprehensive Physiology*, 6:187–214, December 2015.

[219] G. Thiel, A. Lesch, and A. Keim. Transcriptional response to calcium-sensing receptor stimulation. *Endocrinology*, 153(10):4716–28, 2012.

[220] H. Toledano-Katchalski, J. Kraut, T. Sines, S. Granot-Attas, G. Shohat, H. Gil-Henn, Y. Yung, and A. Elson. Protein tyrosine phosphatase epsilon inhibits signaling by mitogen-activated protein kinases. *Mol Cancer Res*, 1(7):541–50, 2003.

[221] Angela Tomasovic, Theresa Brand, Constanze Schanbacher, Sofia Kramer, Martin W Hümmert, Patricio Godoy, Wolfgang Schmidt-Heck, Peter Nordbeck, Jonas Ludwig, Susanne Homann, Armin Wiegering, Timur Shaykhutdinov, Christoph Kratz, Ruth Knüchel, Hans-Konrad Müller-Hermelink, Andreas Rosenwald, Norbert Frey, Jutta Eichler, Dobromir Dobrev, Ali El-Armouche, Jan G Hengstler, Oliver J Müller, Karsten Hinrichs, Friederike Cuello, Alma Zernecke, and Kristina Lorenz. Interference with erk-dimerization at the nucleocytosolic interface targets pathological erk1/2 signaling without cardiotoxic side-effects. *Nature communications*, 11:1733, April 2020.

[222] M. Towatari, G. E. May, R. Marais, G. R. Perkins, C. J. Marshall, S. Cowley, and T. Enver. Regulation of gata-2 phosphorylation by mitogen-activated protein kinase and interleukin-3. *J Biol Chem*, 270(8):4101–7, 1995.

[223] M Khang Tran, Kondababu Kurakula, Duco S Koenis, and Carlie J M de Vries. Protein-protein interactions of the lim-only protein fhl2 and functional implication of the interactions relevant in cardiovascular disease. *Biochimica et biophysica acta*, 1863:219–228, February 2016.

[224] H Traupe, A M van den Ouweland, B A van Oost, W Vogel, U Vetter, S T Warren, M Rocchi, M G Darlison, and H H Ropers. Fine mapping of the human biglycan (bgn) gene within the xq28 region employing a hybrid cell panel. *Genomics*, 13:481–483, June 1992.

[225] M. Udelhoven, U. Leeser, S. Freude, M. M. Hettich, M. Laudes, J. Schnitker, W. Krone, and M. Schubert. Identification of a region in the human irs2 promoter essential for stress induced transcription depending on sp1, nfi binding and erk activation in hepg2 cells. *J Mol Endocrinol*, 44(2):99–113, 2010.

[226] R. B. Vega, J. Yang, B. A. Rothermel, R. Bassel-Duby, and R. S. Williams. Multiple domains of mcip1 contribute to inhibition of calcineurin activity. *J Biol Chem*, 277(33):30401–7, 2002.

[227] Laurine Verset, Lynn Feys, Anne-Laure Trépant, Olivier De Wever, and Pieter Demetter. Fhl2: a scaffold protein of carcinogenesis, tumour-stroma interactions and treatment response. *Histology and histopathology*, 31:469–478, May 2016.

[228] G. P. Vicent, R. Zaurin, C. Ballare, A. S. Nacht, and M. Beato. Erk signaling and chromatin remodeling in mmtv promoter activation by progestins. *Nucl Recept Signal*, 7:e008, 2009.

[229] M. Vidal, T. Wieland, M. J. Lohse, and K. Lorenz. beta-adrenergic receptor stimulation causes cardiac hypertrophy via a gbetagamma/erk-dependent pathway. *Cardiovasc Res*, 96(2):255–64, 2012.

[230] G. Vorbrueggen, J. Lovric, and K. Moelling. Functional analysis of phosphorylation at serine 532 of human c-myb by map kinase. *Biol Chem*, 377(11):721–30, 1996.

[231] Teiji Wada, Tomoki Nakashima, Antonio J Oliveira-dos Santos, Juerg Gasser, Hiromitsu Hara, Georg Schett, and Josef M Penninger. The molecular scaffold gab2 is a crucial component of rank signaling and osteoclastogenesis. *Nature medicine*, 11:394–399, April 2005.

[232] X. Wang, N. Grammatikakis, A. Siganou, M. A. Stevenson, and S. K. Calderwood. Interactions between extracellular signal-regulated protein kinase 1, 14-3-3epsilon, and heat shock factor 1 during stress. *J Biol Chem*, 279(47):49460–9, 2004.

[233] A. J. Waskiewicz, A. Flynn, C. G. Proud, and J. A. Cooper. Mitogen-activated protein kinases activate the serine/threonine kinases mnk1 and mnk2. *EMBO J*, 16(8):1909–20, 1997.

[234] S. Wei, J. H. Liu, P. K. Epling-Burnette, K. Jiang, B. Zhong, M. E. Elkabani, E. W. Pearson, and J. Y. Djeu. Il-2 induces the association of il-2rbeta, lyn,

and map kinase erk-1 in human neutrophils. *Immunobiology*, 202(4):363–82, 2000.

[235] C. Wellbrock, S. Rana, H. Paterson, H. Pickersgill, T. Brummelkamp, and R. Marais. Oncogenic braf regulates melanoma proliferation through the lineage specific factor mitf. *PLoS One*, 3(7):e2734, 2008.

[236] Krister Wennerberg, Kent L Rossman, and Channing J Der. The ras superfamily at a glance. *Journal of cell science*, 118:843–846, March 2005.

[237] F. S. Willard and M. F. Crouch. Mek, erk, and p90rsk are present on mitotic tubulin in swiss 3t3 cells: a role for the map kinase pathway in regulating mitotic exit. *Cell Signal*, 13(9):653–64, 2001.

[238] I. Wortzel and R. Seger. The erk cascade: Distinct functions within various subcellular organelles. *Genes Cancer*, 2(3):195–209, 2011.

[239] Y. Xia, L. Y. Hwang, M. H. Cobb, and R. Baer. Products of the tal2 oncogene in leukemic t cells: bhlh phosphoproteins with dna-binding activity. *Oncogene*, 9(5):1437–46, 1994.

[240] G. Xiao, S. Mao, G. Baumgarten, J. Serrano, M. C. Jordan, K. P. Roos, M. C. Fishbein, and W. R. MacLellan. Inducible activation of c-myc in adult myocardium in vivo provokes cardiac myocyte hypertrophy and reactivation of dna synthesis. *Circ Res*, 89(12):1122–9, 2001.

[241] Kunhong Xiao, Daniel B McClatchy, Arun K Shukla, Yang Zhao, Minyong Chen, Sudha K Shenoy, John R Yates, and Robert J Lefkowitz. Functional specialization of beta-arrestin interactions revealed by proteomic analysis. *Proceedings of the National Academy of Sciences of the United States of America*, 104:12011–12016, July 2007.

[242] R. P. Xiao, H. Cheng, Y. Y. Zhou, M. Kuschel, and E. G. Lakatta. Recent advances in cardiac beta(2)-adrenergic signal transduction. *Circ Res*, 85(11):1092–100, 1999.

[243] A. Xu, P. G. Suh, N. Marmy-Conus, R. B. Pearson, O. Y. Seok, L. Cocco, and R. S. Gilmour. Phosphorylation of nuclear phospholipase c beta1 by extracellular signal-regulated kinase mediates the mitogenic action of insulin-like growth factor i. *Mol Cell Biol*, 21(9):2981–90, 2001.

[244] L. Xu, J. L. Zhou, M. Cohen, D. Bar-Sagi, and K. N. Patel. Spry2 expression correlates with braf mutation in thyroid cancer. *Surgery*, 148(6):1282–7; discussion 1287, 2010.

[245] Clyde W Yancy, Mariell Jessup, Biykem Bozkurt, Javed Butler, Donald E Casey, Monica M Colvin, Mark H Drazner, Gerasimos S Filippatos, Gregg C Fonarow, Michael M Givertz, Steven M Hollenberg, JoAnn Lindenfeld, Frederick A Masoudi, Patrick E McBride, Pamela N Peterson, Lynne Warner Stevenson, and Cheryl Westlake. 2017 acc/aha/hfsa focused update of the 2013 accf/aha guideline for theămanagement of heart failure: A report of the american college of cardiology/american heart association task force on clinical practice guidelines and the heart failure society of america. *Journal of cardiac failure*, 23:628–651, August 2017.

[246] S Ying, A Shiraishi, C W Kao, R L Converse, J L Funderburgh, J Swiergiel, M R Roth, G W Conrad, and W W Kao. Characterization and expression of the mouse lumican gene. *The Journal of biological chemistry*, 272:30306–30313, November 1997.

[247] A Zebisch and J Troppmair. Back to the roots: the remarkable raf oncogene story. *Cellular and molecular life sciences : CMLS*, 63:1314–1330, June 2006.

[248] M. X. Zhang, X. M. Xu, P. Zhang, N. N. Han, J. J. Deng, T. T. Yu, Y. Y. Gan, X. Q. He, and Z. X. Long. Effect of silencing nek2 on biological behaviors of hepg2 in human hepatoma cells and mapk signal pathway. *Tumour Biol*, 37(2):2023–35, 2016.

[249] S. Zhang, M. Fukushi, S. Hashimoto, C. Gao, L. Huang, Y. Fukuyo, T. Nakajima, T. Amagasa, S. Enomoto, K. Koike, O. Miura, N. Yamamoto, and N. Tsuchida. A new erk2 binding protein, naf1, attenuates the egf/erk2 nuclear signaling. *Biochem Biophys Res Commun*, 297(1):17–23, 2002.

[250] J. Zhao, J. Wei, R. Mialki, C. Zou, R. K. Mallampalli, and Y. Zhao. Extracellular signal-regulated kinase (erk) regulates cortactin ubiquitination and degradation in lung epithelial cells. *J Biol Chem*, 287(23):19105–14, 2012.

[251] Ben Zuckerman and David Jefferson. *Human Population and the Environmental Crisis*. Jones & Bartlett Learning, p. 42, 1996.

List of Figures

Part VI.

Appendix

A. Network in xml-format

```
<?xml version="1.0" encoding="UTF-8"?>
<mml level="2">
  <!--Modelomics Markup Language (MML) v2.0-->
  <model />
  <graph>
    <nodes>
      <node id="AND" state="1.0" decay="1.0" gain="10.0" visible="false" posx="297.0" posy="509.0"
/>
      <node id="Elk1" state="0.0" decay="1.0" gain="10.0" visible="true" posx="359.0" posy="658.0"
/>
      <node id="Epac" state="0.0" decay="1.0" gain="10.0" visible="false" posx="407.0"
posy="273.0" />
      <node id="GRK2" state="1.0" decay="1.0" gain="10.0" visible="false" posx="339.0"
posy="416.0" />
      <node id="G_beta__gamma_" state="0.0" decay="1.0" gain="10.0" visible="false" posx="567.0"
posy="337.0" />
      <node id="Gi-coupled_M2_receptor" state="0.0" decay="1.0" gain="10.0" visible="false"
posx="93.5" posy="154.5" />
      <node id="Gq-coupled_AT1_receptor" state="0.0" decay="1.0" gain="10.0" visible="false"
posx="327.5" posy="145.5" />
      <node id="Gs-coupled__beta__1_receptor" state="0.0" decay="1.0" gain="10.0" visible="false"
posx="518.0" posy="150.0" />
      <node id="MEK_1/2" state="0.0" decay="1.0" gain="10.0" visible="false" posx="93.0"
posy="406.0" />
      <node id="MSK1" state="0.0" decay="1.0" gain="10.0" visible="true" posx="444.0" posy="658.0"
/>
      <node id="PKC" state="0.0" decay="1.0" gain="10.0" visible="false" posx="251.0" posy="273.0"
/>
      <node id="RKIP" state="1.0" decay="1.0" gain="10.0" visible="false" posx="251.0"
posy="341.0" />
      <node id="Raf1" state="0.0" decay="1.0" gain="10.0" visible="false" posx="93.0" posy="319.0"
/>
      <node id="Ras_(GTP_bound)" state="0.0" decay="1.0" gain="10.0" visible="false" posx="93.5"
posy="230.0" />
      <node id="angiotensin_II" state="0.0" decay="1.0" gain="10.0" visible="false" posx="326.0"
posy="81.0" />
      <node id="c-Myc" state="0.0" decay="1.0" gain="10.0" visible="true" posx="530.0"
posy="658.0" />
      <node id="carbachol" state="0.0" decay="1.0" gain="10.0" visible="false" posx="95.5"
posy="92.0" />
      <node id="hypertrophic_stimulus" state="0.0" decay="1.0" gain="10.0" visible="false"
posx="415.0" posy="18.0" />
      <node id="isoproterenol" state="0.0" decay="1.0" gain="10.0" visible="false" posx="518.0"
posy="76.5" />
      <node id="non-hypertrophic_stimulus" state="0.0" decay="1.0" gain="10.0" visible="false"
posx="110.5" posy="24.5" />
      <node id="p70S6K" state="0.0" decay="1.0" gain="10.0" visible="true" posx="174.0"
posy="588.0" />
      <node id="p90RSK" state="0.0" decay="1.0" gain="10.0" visible="true" posx="88.0"
posy="588.0" />
```

```
      <node id="pERK(TEY)" state="0.0" decay="1.0" gain="10.0" visible="true" posx="112.5"
posy="509.0" />
      <node id="pERK(Thr188)" state="0.0" decay="1.0" gain="10.0" visible="true" posx="463.0"
posy="509.0" />
      <node id="pRKIPdim" state="0.0" decay="1.0" gain="10.0" visible="false" posx="341.0"
posy="347.0" />
    </nodes>
    <edges>
      <edge id="Gq-coupled_AT1_receptor -- Ras_(GTP_bound)" source="Gq-coupled_AT1_receptor"
target="Ras_(GTP_bound)" sign="positive" weight="1.0" />
      <edge id="G_beta__gamma_ -- pERK(Thr188)" source="G_beta__gamma_" target="pERK(Thr188)"
sign="positive" weight="100.0" />
      <edge id="RKIP -| Raf1" source="RKIP" target="Raf1" sign="negative" weight="0.01" />
      <edge id="pERK(Thr188) -- Elk1" source="pERK(Thr188)" target="Elk1" sign="positive"
weight="8.0" />
      <edge id="pERK(Thr188) -- MSK1" source="pERK(Thr188)" target="MSK1" sign="positive"
weight="7.0" />
      <edge id="PKC -| RKIP" source="PKC" target="RKIP" sign="negative" weight="10.0" />
      <edge id="Gs-coupled__beta__1_receptor -- Ras_(GTP_bound)" source="Gs-
coupled__beta__1_receptor" target="Ras_(GTP_bound)" sign="positive" weight="1.0" />
      <edge id="Gs-coupled__beta__1_receptor -- Epac" source="Gs-coupled__beta__1_receptor"
target="Epac" sign="positive" weight="10.0" />
      <edge id="pERK(TEY) -- p70S6K" source="pERK(TEY)" target="p70S6K" sign="positive"
weight="0.01" />
      <edge id="isoproterenol -- Gs-coupled__beta__1_receptor" source="isoproterenol" target="Gs-
coupled__beta__1_receptor" sign="positive" weight="10.0" />
      <edge id="pERK(TEY) -| AND" source="pERK(TEY)" target="AND" sign="negative" weight="100.0"
/>
      <edge id="hypertrophic_stimulus -- angiotensin_II" source="hypertrophic_stimulus"
target="angiotensin_II" sign="positive" weight="1.0" />
      <edge id="carbachol -- Gi-coupled_M2_receptor" source="carbachol" target="Gi-
coupled_M2_receptor" sign="positive" weight="10.0" />
      <edge id="pERK(TEY) -- p90RSK" source="pERK(TEY)" target="p90RSK" sign="positive"
weight="0.01" />
      <edge id="Raf1 -- MEK_1/2" source="Raf1" target="MEK_1/2" sign="positive" weight="1.0" />
      <edge id="angiotensin_II -- Gq-coupled_AT1_receptor" source="angiotensin_II" target="Gq-
coupled_AT1_receptor" sign="positive" weight="5.0" />
      <edge id="Gi-coupled_M2_receptor -- Ras_(GTP_bound)" source="Gi-coupled_M2_receptor"
target="Ras_(GTP_bound)" sign="positive" weight="10.0" />
      <edge id="Gi-coupled_M2_receptor -- PKC" source="Gi-coupled_M2_receptor" target="PKC"
sign="positive" weight="10.0" />
      <edge id="AND -| pERK(Thr188)" source="AND" target="pERK(Thr188)" sign="negative"
weight="1.0" />
      <edge id="Gs-coupled__beta__1_receptor -- G_beta__gamma_" source="Gs-
coupled__beta__1_receptor" target="G_beta__gamma_" sign="positive" weight="10.0" />
      <edge id="Gq-coupled_AT1_receptor -- G_beta__gamma_" source="Gq-coupled_AT1_receptor"
target="G_beta__gamma_" sign="positive" weight="10.0" />
      <edge id="Epac -- PKC" source="Epac" target="PKC" sign="positive" weight="10.0" />
      <edge id="PKC -- pRKIPdim" source="PKC" target="pRKIPdim" sign="positive" weight="10.0" />
      <edge id="Gq-coupled_AT1_receptor -- PKC" source="Gq-coupled_AT1_receptor" target="PKC"
sign="positive" weight="10.0" />
      <edge id="hypertrophic_stimulus -- isoproterenol" source="hypertrophic_stimulus"
target="isoproterenol" sign="positive" weight="10.0" />
      <edge id="non-hypertrophic_stimulus -- carbachol" source="non-hypertrophic_stimulus"
target="carbachol" sign="positive" weight="10.0" />
      <edge id="pRKIPdim -| GRK2" source="pRKIPdim" target="GRK2" sign="negative" weight="30.0" />
```

```
      <edge id="pERK(Thr188) -- c-Myc" source="pERK(Thr188)" target="c-Myc" sign="positive"
weight="6.0" />
      <edge id="Ras_(GTP_bound) -- Raf1" source="Ras_(GTP_bound)" target="Raf1" sign="positive"
weight="10.0" />
      <edge id="MEK_1/2 -- pERK(TEY)" source="MEK_1/2" target="pERK(TEY)" sign="positive"
weight="0.0010" />
      <edge id="GRK2 -| Gs-coupled__beta__1_receptor" source="GRK2" target="Gs-
coupled__beta__1_receptor" sign="negative" weight="0.1" />
    </edges>
    <states>
      <state id="SS-1">
        <activenode id="AND" statediscrete="1.0" state="1.0" />
        <activenode id="GRK2" statediscrete="1.0" state="1.0" />
        <activenode id="RKIP" statediscrete="1.0" state="1.0" />
      </state>
    </states>
  </graph>
</mml>
```

B. Possible further ERK-Targets

Table B.1.: Possible further ERK targets

Erk-Targets	*official symbol (NCBI)*	*Localisation*	*additional information*	*MAPK isoform*	*cell type*	*reference*
UBF	UBTF	nucleoli	Erk phosphorylates UBF and thus prevents their interaction with DNA, suggest a central role for ribosome biogenesis in growth regulation.	Erk1/2		[213]
TACE	ADAM17	cell surface, golgi apparatus	ERK acts as an intermediate in protein kinase C-regulated TrkA cleavage. The cytosolic tail of TACE is phosphorylated by Erk at threonine 735. ERK and TACE associate.	Erk1/2		[51]
GRK 2	ADRBK1		ERK1 phosphorylates GRK2. Inhibition of ERK activity potentiates GRK2 activity, whereas, conversely, ERK activation inhibits GRK2 activity. An feedback regulatory loop occurs!	Erk1	HEK293 cells	[179]
ALK	ALK	vesicle	ALK mediates growth and differentiation of neurons, ERK is essentially involved.	-	-	[159]

continues on next page

Table B.1.: Possible further ERK targets

Erk-Targets	*official symbol (NCBI)*	*Localisation*	*additional information*	*MAPK isoform*	*cell type*	*reference*
UBF	UBTF	nucleoli	Erk phosphorylates UBF and thus prevents their interaction with DNA, suggest a central role for ribosome biogenesis in growth regulation.	Erk1/2		[213]
p85 betaPIX	ARHGEF7		Erk activates p85 via binding of PAK2 to Erk and as a result of this PAK2 and p85 are building a complex and translocate -> neurite growth	-	PC12 cell lines	[208]
CREB2	ATF2	nucleus	Raf-MEK-Erk pathway induces phosphorylation of ATF2 at Thr71 and Ral-RalGDS-Src-p38 pathway at Thr69 -> both required for activation; but: other study shows that Erk-activation is not required for ATF2-activation GSE 18224 adjusted P-value: 3,4x10-2	-	fibroblasts	[171, 81]

continues on next page

Table B.1.: Possible further ERK targets

Erk-Targets	*official symbol (NCBI)*	*Localisation*	*additional information*	*MAPK isoform*	*cell type*	*reference*
UBF	UBTF	nucleoli	Erk phosphorylates UBF and thus prevents their interaction with DNA, suggest a central role for ribosome biogenesis in growth regulation.	Erk1/2		[213]
bromodomain adjacent to zinc finger domain, 1B	BAZ1B		novel mechanisms of epigenetic regulation of MAPK (amongst others Erk1): Phosphorylation of Williams syndrome transcription factor by them induces a switch between two different chromatin remodeling complexes	Erk1	-	[172]
BRAF	BRAF	cytosol and nucleus	BRAF mutations activate the mitogen-activated protein kinase pathway			[79, 244]
Hyaluronan binding protein1	C1QBP	cytoplasm, nucleus	is an endogenous substrate for MAP kinase, suggestion: ERK activation is requirement for translocation to nucleus			[138]

continues on next page

Table B.1.: Possible further ERK targets

Erk-Targets	*official symbol (NCBI)*	*Localisation*	*additional information*	*MAPK isoform*	*cell type*	*reference*
UBF	UBTF	nucleoli	Erk phosphorylates UBF and thus prevents their interaction with DNA, suggest a central role for ribosome biogenesis in growth regulation.	Erk1/2		[213]
CAD	CAD		allosteric regulation of CAD is mediated by MAPK and PKA-mediated phosphorylations → cell-cycle dependent regulation of pyrimidine biosynthesis			[209]
Calnexin	CANX	endoplasmic reticulum	Phosphorylation by CK2 and MAPK enhances calnexin association with ribosomes → increase in glycoprotein folding GSE 18224 adjusted P-value: 2,17x10-2			[42]
Caspase 8	CASP8		pERK 1/2 inhibit Caspase-8 induced apoptosis	Erk1/2	cancer cells	[34, 3, 166, 141]

continues on next page

Table B.1.: Possible further ERK targets

Erk-Targets	*official symbol (NCBI)*	*Localisation*	*additional information*	*MAPK isoform*	*cell type*	*reference*
UBF	UBTF	nucleoli	Erk phosphorylates UBF and thus prevents their interaction with DNA, suggest a central role for ribosome biogenesis in growth regulation.	Erk1/2		[213]
Caspase 9	CASP9	nucleus and cytoplasm	Erk phosphorylates and inhibits Caspase9 and promotes cell survival and tissue homeostasis			[2, 142]
Caveolin 1	CAV1		"Caveolin-1 and caveolae play a paradoxical role in regulating VEGF-induced ERK2/1 activation and in vitro angiogenesis as evidenced by the similar inhibitory effects of down-regulation and overexpression of caveolin-1 and disruption of caveolae"	ERK 1/2		[126]

continues on next page

Table B.1.: Possible further ERK targets

Erk-Targets	*official symbol (NCBI)*	*Localisation*	*additional information*	*MAPK isoform*	*cell type*	*reference*
UBF	UBTF	nucleoli	Erk phosphorylates UBF and thus prevents their interaction with DNA, suggest a central role for ribosome biogenesis in growth regulation.	Erk1/2		[213]
H4 Gen-produkt	CCDC6		CCDC6-Ret oncogen phosphorylates and activates Erk -> regulation of cell proliferation (CCDC6 Ret genproduct is found in lung adenocarcinoma and papillary thyreoid carcinoma)	Erk 1/2	LAD cell lines	[214, 115]
Cep55	CEP55		amongst others Erk2 phosphorylates Cep55 (centrosome protein) → relocate to midbody →function in cytokinesis and mitotic exit GSE 5500 adjusted P-value: 2,02x10-2	Erk2		[60]

continues on next page

Table B.1.: Possible further ERK targets

Erk-Targets	*official symbol (NCBI)*	*Localisation*	*additional information*	*MAPK isoform*	*cell type*	*reference*
UBF	UBTF	nucleoli	Erk phosphorylates UBF and thus prevents their interaction with DNA, suggest a central role for ribosome biogenesis in growth regulation.	Erk1/2		[213]
Cortactin	CTTN	cytoplasm	ERK regulates cortactin ubiquitination and degradation in lung epithelial cells GSE 18224 adjusted P-value: 1,03x10-2			[250]
DCC	DCC		DCC activates Erk and this contributes to netrin signalling in axon growth and guidance	Erk 1/2		[66, 84]
Elk1	ELK1	nucleus and cytoplasm	IN CASCADE, phosphorylated Erk1/2 translocated to the nucleus and phosphorylates Elk1 GSE 18224 adjusted P-value: 5,09x10-3	Erk1/2		[137]

continues on next page

Table B.1.: Possible further ERK targets

Erk-Targets	*official symbol (NCBI)*	*Localisation*	*additional information*	*MAPK isoform*	*cell type*	*reference*
UBF	UBTF	nucleoli	Erk phosphorylates UBF and thus prevents their interaction with DNA, suggest a central role for ribosome biogenesis in growth regulation.	Erk1/2		[213]
Elk 4	ELK4	nucleus and cytoplasm	Elk4 is phosphorylated by Erk2 (and MAPK8), Elk4 directly links Erk signaling to the transcriptional events required for thymocyte positive selection, Elk4 is direct androgen receptor target in prostate cancer	Erk2		[44, 139]
TNF - R	f.e. FAS		Polyphenols from Korean prostrate spurge Euphorbia supina induce apoptosis through the Fas-associated extrinsic pathway and activation of ERK in human leukemic U937 cells			[78]

continues on next page

Table B.1.: Possible further ERK targets

Erk-Targets	*official symbol (NCBI)*	*Localisation*	*additional information*	*MAPK isoform*	*cell type*	*reference*
UBF	UBTF	nucleoli	Erk phosphorylates UBF and thus prevents their interaction with DNA, suggest a central role for ribosome biogenesis in growth regulation.	Erk1/2		[213]
FCGR2B	FCGR2B	nuclear membrane and cytoplasm	Erk1/2 binds to FCGR2B and phosphorylates a serine residue → thr binding of Lyn to FCGR2B is modified → thus might negatively regulate phosphorylation of ITIM → signal transduction is not inhibited anymore	Erk1/2		[146]
FHL2	FHL2	nucleus	FHL2 serves a repressor function, it inhibits ERK 1/2 transcriptional coupling GSE 18224 adjusted P-value: 4,63x10-2	Erk1/2		[183, 168, 227]
c - fos	FOS	nucleus	Erk phosphorylates c-fos, as an result the transcriptional activity is increased			[158]

continues on next page

Table B.1.: Possible further ERK targets

Erk-Targets	*official symbol (NCBI)*	*Localisation*	*additional information*	*MAPK isoform*	*cell type*	*reference*
UBF	UBTF	nucleoli	Erk phosphorylates UBF and thus prevents their interaction with DNA, suggest a central role for ribosome biogenesis in growth regulation.	Erk1/2		[213]
GAB2	GAB2	cytoplasm	Erk-mediated phosphorylation of Gab2 regulates assosication with SHP2 and decreases STAT5 activation → fine tuning of proliferative answer of t-lymphocytes to IL-2		t-lymphocytes	[5, 231, 26]
GATA2	GATA2	nucleus	Erk possibly phosphorylates GATA2, involved in growth factor responsiveness and proliferation of hematopoietic progenitor cells		hematopoietic progenitor cells	[222]
GATA4	GATA4	mainly nucleus	Erk1/2 regulates cardiomyocyte hypertrophic growth via GATA4 through direct phosphorylation	Erk1/2	cardiomyocyte	[125]

continues on next page

Table B.1.: Possible further ERK targets

Erk-Targets	*official symbol (NCBI)*	*Localisation*	*additional information*	*MAPK isoform*	*cell type*	*reference*
UBF	UBTF	nucleoli	Erk phosphorylates UBF and thus prevents their interaction with DNA, suggest a central role for ribosome biogenesis in growth regulation.	Erk1/2		[213]
Connexin 43	GJA1		hexameric connexin (Cx)-43 hemichannels are the essential transducers of the Erk-activating/anti-apoptotic effects of bisphosphonates	Erk1/2		[180]
GRB10	GRB10	nucleus and cytoplasm	is a direct substrate of Erk1/2, regulates insulin signaling	Erk1/2	-	[120]
general transcription factor IIi	GTF2I	nucleus	ERK regulates the activity of TFII-I by direct phosphorylation, regulates its activation of the c-fos promoter	Erk1		[104, 105]

continues on next page

Table B.1.: Possible further ERK targets

Erk-Targets	*official symbol (NCBI)*	*Localisation*	*additional information*	*MAPK isoform*	*cell type*	*reference*
UBF	UBTF	nucleoli	Erk phosphorylates UBF and thus prevents their interaction with DNA, suggest a central role for ribosome biogenesis in growth regulation.	Erk1/2		[213]
hyaluronan-mediated motility receptor (RHAMM)	HMMR		RHAMM (an intracellular cytoskeletal protein) modulates ERK1/2 signal transduction at microtubules, which can act as barriers to mESC pluripotency	Erk1/2		[95]
heat shock transcription factor 1	HSF1	nucleus and cytoplasm	association of HSF1 with ERK and 14-3-3ε during heat shock may thus modulate the amplitude of the response and lead to efficient termination of HSP expression on resumption of growth conditions	Erk2		[232]

continues on next page

Table B.1.: Possible further ERK targets

Erk-Targets	*official symbol (NCBI)*	*Localisation*	*additional information*	*MAPK isoform*	*cell type*	*reference*
UBF	UBTF	nucleoli	Erk phosphorylates UBF and thus prevents their interaction with DNA, suggest a central role for ribosome biogenesis in growth regulation.	Erk1/2		[213]
Hsp90	HSP90	cytosol	extracellular Hsp90 serves as an important co-factor for KSHV-initiated MAPK activation (proof-of-concept for the potential benefit of targeting csHsp90 for the treatment or prevention of KSHV-associated illnesses)	MAPK general		[185]
heat shock 22kDa protein 8	HSPB8	nucleus and cytoplasm	involved in regulation of cell proliferation, apoptosis; HSPB8 is phosphorylated by amongst others Erk1 (at residues Ser(27) and Thr(87)) GSE 18224 adjusted P-value: 9,8x10-3	Erk1	in vivo	[173]

continues on next page

Table B.1.: Possible further ERK targets

Erk-Targets	*official symbol (NCBI)*	*Localisation*	*additional information*	*MAPK isoform*	*cell type*	*reference*
UBF	UBTF	nucleoli	Erk phosphorylates UBF and thus prevents their interaction with DNA, suggest a central role for ribosome biogenesis in growth regulation.	Erk1/2		[213]
IEX1	IER3		IEX1 is a substrate of Erk, they regulate each other, phosphorylated IEX1 is able to inhibit cell death	Erk2	in vivo	[71]
JAK 2	JAK2		the interaction between TFII-I and ERK, which is essential for its activity, can be regulated by JAK2 through phosphorylation of TFII-I	Erk general		[105]
Sam68	KHDRBS1	nucleus	Sam68 acts as a convergence point for ERK signaling to cell migration; blockade of phospho-Sam68 may provide a new avenue for therapeutic inhibition of metastatic cancers GSE 18224 adjusted P-value: 4,7x10-3	Erk1/2/5		[130]

continues on next page

Table B.1.: Possible further ERK targets

Erk-Targets	*official symbol (NCBI)*	*Localisation*	*additional information*	*MAPK isoform*	*cell type*	*reference*
UBF	UBTF	nucleoli	Erk phosphorylates UBF and thus prevents their interaction with DNA, suggest a central role for ribosome biogenesis in growth regulation.	Erk1/2		[213]
KSR1	KSR1		KSR1 is a scaffold, enhances signaling between Raf, MEK and ERK, Erk phosphorylates KSR1	MAPK general	in vivo	[190, 33]
LIFR	LIFR		ERK-induced event was required, in addition to CREB/ATF-1 phosphorylation, for CREB/ATF-1-mediated transcription of C/EBP genes; essential role for adipocyte differentiation GSE 18224 adjusted P-value: 1,08x10-2	Erk1/2		[14]
hormonsensitive Lipase	LIPE		Erk phosphorylates LIPE in fat cells, in muscle via PKC		fat cells, muscle cells	[52, 53]

continues on next page

Table B.1.: Possible further ERK targets

Erk-Targets	*official symbol (NCBI)*	*Localisation*	*additional information*	*MAPK isoform*	*cell type*	*reference*
UBF	UBTF	nucleoli	Erk phosphorylates UBF and thus prevents their interaction with DNA, suggest a central role for ribosome biogenesis in growth regulation.	Erk1/2		[213]
Lyn	LYN		Interleukin 2 activates polymorph cored, neutrophil granulocytes. In signal transduction the MAP/ERK cascade plays a role. ERK 1 binds Lyn in IL-2 activated neutrophil granulocytes.	Erk1	neutrophil granulo-cytes	[234]
Mxi - 2	MAPK14	nucleus and cytoplasm	Could play a pivotal role in the balance between ERK1/2 nuclear and cytoplasmic signals. GSE 18224 adjusted P-value: 8,74x10-3			[38, 37, 201]

continues on next page

Table B.1.: Possible further ERK targets

Erk-Targets	*official symbol (NCBI)*	*Localisation*	*additional information*	*MAPK isoform*	*cell type*	*reference*
UBF	UBTF	nucleoli	Erk phosphorylates UBF and thus prevents their interaction with DNA, suggest a central role for ribosome biogenesis in growth regulation.	Erk1/2		[213]
Ubiquitin - Protein - Ligase E3	MDM2		Mdm2 phosphorylation is regulated via MEK-ERK, might be important for the regeneration of hepatocytes after centrilobular cell death		hepatocytes	[140]
MI	MITF	cytoplasm	becomes phosphorylated by ERK -> activation, also targets it for degradation through the ubiquitin-proteosome pathway, involved in melanoma proliferation regulation GSE 18224 adjusted P-value: 6,01x10-3	Erk2	melanocytes	[235, 83]

continues on next page

Table B.1.: Possible further ERK targets

Erk-Targets	*official symbol (NCBI)*	*Localisation*	*additional information*	*MAPK isoform*	*cell type*	*reference*
UBF	UBTF	nucleoli	Erk phosphorylates UBF and thus prevents their interaction with DNA, suggest a central role for ribosome biogenesis in growth regulation.	Erk1/2		[213]
Mnk1 und 2	MKNK1/2	nucleus	after activation through phosphorylation by Erk Mnk 1 and 2 both phosphorylate eukaryotic initiations factor 4E	Erk1/2		[233]
c - Myb	MYB		MAPKs can phoyphorylate c-Myb and thus modulate the cellular function of c-Myb			[230]

continues on next page

Table B.1.: Possible further ERK targets

Erk-Targets	*official symbol (NCBI)*	*Localisation*	*additional information*	*MAPK isoform*	*cell type*	*reference*
UBF	UBTF	nucleoli	Erk phosphorylates UBF and thus prevents their interaction with DNA, suggest a central role for ribosome biogenesis in growth regulation.	Erk1/2		[213]
c-myc	MYC	nucleus	hypertrophic target in our cascade, becomes phosphorylated by Erk, enables post-mitotic cardiomyocytes to reenter the cell cycle and increases gene expression of genes that play a decisive role in cardiac hypertrophy, c-Myc is known for elevating both, protein synthesis and cell mass GSE 18224 adjusted P-value: 1,89x10-2			[64, 181, 240]

continues on next page

Table B.1.: Possible further ERK targets

Erk-Targets	*official symbol (NCBI)*	*Localisation*	*additional information*	*MAPK isoform*	*cell type*	*reference*
UBF	UBTF	nucleoli	Erk phosphorylates UBF and thus prevents their interaction with DNA, suggest a central role for ribosome biogenesis in growth regulation.	Erk1/2		[213]
MLCK	MYLK		Erk phosphorylates MLCK, involved in cell migration, in GSE 18224: MYLK4 GSE 18224 adjusted P-value: 1,36x10-2			[163, 161]
SPIN90	NCKIPSD		SPIN90 is a binding partner to Nck, which plays a role in the formation of sarcomeres during differentiation of cardiomyocytes. Cell adhesion and PDGF activate Erk1, which results in phosphorylation of SPIN90. Finally this is of essential importance for solid cell adhesion	Erk1		[127, 167]

continues on next page

Table B.1.: Possible further ERK targets

Erk-Targets	*official symbol (NCBI)*	*Localisation*	*additional information*	*MAPK isoform*	*cell type*	*reference*
UBF	UBTF	nucleoli	Erk phosphorylates UBF and thus prevents their interaction with DNA, suggest a central role for ribosome biogenesis in growth regulation.	Erk1/2		[213]
AIB1	NCOA3		assumption: the ability of growth factors to modulate estrogen action may be mediated through MAPK activation of the nuclear receptor coactivator AIB1	MAPK general		[65]
Nek2A	NEK2	centrosome	NEK2 may regulate proliferation, apoptosis, and other biological behaviors via MAPK signal pathway -> therapeutic target in liver cancer	Erk general	Hep G2 cells	[248]

continues on next page

Table B.1.: Possible further ERK targets

Erk-Targets	*official symbol (NCBI)*	*Localisation*	*additional information*	*MAPK isoform*	*cell type*	*reference*
UBF	UBTF	nucleoli	Erk phosphorylates UBF and thus prevents their interaction with DNA, suggest a central role for ribosome biogenesis in growth regulation.	Erk1/2		[213]
PAK2	PAK2		PAK2 plays a role in a new signal transduction pathway, which induces growth of neurites by bfGF. The PAK2-p85 betaPIX – complex phosphorylates the Erk-cascade and following translocations of this complex		PC12 cell lines	[101]
PEA-15	PEA15		PEA – 15 binds Erk and prevents its translocation into the nucleus -> blockade of cell proliferation, amongst others involved in ovarian cancer			[114, 13]

continues on next page

Table B.1.: Possible further ERK targets

Erk-Targets	*official symbol (NCBI)*	*Localisation*	*additional information*	*MAPK isoform*	*cell type*	*reference*
UBF	UBTF	nucleoli	Erk phosphorylates UBF and thus prevents their interaction with DNA, suggest a central role for ribosome biogenesis in growth regulation.	Erk1/2		[213]
PECAM1	PECAM1		Erk phosphorylates platelet endothelial cell adhesion molecule 1 (PECAM-1) and regulates its function as a binding partner and modulator of catenins			Platelet Web [23]
progesterone receptor	PGR	nucleus	Progesterone receptor ligand binding induces rapid and transient ERK1/2 activation via EGFR	Erk1/2		[61]
Phospholipase A2, CA-2+ abhängig	PLA2	cytosol	stretch induced ERK2 phosphorylation depends on PLA2 activity in skeletal myotubes GSE 18224 adjusted P-value: G5 8,18x10-4, G4a 1,03x10-2	Erk2		[31]

continues on next page

Table B.1.: Possible further ERK targets

Erk-Targets	*official symbol (NCBI)*	*Localisation*	*additional information*	*MAPK isoform*	*cell type*	*reference*
UBF	UBTF	nucleoli	Erk phosphorylates UBF and thus prevents their interaction with DNA, suggest a central role for ribosome biogenesis in growth regulation.	Erk1/2		[213]
Phospholipase c beta 1	PLCB1	nucleus	Erk phosphorylates PLCB1 and leads to mitogenic action of the insulin like growth factor GSE 18224 adjusted P-value: 3,43x10-2	Erk1/2		[243]
PPARalpha	PPARA		Erk1/2-dependent Cox 2-expression is one of the mechanisms of PPARA activation -> may control atherosclerosis	Erk1/2	macrophages	[216]
PP2Calpha	PPM1A		PPM1A functions as an extracellular signal-regulated kinase phosphatase (regulates it negatively) GSE 18224 adjusted P-value: 1,29x10-2	Erk general		[123]

continues on next page

Table B.1.: Possible further ERK targets

Erk-Targets	*official symbol (NCBI)*	*Localisation*	*additional information*	*MAPK isoform*	*cell type*	*reference*
UBF	UBTF	nucleoli	Erk phosphorylates UBF and thus prevents their interaction with DNA, suggest a central role for ribosome biogenesis in growth regulation.	Erk1/2		[213]
PP1C	PPP1CC	cytoplasm	in IGF1 treated neuronal cells ERK associates with PP1C (protein phosphatase 1 catalytic subunit c), which results in an enhanced activation level and however activates elF2b (= endogenous initiation factor 2B)	Erk1/2	neuronal cells	[186]
STEP	PTPN5	cytosol	PTPN5 specifically inactivates MAPKs and block nuclear translocation, missense variant of PTPN5 involved in appearance of hypertrophic scarring	mostly Erk1/2, p38MAPK		[57, 212]

continues on next page

Table B.1.: Possible further ERK targets

Erk-Targets	*official symbol (NCBI)*	*Localisation*	*additional information*	*MAPK isoform*	*cell type*	*reference*
UBF	UBTF	nucleoli	Erk phosphorylates UBF and thus prevents their interaction with DNA, suggest a central role for ribosome biogenesis in growth regulation.	Erk1/2		[213]
PTP-E	PTPRE	cytosol	inhibits Erk1/2 kinase activity, functions to prevent inappropriate activation and to stop prolonged activation	Erk1/2		[220]
Stomach Cancer-associated Protein-tyrosine Phosphatase-1	PTPRH		inhibits growth factor induced activation of Erk2			[165, 154]

continues on next page

Table B.1.: Possible further ERK targets

Erk-Targets	*official symbol (NCBI)*	*Localisation*	*additional information*	*MAPK isoform*	*cell type*	*reference*
UBF	UBTF	nucleoli	Erk phosphorylates UBF and thus prevents their interaction with DNA, suggest a central role for ribosome biogenesis in growth regulation.	Erk1/2		[213]
PTP - SL	PTPRR	cytosol	inactivates MAPKS and inhibits nuclear translocation, therapeutic target for treating neurodegenerative diseases	mostly Erk1/2, p38MAPK		[10, 57]
PTPN7	PTPN7	cytosol	inactivates MAPKS and inhibits nuclear translocation, therapeutic target for treating acute myeloblastic leukaemia	mostly Erk1/2, p38MAPK		[57]
RAB4A	RAB4A		is phosphorylated by insulin-activated Erk1	Erk1	in vitro	[43]

continues on next page

Table B.1.: Possible further ERK targets

Erk-Targets	*official symbol (NCBI)*	*Localisation*	*additional information*	*MAPK isoform*	*cell type*	*reference*
UBF	UBTF	nucleoli	Erk phosphorylates UBF and thus prevents their interaction with DNA, suggest a central role for ribosome biogenesis in growth regulation.	Erk1/2		[213]
MCIP 1	RCAN1		Erk1/2 phosphorylates RCAN1, phosphorylated RCAN1 inhibits calcineurin which plays a role in cardiac hypertrophy, but there are different mechanisms of inhibition and they are not finally clarified GSE 18224 adjusted P-value: 5,21x10-4	Erk1/2	in vitro	[226]

continues on next page

Table B.1.: Possible further ERK targets

Erk-Targets	*official symbol (NCBI)*	*Localisation*	*additional information*	*MAPK isoform*	*cell type*	*reference*
UBF	UBTF	nucleoli	Erk phosphorylates UBF and thus prevents their interaction with DNA, suggest a central role for ribosome biogenesis in growth regulation.	Erk1/2		[213]
RSK1	RPS6KA1	nucleus and cytoplasm	non-hypertrophic target in our cascade, mediates mitogenic and stress-induced activation of transcription factors, regulates translation through phosphorylation, and mediates cellular proliferation, survival, and differentiation by modulating mTOR signaling and repressing pro-apoptotic functions			[195, 207, 174, 68]

continues on next page

Table B.1.: Possible further ERK targets

Erk-Targets	*official symbol (NCBI)*	*Localisation*	*additional information*	*MAPK isoform*	*cell type*	*reference*
UBF	UBTF	nucleoli	Erk phosphorylates UBF and thus prevents their interaction with DNA, suggest a central role for ribosome biogenesis in growth regulation.	Erk1/2		[213]
RSK3	RPS6KA2		non-hypertrophic target in our cascade, serine/threonine-protein kinase that acts downstream of Erk1/2 signaling and mediates mitogenic and stress-induced activation of transcription factors, regulates translation, and mediates cellular proliferation, survival, and differentiation, may function as tumor suppressor in epithelial ovarian cancer cells, prolonged Erk association increased the duration of RSK3 activation	Erk 1/2		[194, 237]

continues on next page

Table B.1.: Possible further ERK targets

Erk-Targets	*official symbol (NCBI)*	*Localisation*	*additional information*	*MAPK isoform*	*cell type*	*reference*
UBF	UBTF	nucleoli	Erk phosphorylates UBF and thus prevents their interaction with DNA, suggest a central role for ribosome biogenesis in growth regulation.	Erk1/2		[213]
RSK2	RPS6KA3		after EGF-stimulation, Erk activates RSK2	Erk1/2		[99]
MSK1	RPS6KA5		hypertrophic target in our cascade, mediates stress and growth factor induced activation of CREB GSE 18224 adjusted P-value: 1,43x10-2	Erk1/2		[210, 35, 46, 228]
p70S6K	RPS6KB1	nucleus and cytoplasm	non-hypertrophic target in our cascade, involved in the activation of protein synthesis after physical exercise and thus in the building of muscle	Erk1/2		[8, 145]

continues on next page

Table B.1.: Possible further ERK targets

Erk-Targets	*official symbol (NCBI)*	*Localisation*	*additional information*	*MAPK isoform*	*cell type*	*reference*
UBF	UBTF	nucleoli	Erk phosphorylates UBF and thus prevents their interaction with DNA, suggest a central role for ribosome biogenesis in growth regulation.	Erk1/2		[213]
RXRalpha	RXRA	nucleus	in hepatocellular carcinoma, RXRα is constitutively phosphorylated by Erk and thereby losing its transactivation activity and becoming resistant to degradation			[110]
Na(+)/H(+) exchanger fusion protein, His182	SLC9A1		positive feedback loop between both proteins, this could pose a barrier against apoptosis			[112, 176]

continues on next page

Table B.1.: Possible further ERK targets

Erk-Targets	*official symbol (NCBI)*	*Localisation*	*additional information*	*MAPK isoform*	*cell type*	*reference*
UBF	UBTF	nucleoli	Erk phosphorylates UBF and thus prevents their interaction with DNA, suggest a central role for ribosome biogenesis in growth regulation.	Erk1/2		[213]
SMAD1	SMAD1		Smad signaling becomes activated via Erk1/2 pathway, signaling crosstalk could be a key mechanism in diabetic scarring GSE 18224 adjusted P-value: 7,15x10-3	Erk1/2, p38MAPK		[122]
SMAD2	SMAD2		Ras inhibitory signal on Smad2 is mediated by Erk MAPKs, regulates cell proliferation, differentiation and apoptosis.	Erk1/2		[91, 113, 188]
Vinexin	SORBS3	cytoplasm	Erk phosphorylates vinexin, plays important roles in cell spreading, migration and anchorage-independent growth	Erk2		[155]

continues on next page

Table B.1.: Possible further ERK targets

Erk-Targets	*official symbol (NCBI)*	*Localisation*	*additional information*	*MAPK isoform*	*cell type*	*reference*
UBF	UBTF	nucleoli	Erk phosphorylates UBF and thus prevents their interaction with DNA, suggest a central role for ribosome biogenesis in growth regulation.	Erk1/2		[213]
Sos1	SOS1		Ras–Raf–ERK pathway in placentas is highly dependent upon Sos1	Erk2		[184]
SP1 transcription factor	SP1	nucleus	SP1 mediates stress-induced activity of IRS2 promoter via Erk	Erk1/2	HepG2 cells	[225]
SRC1	SRC	nucleus	SRC can modulate pathways by the phosphorylation of hSpry2WT and following inhibition of Erk1/2	Erk1/2	in vitro	[124]
SREBP-1a	SREBF1		gets phosphorylated by Erk	Erk1/2	in vitro	[192]
TAL2	TAL2		Erk1 phosphorylates TAL2, involved in T-ALL	Erk1	in vitro	[239]

continues on next page

Table B.1.: Possible further ERK targets

Erk-Targets	*official symbol (NCBI)*	*Localisation*	*additional information*	*MAPK isoform*	*cell type*	*reference*
UBF	UBTF	nucleoli	Erk phosphorylates UBF and thus prevents their interaction with DNA, suggest a central role for ribosome biogenesis in growth regulation.	Erk1/2		[213]
E47	TCF3		Notch-induced E2A ubiquitination and degradation are controlled by Erk1/2 kinase activity → crucial for B and T lymphocyte development	Erk1/2	B/T lymphocyte	[164]
TGIF1	TGIF1	cytoplasm	Smad2 – co-repressor GSE 18224 adjusted P-value: 4,58x10-2	Erk1		[129]
Naf1alpha	TNIP1		Naf1alpha inhibits the translocation of Erk2 in the nucleus and consequently the transcriptional activation, is an attenuator of activated Erk2 GSE 18224 adjusted P-value: 1,56x10-3	Erk2	in vitro and in vivo	[249]

continues on next page

Table B.1.: Possible further ERK targets

Erk-Targets	*official symbol (NCBI)*	*Localisation*	*additional information*	*MAPK isoform*	*cell type*	*reference*
UBF	UBTF	nucleoli	Erk phosphorylates UBF and thus prevents their interaction with DNA, suggest a central role for ribosome biogenesis in growth regulation.	Erk1/2		[213]
Tob	TOB1		The phosphorylation of Erk negatively regulates the anti proliferative effect of Tob.	Erk2	in vitro	[136]
Tpr	TPR		protein-protein interaction	Erk2	in vitro	[32]
YBX1	YBX1		shows interaction	Erk2	HEK293 cells	[241]

Danksagung

Zunächst möchte ich Herrn Prof. Dr. Thomas Dandekar für die Überlassung des interessanten Promotionsthemas und die Möglichkeit in seinem Institut meine Promotionsarbeit anfertigen zu dürfen danken. Herr Prof. Dr. Dandekar engagierte sich weit über das notwendige Mass hinaus und trug so massgeblich zum Gelingen dieser Promotion bei. Herr Prof. Dr. Dandekar war mir ein stets verständnisvoller und nachsichtiger Mentor und gab mir Rückhalt und die entscheidende Sicherheit auch schwierige Hürden und Herausforderungen zu bestehen. Besonders möchte ich mich auch für das wiederholte und stets zügige Korrekturlesen der Dissertation bedanken.

Bei Frau Prof. Dr. Kristina Lorenz und ihrer Arbeitsgruppe am Institut für Pharmakolgie und Toxikologie der Universität Würzburg, welche die in dieser Arbeit beschriebenen in-vitro Experimente durchführte, bedanke ich mich herzlich für die reibungslose Zusammenarbeit. Es bestand ein reger Austausch von Daten und Informationen, der sich durch viel Kollegialität auszeichnete.

Meinen Kollegen am Lehrstuhl für Bioinformatik der Universität Würzburg, hier insbesondere Frau Dr. Astrid Fieselmann, Frau Dr. Gaby Wangorsch und Herrn Dr. Alexander Cecil, danke ich für die stete Hilfsbereitschaft und angenehme Arbeitsatmosphäre. Sie waren mir als Medizinerin bei der Einführung und Einarbeitung in die zunächst fachfremde Thematik der Bioinformatik eine groSSe Hilfe. Ich danke Ihnen für viele fruchtbare Gespräche und Anregungen.

Desweiteren danke ich Frau Anke Fischbach, Herr Dr. Dennis Wiebusch und Herr Dr. Martin Fischbach vom Lehrstuhl für Mensch-Computer-Interaktion der Universität Würzburg, die mir mit wertvoller Erfahrung aus ihren wissenschaftlichen Tätigkeiten und nicht zuletzt als Freunde über die letzten Jahre eine unermessliche Hilfe waren. Ich danke meinen Eltern, die mir das Studium der Humanmedizin ermöglichten und mich im gesamten Studium und während der Promotion liebevoll unterstützten. Ganz besonders danke ich meinem Ehemann Simon, der mir sowohl bei der beruflichen Tätigkeit als auch bei der Erstellung der Dissertation viel Verständnis und Geduld entgegenbrachte und mich stets motivierte.

Allen Mitwirkenden spreche ich meinen besonderen Dank aus!

Vita

Der Lebenslauf wird aus Gründen des Datenschutzes in der elektronischen Version nicht veröffentlicht.